Characterization of the interaction of synemin-L & nestin with desmin, a major structural protein in muscles

Petra Zugschwerdt

Doctoral Thesis

German Cancer Research Centre (DKFZ)

Dissertation

submitted to the

Combined Faculties for the Natural Sciences

and for Mathematics

of the Ruperto-Carola University of Heidelberg, Germany

for the degree of

Doctor of Natural Sciences

Presented by: Petra Zugschwerdt, Dipl. Biology

Born in: Bensheim, Germany

Oral examination: 2015

Characterization of the interaction of synemin-L & nestin with desmin, a major structural protein in muscles

Referees: Prof. Dr. Harald Herrmann-Lerdon

PD Dr. Karsten Rippe

Declaration by the PhD Candidate

I hereby declare that the data described and presented in this thesis are a result of my own work and effort. In cases other sources of information have been used, they have been appropriately indicated and referenced. The particular experiments performed by others, as well as figures supplemented by them, have been rightfully acknowledged

Heidelberg _____

Petra Zugschwerdt

Meinen Eltern

Acknowledgments

Zuerst danke ich Herrn Professor Herrmann für seine Unterstützung während meiner Doktorarbeit. Mit seinem immensen Wissensschatz über IF-Proteine in der Theorie und Praxis half er mir durch alle Phasen der Doktorarbeit.

Herrn Doktor Karsten Rippe möchte ich für die Übernahme des Zweitgutachtens und den hilfreichen Kommentaren während der TAC-Meetings danken. Darüber hinaus danke ich Herrn Professor Frings und Herrn Professor Lichter für die Bereitschaft, meine Prüfer zu sein. Ebenso danke ich Professor Dieter Fürst für seine Unterstützung bei meinen TAC-Meetings.

Herrn Doktor Norbert Mücke danke ich für seine Bereitschaft, mir die AUZ für meine Versuche zu überlassen. Herrn Doktor Karsten Richter danke ich für seinen Support am Elektronenmikroskop und die Hilfe beim Rotary Shadowing.

Bei der Arbeitsgruppe von Professor Herrmann möchte ich mich herzlich für die wundervollen, familiären Jahre in ihrer Mitte bedanken. Es war mir eine Ehre, mit euch zu arbeiten und zu lachen: Tatjana Wedig, Monika Mauermann, Tanja Tourgaidis, Michaela Hergt Kendra Maass, Domenic Hartmann, Dorothee Möller, Thorsten Kolb (Frühere Mitglieder: Pavle Krsmanovic, Sarika Sharma, Helga Kleiner).

Der gleiche Dank gilt meiner Familie, ohne die all das nicht möglich gewesen wäre. Sie hat mich immer darin unterstützt, meine eigenen Wege zu gehen und hat mir stets das Gefühl gegeben, ein großes Netz unter dem Seil zu haben: meine Eltern Monika und Michael Zugschwerdt genauso wie meine Schwester Tanja mit Martin und Charlotte.

Ich möchte Melanie und Dominik für ihre Treue die letzten Jahre danken.

Auch Björn möchte ich für seine treue Unterstützung danken.

Summary

In desminopathies, protein aggregates of desmin (*des)* are found together with other proteins from the intermediate filament (IF) protein family such as nestin (*nes*) and synemin (*syn*) within the muscle of patients. It is not known if or what role *des* associated proteins play within the aggregation process of mutant *des*. We have systematically characterized the biochemical properties of both human *syn*-L and tail truncated *nes* as well as their interaction with *des* and vimentin (*vim*). After renaturation into buffers of low ionic strength, s*yn* was determined to be a monomer, and it only formed oligomeric structures of distinct size under IF assembly conditions. A major topic of this thesis was to characterize its *in vitro* interaction with *des* and *vim*. Surprisingly, *syn* exhibited a strong negative impact on the filament forming process of *des* and *vim,* both when proteins were mixed before or after renaturation. The addition of *syn* to pre-assembled filaments caused the formation of globular protein structures within the filament network and at its ends. Employing domain-truncated variants of *des* and *vim* for assembly experiments of *syn*, we determined the rod domain of *des* and *vim* as binding site for *syn*. The study of the tail-truncated variant of *nes* revealed a significant pH-sensitive solubility. Aggregates formed by *nes* under assembly conditions seemed to be unordered. *Nes* interacted with *des* during renaturation but not afterwards. “Unit length filament”-like structures formed by mutant *vim*Y117L and *des*Y122L were covered by a proteinacous mass assembled in the presence of *nes*. No filaments but huge protein aggregates were visualized when *nes* was renaturated and co-assembled with *des* under assembly conditions, but addition of *nes* after renaturation of *des* caused the occasional decoration of seemingly intact *des* IFs with irregular protein structures. Addition of *nes* before or after renaturation of *vim* altered the size of protein aggregates found besides intact filaments. Our *in vitro*-data suggest that *syn* and *nes* are no *bona fide* IF proteins but IF-associated proteins. Because *nes* is only coating filaments and *syn* aggressively integrates into pre-existing IFs, and because both are not able to form IFs, the role of *syn* and *nes* as structural components in both normal and diseased muscle should be analysed now from a completely different point of view.

Keywords: cytoskeleton, intermediate filament, desmin, vimentin, synemin, nestin, assembly, electron microscopy, cosedimentation, preparative and analytical ultracentrifugation, rotary shadowing.

Zusammenfassung

In Desminopathien sind Proteinaggregaten von Desmin (*Des)* zusammen mit anderen Proteinen der Intermediärfilament (IF)- Proteinfamilie wie Nestin (*Nes*) und Synemin (*Syn*) in den Muskeln von Patienten zu finden. Es ist nicht bekannt, ob oder welche Rolle *Des*-assoziierte Proteine innerhalb des Aggregationprozesses vom mutanten *Des* spielen. Wir haben systematisch die biochemischen Eigenschaften von humanem *Syn*-L und einer Tail-verkürzten Form von *Nes* sowie deren Interaktionen mit *Des* und Vimentin (*Vim*) charakterisiert. Nach der Renaturation in Puffer geringer ionischer Stärke wurde *Syn* als Monomer bestimmt, und es formte nur oligomerische Strukturen definierter Größe in IF-Assemblierungsbedingungen. Ein Hauptthema dieser Thesis war seine *in vitro*-Interaktion mit *Des und Vim zu* charakterisieren*.* Überraschenderweise hat *Syn* einen starken negativen Einfluß auf den Filamentformationsprozess von *Des* und *Vim*, wenn die Proteine vor oder nach der Renaturation gemischt worden sind. Die Zugabe von *Syn* zu vor-assemblierten Filamenten verursachte globuläre Proteinstrukturen innerhalb des Filament-netzwerkes und an seinen Enden. Durch das Nutzen von Domänen-verkürzten Varianten von *Des* und *Vim* für Assemblierungsexperimenten von *Syn* konnte die Rod-Domäne von *Des* und *Vim* als Bindungsstelle für *Syn bestimmt werden*. Die Studie der Tail-verkürzten Variante von *Nes* zeigte eine signifikante pH-sensitive Löslichkeit. Von *Nes* unter Assemblierungsbedingungen geformte Aggregate schienen ungeordnet zu sein. *Nes* interagiert mit *Des* während der Renaturation, aber nicht danach. „Einheitslängenfilament“-ähnliche Strukturen von in der Anwesenheit von *Nes* assemblierten *Vim*Y177L und *Des*Y122L waren von einer Proteinmasse überzogen. Keine Filamente, aber riesige Proteinaggregate waren sichtbar, wenn *Nes* mit *Des* zusammen renaturiert und ko-assembliert wurde, aber die Zugabe von *Nes* nach der Renaturation von *Des* verursachte die teilweise Dekoration von anscheinend intakten *Des* IFs mit irregulären Proteinstrukturen. Gleichzeitig ändert die Zugabe von *Nes* vor oder nach Renaturierung von *Vim* die Größe der Proteinaggregate, die neben den intakten Filamenten gefunden werden. Unsere *in vitro*-Daten legen nahe, dass *Syn* und *Nes* keine *bona fide* IF-Proteine, aber IF-assoziierten Proteine sind. Da *Nes* Filamente umhüllt und *Syn* aggressiv in existierende IFs integriert, und weil beide nicht fähig sind, IFs zu formen, sollte die Rolle von *Syn* und *Nes* als Strukturkomponenten in gesundem und krankem Muskel jetzt von einem komplett anderen Gesichtspunkt untersucht werden.

Schlüsselworte: Zytoskelett, Intermediärfilamente, Desmin, Vimentin, Synemin, Nestin, Assemblierung, Elektronenmikroskopie, Kosedimentation, präparative und analytische Ultrazentrifugation, hochauflösende Metallbeschattung („rotary shadowing“).

Contents

1 Introduction

The cytoskeleton plays an important role in different processes in most vertebrate cells like stabilization, transport, movement, cell division and resistance against mechanical stress. Various diseases are connected to mutations in single cytoskeleton proteins. Therefore, it is necessary to develop a detailed understanding of this complex network within the cell.

1.1 The cytoskeleton

The cytoskeleton of most animal cells is dominated by three distinct major network systems; the microtubule network, the intermediate filament (IF) network and the microfilament network. These protein systems differ in structure, polymerization process and function. Microtubules (with a diameter of 25 nm) work as a platform for intracellular transport, while actin microfilaments are important for the cell polarity, cell motility and contraction (Pollard 2002). The role of IF filaments named after the intermediate diameter of 10 – 12 nm is the stabilization of cell structures (Herrmann et al 2007).

Microfilaments are formed by globular actin monomers with the help of ATP hydrolysis (Wegner and Engel 1975), while microtubules are constituted by globular αβ tubulin heterodimers through GTP hydrolysis (Voter and Erickson 1984). The polarity of the modules leads to a dynamic structure of these filaments by growth and shrinking (Pollard 2002; Kerssemakers et al. 2006). IFs (with a diameter of 8 - 14 nm) lack an enzymatic activity and therefore differ in their filament forming process, which is arranged by lateral and longitudinal alignment of the fibrillar proteins (Herrmann and Aebi 2004). IF filaments were first described in metaphase myocytes that stained negative for actin and myosin (Ishikawa, Bischoff, and Holtzer 1968). The three network systems can be distinguished by immunofluorescence microscopy or electron microscopy in different myogenic cultured cells (Franke et al. 1978). In most

metazoan cells, two IF networks can be distinguished: the cytoplasmic IF network und the nuclear IF network. The nuclear membrane- and chromatin-bound IF network, called lamina, is formed by lamins (Aebi et al. 1986). Nuclear membrane proteins like plectin and nesprin-3α and linker proteins connect the nuclear envelope to the cytoplasmic IFs (Favre et al. 2011). The cytoplasmic IF network is also connected to the plasma membrane-associoated junctions like desmosomes and hemidesmosomes in epithelial cells or costameres in striated muscle (Rezniczek et al. 1998; Green et al. 2005; Herrmann et al. 2007). The three filament networks are interconnected by cross-bridging factors supported by a large group of associated proteins (Fuchs and Yang 1999).

1.2 The family of IF proteins

The family of IF proteins is encoded by at least 70 different genes located on different chromosomes (Szeverenyi et al. 2008; Hesse, Magin, and Weber 2001). The different IF proteins share only 20% sequence identity implying different physical and biochemical properties (Fuchs and Weber 1994). IF proteins are expressed in a development - and tissue specific kind (Toivola et al. 2005). Besides their mentioned role in cell integretiy and scaffolding, IF proteins have organelle-related and protein-targeting functions within the cell (Toivola et al. 2005). For example is mitochondrial positioning and functionality dependent of IFs such as desmin or keratin filaments (Reipert et al. 1999; Tao et al. 2009). Moreover, the IF network have been shown to interact with the endo-lysosomal sorting system (Styers et al. 2004). IF proteins are important for lipid biosynthesis and metabolism as shown for vimentin in case of glycosphingolipids and lipoprotein-derived cholesterol (Gillard et al. 1994; Sarria, Panini, and Evans 1992). This diversity in function and expression of the different IF proteins is supplemented by their diversity of assembly.

IF proteins are divided into three assembly groups based on their differences in co-polymerization (Herrmann and Aebi 2000). While IF proteins of assembly group 1 do only form heteropolymers, IF proteins of assembly group 2 are able to form homo- and heteropolymers. Based on sequence homology, IF proteins are categorized into six sequence homology classes (SHC). The proteins of class I and II are the acidic and basic keratins which form heteropolymers together. Class III is determined by vimentin, desmin, peripherin and GFAP, which can build filaments alone or together

with proteins of group IV and VI. The proteins of SHC IV are not able to form filaments on their own and are mostly found in nerve cells (NF-L, NF-M, NF-H, α-internexin, L-synemin). But SHC IV proteins H-synemin and M-synemin are expressed in muscle tissue. In contrast to the other IF proteins, the proteins of SHCV, the lamins are only found within the nucleus (Aebi et al. 1986). These proteins determine the third assembly group, because they are not able to form filaments with proteins of the other sequence homology classes. The proteins phakinin and filensin are found within the eye lens and build SHC VI (Ireland et al. 2000).

SHC	Member	Tissue	Assembly group	Example of associated diseases
I	acidic keratins	Epithelia, hair	1	Epidermolysis bullosa simplex, epidermolytic hyperkeratosis
II	basic keratins	Epithelia, hair	1	Epidermolysis bullosa simplex, epidermolytic hyperkeratosis
III	desmin vimentin GFAP	Muscle Mesenchyma Glial cells	2 2 2	Desminopathies Cataract Alexander disease
IV	synemin nestin NFL, NFM, NFH	Muscle Pluripotent cells neurons	2 2 2	? ? Charcot-Marie-Tooth disease, Parkinson
V	A-type lamins B-type lamins	All metazoan cells All metazoan cells	3 3	Hutchinson-Gilford progeria syndrome, emery-dreifuss muscular dystrophy Acquired partial lipodystrophy
VI	filensin phakinin	Eye lens Eye lens	? ?	Autosomal dominant cataract Autosomal recessive cataract

Table 1 Adapted from (Eriksson et al. 2009; Omary 2009). SHC: Sequence homology class

IF proteins are a heterogeneous group of unpolar proteins. They differ in protein sequence but share the tripartite composition of an amino terminal head domain, an α-helical rod domain and a carboxy terminal tail domain (Herrmann et al. 2009). The central rod domain is ~310 amino acids long and its amino acid sequence is organized by heptadic repeats $(abcdefg)_n$ with hydrophobic amino acids like Leu, Ile, Met or Val at position *a* and *d* (Geisler, Kaufmann, and Weber 1982; Parry 2005).

The α-helical structural elements called coil1A, coil1B and coil2 of the rod domain are interrupted by two linker domains called L1 and L12 (Chernyatina et al. 2012).

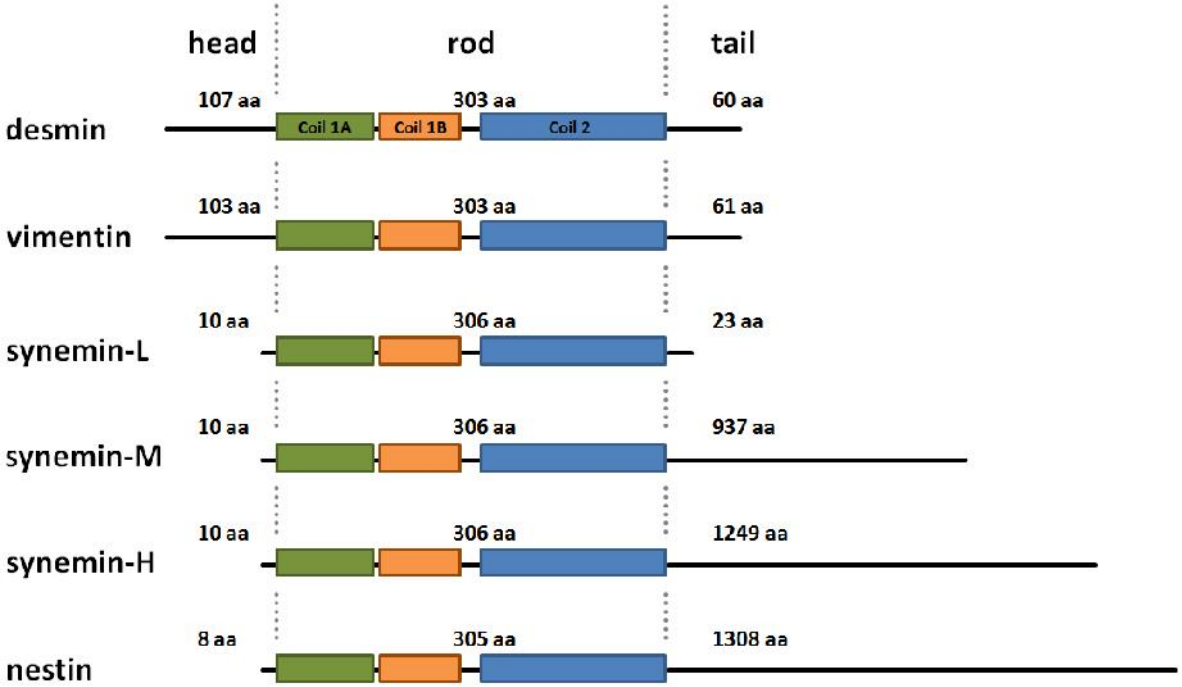

Figure 1: Comparison of different IF proteins. Desmin and vimentin are type III IF proteins while synemin-L, -M, -H and nestin are characterized as type IV IF proteins.

The heptadic repeats lead two IF proteins to align into coiled-coil dimer. Within coil2 is a discontinuity of the helical repeats called “stutter” where two helices are aligned in parallel. These dimers are the starting units for the assembly process. Truncation studies lead to the insight that the highly conserved TYRKLLEGEE motif at the end of the rod domain is crucial for the tetramer forming process and the filament width (Herrmann and Aebi 2004). The TYRKLLEGEE motif at the end and the LNDR motif at the beginning of the rod domain are highly conserved sequences within all IF proteins, and therefore have been called IF consensus motifs (Magin, Hatzfeld, and Franke 1987). Head and tail domains differ in size (Figure 1) and composition. For example, the head domain of nestin is five amino acids long while the head domain of vimentin is 103 amino acids long. The head domain is important for building tetramer complexes (Herrmann et al. 1996) and posttranslational modifications such as serine-phosphorylation are predominant found within the head and tail domains (Inagaki et al. 1996).

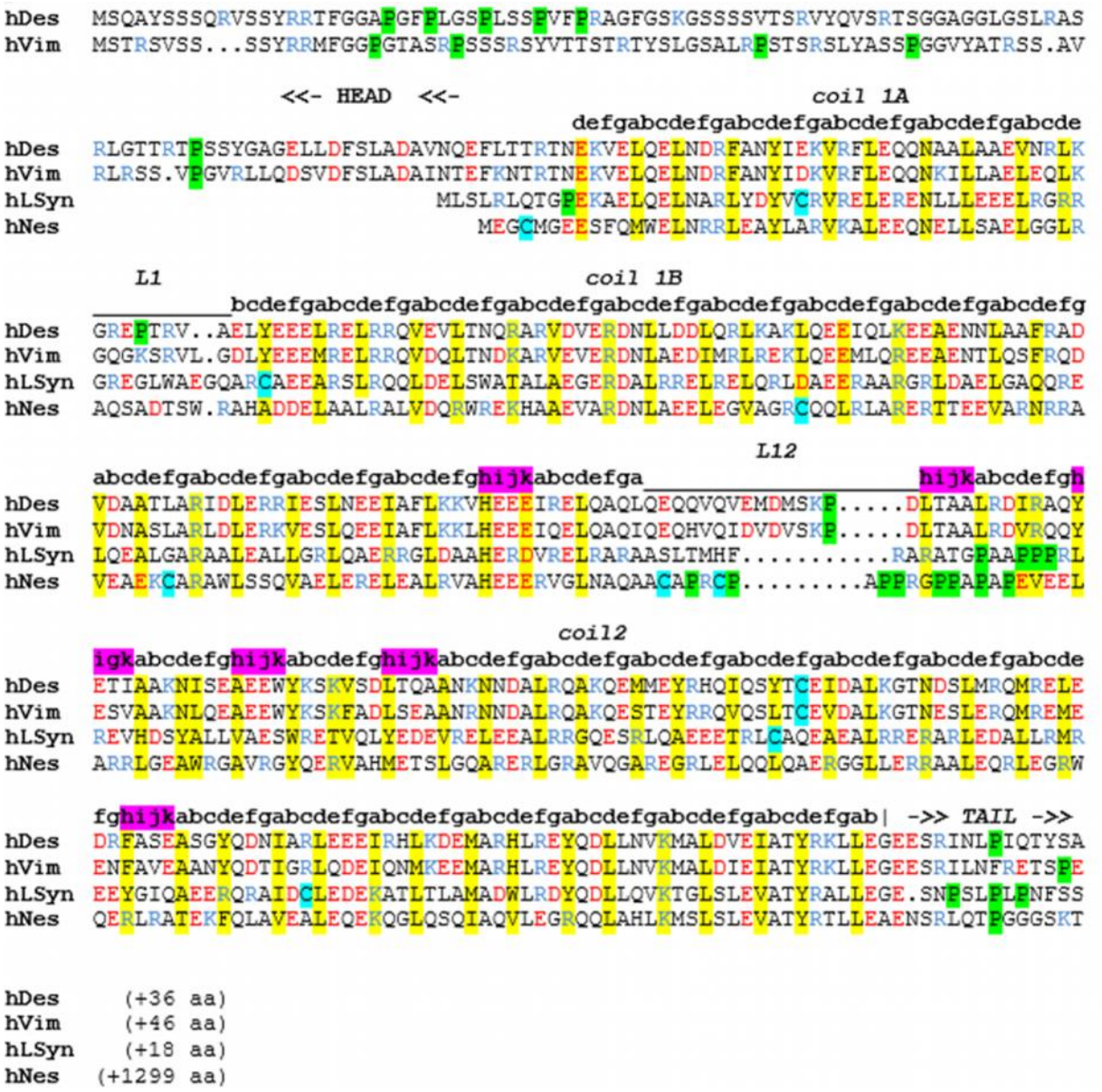

Figure 2: Comparison of the amino acid sequence of the head and rod domain of human desmin (hDes), vimentin (hVim), synemin-L (hLSyn) and nestin (hNes). Amino acids are written in the one-letter-code. Above the sequence repeat pattern were indicated. The tail domain is not completely shown.

1.2.1 *In vitro* assembly of IF proteins

The assembly process of IF proteins is cofactor-independent. The tetramers are formed by two anti-parallel coiled-coil dimers. The IF proteins of the nuclear and cytoskeletal IF networks differ in their *in vitro* assembly process. While lamins form dimers at high pH (pH 8.0 – 9.0) and salt conditions (150 – 300 mM NaCl) and paracrystal fibres at pH 9.0 in 20-25 mM $CaCl_2$, cytoplasmic proteins like vimentin

form tetramers under buffer conditions of low ionic strength and high pH (5 mM Tris, pH 8.4) (Herrmann and Aebi 2004).

These tetramers form “unit-length filaments” (ULFs) within 10 seconds in buffers of physiological pH and ionic strength (25 mM Tris, 50 mM NaCl, pH 7.5). While the ULFs at the beginning are ~17nm wide and ~60 nm long, which are compacted through a process called radial compaction following the filament forming process of lateral and longitudinal alignment (Herrmann et al. 1996). This process leads to the mature filaments with a width of 10-12 nm without reducing the mass-per-length (MPL), which is an quantitative term for the molecules per filament diameter (kDa/nm) (Wickert et al. 2005). For vimentin filaments under assembly conditions, the MPL value is 30±4 kDa/nm corresponding to ~30 molecules per cross-section, while for desmin filaments the MPL value is 48±8 kDa/nm corresponding to ~37 desmin subunits per filament cross section (Wickert et al. 2005).

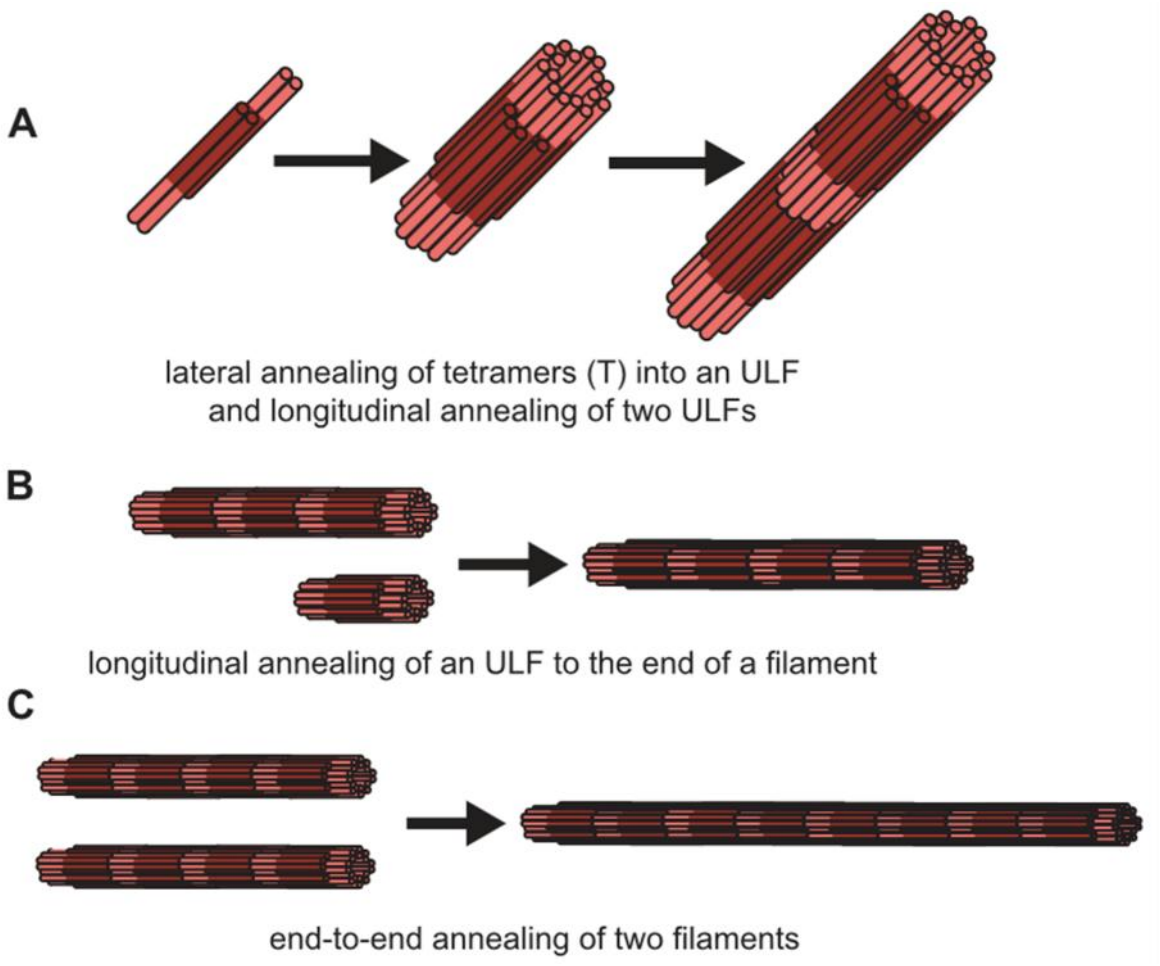

Figure 3: The assembly process of IF proteins (Kirmse et al. 2007)

1.3 The expression of intermediate filament proteins within muscle cells

The expression of IF proteins is highly dynamic during the development of muscle fibers (Lazarides 1982). During division of myoblasts and the following cell alignment, the major IF proteins found are vimentin together with nestin and synemin. During the cell fusion, instead of vimentin desmin becomes the major IF protein and remains for life in the intact muscle fibre besides synemin and syncoilin (Figure 4). The expression of vimentin and nestin is down-regulated, but in case of injury they are expressed again during regeneration.

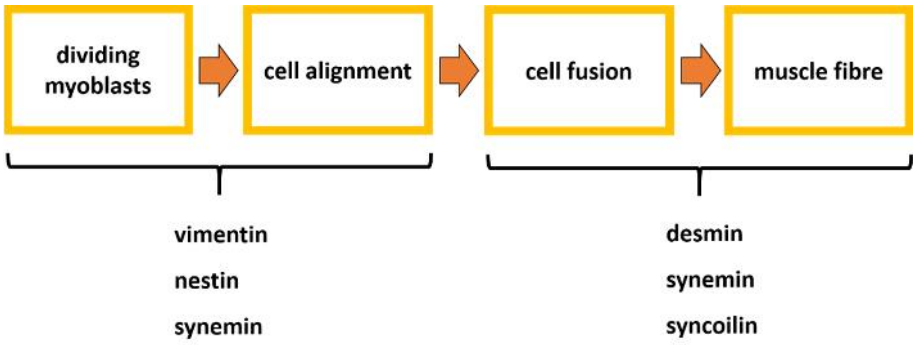

Figure 4: Distribution of different muscle specific IF proteins during muscle development. In the first stages of development, vimentin is the major IF protein. In the later stages, desmin is the major IF protein within muscle cells.

1.4 Desmin is a major cytoskeletal protein in muscle

Desmin (from the greek word *desmos*: bond or link) is specially expressed in all kinds of muscle cells (Lazarides 1980). The single copy gene (DES) is located with nine exons on chromosome 2q35. Due to its appearance at embryonic day 7.5, the 476 aa long protein is one of the earliest muscle-specific markers (Paulin and Li 2004). Desmin filaments are part of the extrasarcomeric cytoskeleton in mature skeletal muscles and form a scaffold around Z-discs to connect the neighbouring myofibrils (Konieczny et al. 2008). Moreover, the desmin filaments are connected with the nuclei, subsarcolemmal cytoskeleton and organelles like mitochondria by different isoforms of a linker-protein called plectin (Konieczny et al. 2008). Therefore, desmin is an important connective platform of different compartments within the muscle cells

(Goldfarb et al. 2004; Hijikata et al. 2008). A lack of desmin as obtained by a corresponding gene knockout in mice does not lead to an abnormal sarcomeric organization but the muscles (DES-/-) mice degenerate upon repeated contractions (Li et al. 1996; Li et al. 1997; Milner et al. 1996). Mice lacking desmin exhibit reduced life spans and suffer from cardiomyopathy besides skeletal myopathies and smooth muscle dysfunction (Capetanaki and Milner 1998).

1.5 Synemin and nestin, two non-self-assembling IF proteins

Synemin (also called desmulin) and its co-localization with desmin and vimentin was first described 1980 in developing avian muscles (Granger and Lazarides 1980). It is categorized into SHC IV as a non-self-assembling protein which needs vimentin or desmin to co-polymerize (Khanamiryan et al. 2008; Bellin et al. 1999). Today, three splice variants of the synemin coding gene DMN on chromosome 15qn6.3 are known (Xue et al. 2004). Besides lamin A and B and GFAP, synemin is the only IF protein with different splice variants. These splice variants are expressed in a development- and tissue specific manner (Izmiryan et al. 2009). The three isoforms are designated, according to their molecular weight, synemin-H, synemin-M and synemin-L. They are expressed in astrocytes and neurons. They share the short head domain (10 amino acids) and the rod domain (306 amino acids), but differ in the length of the tail domain (Figure 1). The muscle specific isoforms synemin-H and synemin-M differ only by a 312 amino acids long insertion within the tail domain of synemin-H. Like desmin, synemin is expressed in all four classes of muscles (Hirako et al. 2003), where it is associated with desmin (Xue et al. 2004). The carboxy-terminal tail domain of synemin contains binding motifs for different non-IF proteins such as α-actinin (Olivé et al. 2003), zyxin (Sun et al. 2010), talin (Sun et al. 2008), vinculin and meta-vinculin (Bellin et al. 2001) as well as dystrophin and utrophin (Bhosle et al. 2006). These findings suggest a role of synemin in cell adhesion and cell migration.

Nestin was first described in neuroepithelial stem cells with a monoclonal antibody by Hockfield and McKay (Hockfield and McKay 1985). Based on the low sequence homology of the rod domain in comparison to the other IF proteins, nestin was definded as a type IV IF protein (Liem 1993). Nestin is the IF protein with the shortest head domain (5 amino acids) and the longest tail domain (1308 amino acids) which interacts with other cytoskeletal components like microfilaments and microtubules

(Hockfield and McKay 1985). Because of its expression during mammalian embryogenesis in a variety of embryonal and fetal tissues, nestin is thought to be important for multi-lineage progenitor cells (Wiese et al. 2004). In the central nervous system, stem cells of the central nervous system in the neural tubes, nestin is replaced by neurofilaments upon terminal neural differentiation. Moreover, nestin has been shown to be upregulated during neuroregeneration (Frisén et al. 1995; Pekny et al. 1999). The colocalization of nestin with desmin and vimentin was shown in developing skeletal myotubes by three-dimensional fluorescence digital imaging microscopy (Sjöberg et al. 1994).

Nestin is expressed in pediatric rhabdomyosarcomas besides desmin (Kobayashi et al. 1998). After muscle injuries, the expression of nestin is correlated with the expression of vimentin indicating that they are essential during the early dynamic phase of the myofiber regenartion, when migration, fusion and structural modelling of myogenic cells occur (Vaittinen et al. 2001). Nestin is unable to self-assemble (Herrmann and Aebi 2000). Nestin purified from BHK-21 cells has been shown to be able to form homodimers and homotetramers and to assemble *in vitro* together with vimentin as long as the share of nestin does not exceed about 25% (Steinert et al. 1999).

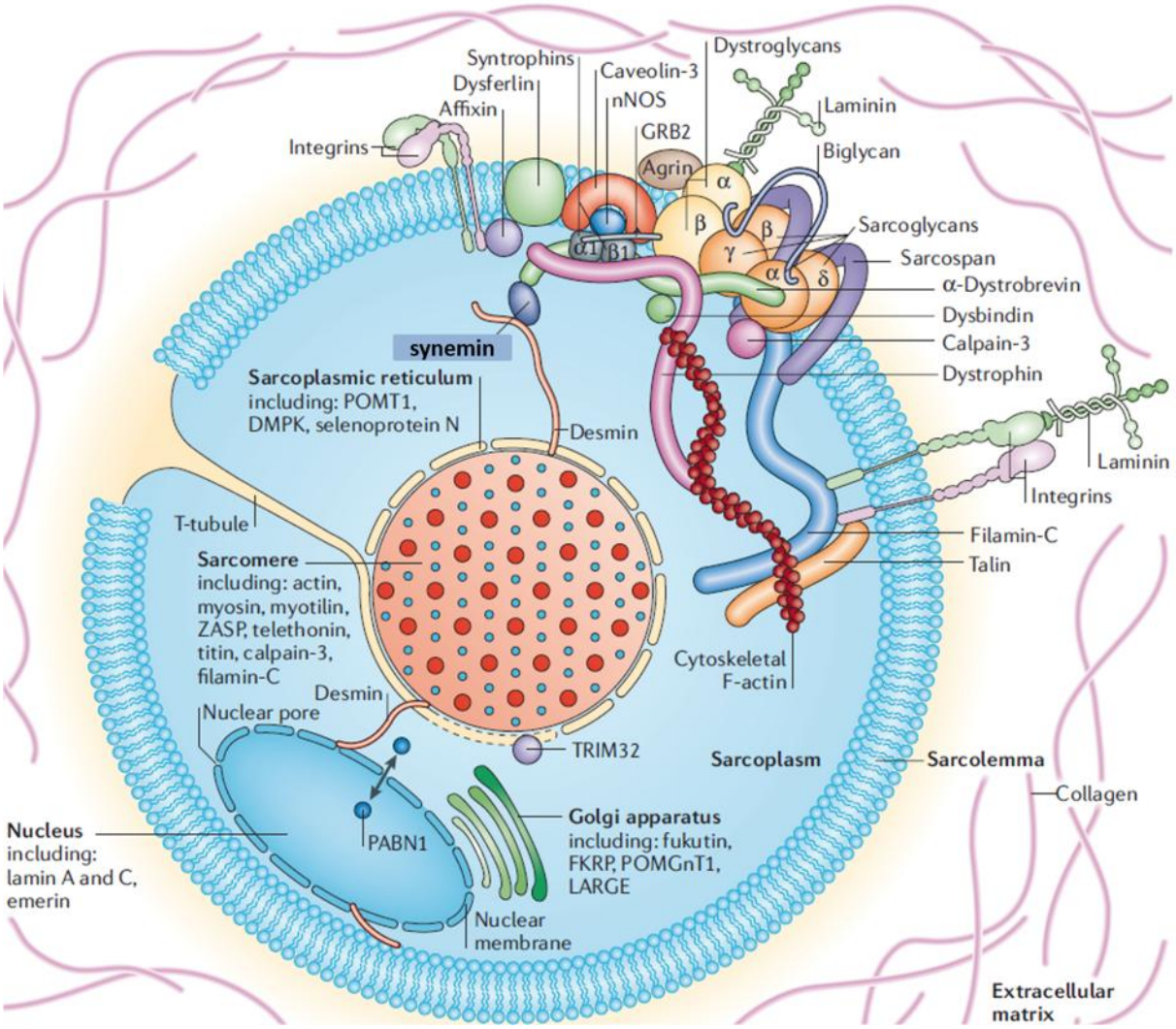

Figure 5: A cross-section of a myofibre (adapted from Davies and Nowak 2006)

1.6 Desminopathies

Desmin-positive sarcoplasmic protein aggregates and myofibrillar degeneration are the major pathophysiological features in myopathies. The protein accumulation interferes with dynamic protein turnover and cellular homeostasis. Myofibrillar myopathies (MFM) are hereditary protein aggregate myopathies with a general autosomal-dominant mode of inheritance. MFMs are thought to be affecting a subgroub of stress-responsive Z-disc proteins (Claeys et al. 2009). More than half of all myofibrillar myopathies (MFMs) are connected to desmin and desmin related proteins (Schröder, Vrabie, and Goebel 2007; Selcen, Ohno, and Engel 2004). *In vitro* studies with MFM causing desmin mutants showed that the mutant proteins

differ from wildtype proteins in their assembly behaviour as they are unable to form filamentous networks but do form abnormal IF structures or are able to induce the collapse of a pre-existing IF network (Bär, Mücke, et al. 2005; Bär, Fischer, et al. 2005).

1.7 Motivation

The *in vitro* assembly process of type III intermediate filament proteins desmin and vimentin gives an impression of the assembly process within the cell. In *in vitro* approach, tetramers are the starter units of assembly induced through increasing the ionic strength and lowering the pH. The head and rod domain of desmin are needed to form tetramers through renaturation and filaments through *in vitro* assemby. Synemin and nestin are characterized as type IV intermediate filament proteins based on sequence aligment and co-localization with desmin and vimentin. The *in vitro* characteristics of synemin and nestin have not been systematically analysed. As non-self-assembling proteins they are supposed to form heteropolymers with type III intermediate filament proteins, but the interaction of synemin and nestin with desmin and vimentin has not been characterized in detail.

During this Ph.D. thesis, we aim at understanding the *in vitro* properties of type IV intermediate filament proteins synemin and nestin in standard *in vitro* conditions used for type III intermediate filament proteins desmin and vimentin. First, we want to understand how synemin and nestin react to the standard renaturation protocols. Second, we aim at analyzing the interaction of synemin and nestin with desmin or vimentin on a monomeric, tetrameric, ULF-like and filamentous stage of *in vitro* assembly. The third objective is the characterization of the binding site of desmin and vimentin for synemin and nestin. To achieve our first objective, we aim at characterizing soluble syemin and nestin using recombinant proteins. The soluble structures of synemin and nestin are analyzed by sedimentation assays with the airfuge as well as analytical ultracentrifugation and rotary shadowing. We investigate the ability of synemin and nestin to assemble by using sucrose gradient centrifugation and electron microscopy. These data should give us a first impression of the *in vitro* characteristics of synemin and nestin. In order to analyze the interaction of synemin and nestin with desmin and vimentin on different stages during renaturation and assembly, electron microscopy, sedimentation assay with the

airfuge and sucrose gradient centrifugation have been used. These data should give us an understanding of the intergration of synemin and nestin in the heterofilaments besides desmin and vimentin. As a third objective, we aim at analyzing the binding site of type III intermediate filament proteins for synemin and nestin. We use truncated variants of desmin and vimentin for the characterization of the binding domain with sucrose gradient centrifugation, sedimentation assays with the airfuge and electron microscopy.

2 Results

Results Part I

Characterization of the *in vitro* properties of synemin-L

Part I focus on the *in vitro* characterization of synemin and its interaction with type III IF proteins desmin and vimentin. The soluble structures formed by synemin during renaturation are analyzed using analytical ultracentrifugation (**2.1.2**). The behavior of synemin have been analyzed under standard assembly conditions (**2.1.3**). In order to investigate the differences of the interaction of synemin with desmin on a monomeric or tetrameric state, both proteins were renatured alone or together and analyzed using analaytical ultracentrifugation and rotary shadowing (**2.2.1**). For analyzing the possible interaction of synemin with ULFs formed by type III IF proteins, mutant vimentin Y117L and desminY122L have been used due to the fact that the assembly of vimentinY117L ends on a ULF-like state (**2.2.2**). DesminY122L has the mutation on the comparable position within desmin and is able to form longer filaments but no intact filamenteous network. Finally, the interaction of synemin with wildtype desmin and vimentin under assembly conditions have been analyzed (**2.2.3** and **2.2.4**).

2.1 Characterization of the solubility properties of synemin-L

Synemin is classified as a type IV intermediate filament protein based on protein sequence similarities and co-localization with desmin and vimentin in developing avian myotubes (Granger and Lazarides 1980). Synemin has not been analysed for its *in vitro* characteristics in detail. Therefore, the first section of the results focuses the characterization of synemin based on standard *in vitro* conditions established for type III IF proteins vimentin and desmin.

2.1.1 Recombinant production of human synemin-L

The protein sequences of synemin-M and synemin-H posses a very long tail domain which could interfere with the normal assembly forming process of IF proteins. Hence the smallest splice form of synemin, synemin-L, has been used for the *in vitro* studies. The head and predicted alpha-helical rod domain of the three splice variants are the same and in the case of a hetero-coiled-coil formation with, for example, desmin it is the rod domain that mediates the dimerization according to coiled-coil forming principles .

For protein expression and purification, wild-type cDNA of synemin-L was subcloned into the prokaryotic expression vector pDS5 as described previously (H Herrmann et al. 1999). The clone was expressed in *E.coli* strain TG1 for protein purification. First, an inclusion body preparation was performed to purify the exogenously expressed protein. In all washing steps of the inclusion bodies, some synemin was lost, but the highest amount of protein was found within the final pellet. For further purification, inclusion bodies were dissolved in 9.5 M urea and centrifuged at 35.000 rpm in order to remove bacterial cell wall contaminations (Figure 6). Anionic and cationic exchange chromatography followed by analytical SDS-geles to inspect the purity of the individual fractions was applied (Figure 7). The anionic exchange chromatography was performed using DEAE sepharose, pH 7.5. No synemin-L was found within the samples representing the void volume, flow-through and washing volume. For elution, a continuous gradient of 0 to 0.3 M NaCl in 8 M urea was used. The fractions 36 to 50 were analysed using gel electrophoresis. Based on their amount of purified synemin-L, the fractions 40 to 50 were pooled. A dialysis into 8 M urea, pH 8.4, was performed to remove the NaCl in the pooled sample. For the

following cationic exchange chromatography steps we used CM sepharose, pH 4.0. Again, no synemin-L was found within the void volume, flow-through and washing volume suggesting that the protein bound strongly to the matrix. For elution, a continuous gradient of 0 to 0.5 M NaCl in 8 M urea was used and fractions 32 to 37 were pooled based on their purity and amount of synemin-L.

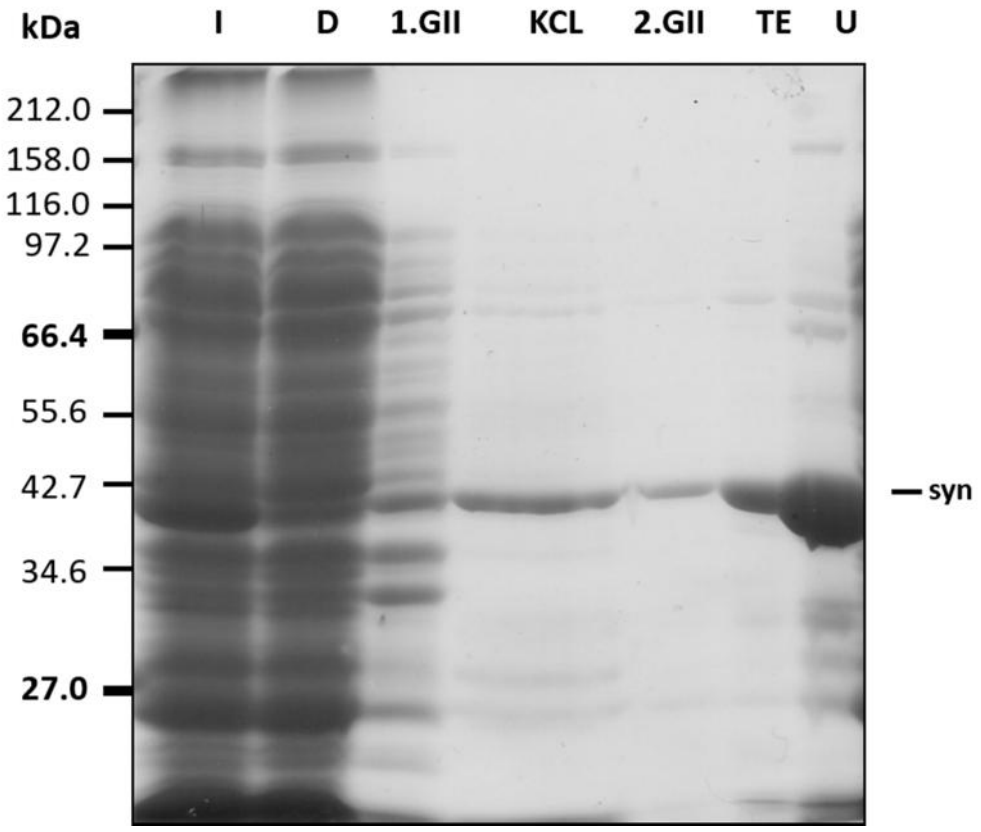

Figure 6: Inclusion body purification of recombinant synemin. I: Input; D: detergent buffer; 1.GII: first washing step with GII buffer; KCL: GII + 1.5 M KCl buffer; 2.GII: second washing step with GII buffer; TE: TE buffer; U: 9.5 M urea buffer.

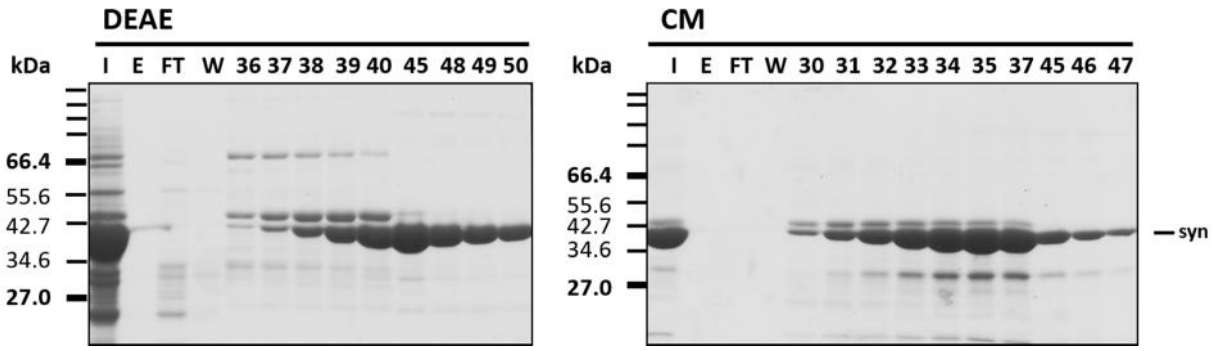

Figure 7: Purification of recombinant human synemin-L using ionic exchange chromatography. Anionic exchange chromatography was performed using DEAE sepharose, pH 7.5 with a 0.3 M gradient of NaCl. For cationic exchange chromatography, CM sepharose, pH 4.0 with a 0.5 M gradient of NaCl was used. (I: input; E: void volume; FT; flow-through; W: washing volume)

The purified protein synemin-L was analyzed for its stability and quality (Figure 8). The quality control in 8 M urea, pH 8.4, unveiled a smaller band at 30 kDa suggesting a former degradation during expression or purification of the protein. But the protein showed no signs of proceeding degradation after 9 days of storage at room temperature in 5 mM Tris-HCl, pH 8.4, representing the absence of proteases in the preparation.

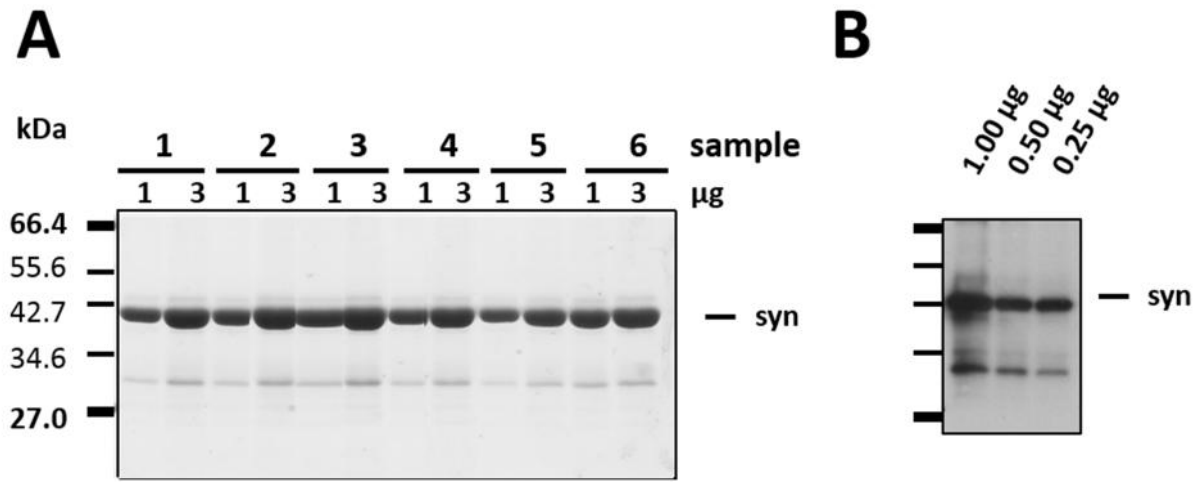

Figure 8: Analysis of purified synemin-L. (A): Time-dependent stability control of synemin. 1 and 3 µg of purifiyed synemin were loaded on a 10% SDS-gel performing a SDS-PAGE. Afterwards, the gel was coomassie®-stained (Sample 1: before renaturation; sample 2: after renaturation; sample 3: one day after renaturation; sample 4: 3 days after renaturation; sample 5: 6 days after renaturation; sample 6: 9 days after renaturation). **(B): Quality control of synemin.** For analyzing degradation, 1 µg, 500 ng and 250 ng were loaded. First antibody: α-synemin antiserum, produced in guinea pigs (1:500). Second antibody: HRP-coupled α-guinea pig (1:5000).

2.1.2 Soluble forms of synemin-L after renaturation into different buffer systems

Under urea-dependent conditions, vimentin and desmin are known to form during renaturation tetramers, the basic unit for *in vitro* IF assembly. A dialysis step of the proteins from 6 M urea into 5 M urea leads to the tetramerization of dimers (Strelkov, Herrmann, and Aebi 2003). For characterization of complexes formed by synemin after renaturation, we chose a set of buffers that have proven to yield functional IF protein complexes in the case of vimentin and desmin. The different buffer systems have been used for analytical ultracentrifugation (Table 2). Besides the established standard renaturation protocols into 5 mM Tris-HCl, pH 8.4, or 2 mM NaPi, pH 7.5, buffers containing 2.5 mM and 5 mM HEPES were tested for reconstitution of the protein. Moreover, to analyse the influence of changes of the pH, synemin has been analysed after step-wise analysis from 8 M urea into 5 mM Tris-HCl, pH 7.5. After dialyzing a purified protein sample into the standard dialysis buffer, 5 mM Tris-HCl, pH 8.4, the protein was centrifuged for 30 minutes at 13.000 rpm.

The soluble structures formed by synemin were analyzed by sedimentation velocity runs using analytical ultracentrifugation and compared to those of vimentin and desmin under the same conditions (Figure 9). Vimentin and desmin are known to form tetramers if dialysed stepwise from 8 M urea into 5 mM Tris-HCl, pH 8.4. The typical *s*-value of vimentin tetramers is 5.1 S, the *s*-value of desmin tetramers 4.8 S. Synemin had an *s*-value of 2.4 S under these conditions and thereby differs from the typical *s*-value of the desmin and vimentin tetramers (Table 2). Synemin's *s*-value of 2.6 S in 2 mM NaPi, pH 7.5 is comparable to the *s*-value in 5 mM Tris-HCl, pH 8.4. As the protein precipitated completely during dialysis, no sedimentation velocity run was performed with synemin dialyzed into 2.5 mM HEPES or 5 mM HEPES. By decreasing the pH of the 5 mM Tris-HCl buffer from pH 8.4 to pH 7.5, the *s*-value of synemin slightly increased from 2.4 S to 2.6 S. Synemin is a monomer based on the small *s*-value obtained in all tested renaturation buffers (Table 2).

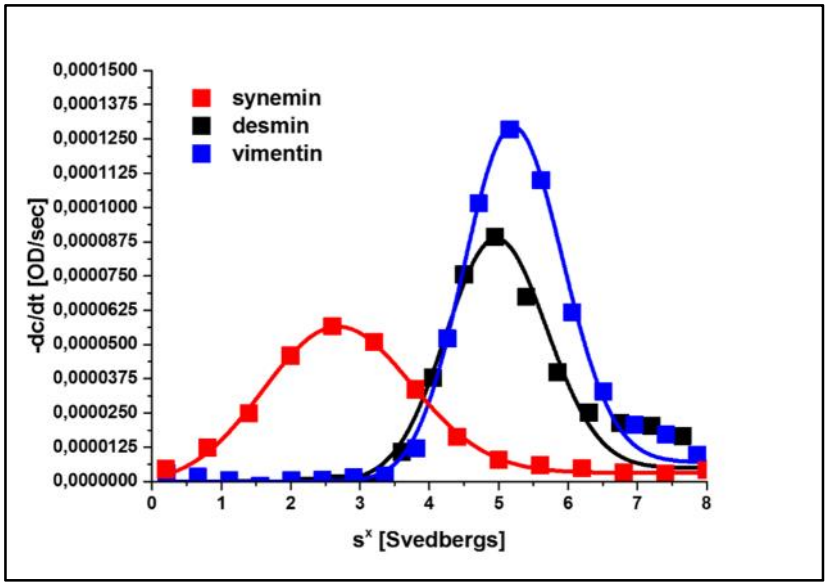

Figure 9: Distribution of the sedimentation coefficients of synemin-L, desmin and vimentin after renaturation from 8 M urea into 5 mM Tris-HCl, pH 8.4. Red line: synemin; black line: desmin; blue line: vimentin. Vimentin and desmin occur as tetramers after renaturaion. Synemin was not able to form dimer or tetramers through renaturation and remained monomeric. The protein concentration of all samples is 0.1 g/l. Centrifugation was performed at 40.000 rpm and 20°C and protein movement was measured at 230 nm.
s* indicates the Svedberg sedimentation coefficient. Data analysis was performed using the software DCDT+.

buffer	protein	S-profile	$s_{20,w}$ [S]*	M_{sed} [kDa]
5 mM Tris-HCl, pH 8.4	synemin	40 - 61	2.4 ± 0.0	47.1 ± 0.7
	vimentin	45 - 66	5.1 ± 0.0	212.0 ± 5.4
	desmin	45 - 66	4.8 ± 0.0	189.4 ± 8.2
5 mM Tris-HCl, pH 7.5	synemin	30 - 59	2.6 ± 0.0	41.4 ± 0.5
2 mM NaPi, pH 7.5	synemin	30 - 59	2.6 ± 0.0	38.4 ± 0.5
2.5 mM HEPES, pH 7.5**	synemin	-	Not determined	-
5 mM HEPES, pH 7.5**	synemin	-	Not determined	-

Table 2: Comparison of the *s*-values of soluble structures formed by synemin-L through renaturation into different buffers. All runs in AUC were performed after step-wise renaturation of samples from 8 M urea into the depicted buffers. Sedimentation was measured at 230 nm and at 40.000 rpm, 20°C. The concentration of all protein samples was 0.1 g/l. The values were rounded to one decimal place.
* Peak value s*(20,w) indicates sedimentation coefficient that has been corrected for the viscosity and density of solvent, relative to that of water at 20°C.
** The samples precipitated during dialysis.

2.1.3 Analysis of structures formed by synemin-L under different *in vitro* assembly conditions.

Due to the fact that the sedimentation characteristics of synemin differ from those of desmin and vimentin in standard renaturation conditions, we initiated a series of solubilisation studies necessary to analyse the influence of ionic strength and buffer conditions on synemin-L. Therefore, different concentrations of Tris-HCl buffer, pH 7.5, were tested.

First, the ionic strength of the Tris-buffer was increased by the addition of NaCl (Table 3). Interestingly, the s-value of synemin was increased through decreasing the pH from 8.4 to 7.5 from 2.4 S as shown previously (Table 2) to 2.6 S. However, by increasing the ionic strength, the *s*-value was increased from 3.0 S in 5 mM Tris, 5 mM NaCl, pH 7.5 to 3.4 S in 5 mM Tris, 50 mM NaCl, pH 7.5 (Table 3). The data indicates a minor role of the ionic strength for the aggregation process of synemin-L in the employed range.

5 mM Tris, pH 7.5	S - profile	$s_{20,w}$ [S]*	c_0 (OD_{230nm})
+ 0 mM NaCl	15 - 34	2.8 ± 0.0	0.29 ± 0.00
+ 5 mM NaCl	15 - 34	3.0 ± 0.0	0.41 ± 0.00
+ 10 mM NaCl	15 - 34	3.1 ± 0.0	0.40 ± 0.00
+ 20 mM NaCl	15 - 34	3.3 ± 0.0	0.39 ± 0.00
+ 30 mM NaCl	15 - 34	3.3 ± 0.0	0.38 ± 0.00
+ 40 mM NaCl	15 - 34	3.4 ± 0.0	0.38 ± 0.00
+ 50 mM NaCl	15 - 34	3.4 ± 0.0	0.38 ± 0.00

Table 3: Comparison of the *s*-values of structures formed by synemin-L in 5 mM Tris-HCl, pH 7.5 with different concentrations of NaCl. All runs in AUC were performed after step-wise renaturation of samples from 8 M urea into the depicted buffers. Sedimentation was measured at 230 nm and at 40.000 rpm, 20°C. The concentration of all protein samples was 0.1 g/l. The *s*-values were rounded to one decimal place and the concentration values were rounded to two decimal places.
* Peak value s*(20,w) indicates sedimentation coefficient that has been corrected for the viscosity and density of solvent, relative to that of water at 20°C.

In another experimental series, the concentration of Tris-buffer was increased up to 25 mM. In addition, the concentration of NaCl was increased (Table 4). Under these conditions, synemin-L started to aggregate. In 25 mM Tris-HCl, pH 7.5, two *s*-values, one at 3.7 S and the other at 10.7 S, occured. These *s*-values were increased up to 6.5 S and 29.3 S by increasing the ionic strength in 25 mM Tris-HCl, 40 mM NaCl, pH

7.5 (Table 4). Interestingly, the higher *s*-value was four times higher than the smaller *s*-value suggesting an ordered aggregation process. In order to analyse the influence of the Tris buffer on the aggregation process, different concentrations were used ranging from 10 mM Tris-HCl, pH 7.5 to 50 mM Tris-HCl, pH 7.5 (Table 4). While in 10 mM Tris, pH 7.5, only one *s*-value of 3.0 was obtained, the increasing of the ionic strength to 30 mM Tris-HCl, pH 7.5, led to 3 different *s*-values: 3.3 S, 13.3 S and 27.0 S. This altered behaviour might illustrate an aggregation process of synemin-L (Table 4).

Once again, the second *s*-value is four times higher than the first. The third *s*-value is two times higher than the second *s*-value. Further increase of the ionic strength to 50 mM Tris-HCl, pH 7.5 led to an increase of the three *s*-values to 13.4 S, 27.8 S and 39.9 S. The first and the second *s*-value observed in the experiment employing 50 mM Tris-HCl, pH 7.5, are comparable with the second and third *s*-value of synemin-L in 30 mM Tris-HCl, pH 7.5. The concentration of Tris-HCl has a higher impact on the assembly process of synemin than the concentration of NaCl. An increase of both variables increased the effect of aggregation by changing a three-step process into a two-step process.

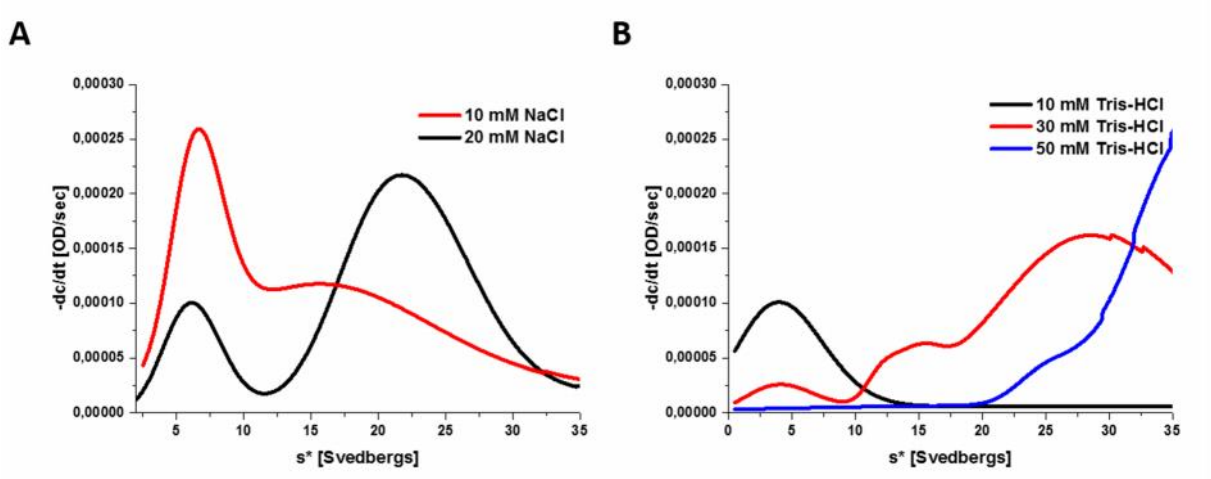

Figure 10: Influence of the ionic strength and the buffer conditions on the aggregation process of synemin-L (A) comparison of the contribution of the sedimentation coefficients of synemin-L in 25 mM Tris, 10 mM NaCl, pH 7.5 and 25 mM Tris, 20 mM NaCl, pH 7.5. Centrifugation was performed at 30.000 rpm and at 20°C. **(B) comparison of the contribution of the sedimentation coefficients of synemin-L in 10 mM Tris-HCl, pH 7.5, 30 mM Tris-HCl, pH 7.5, and 50 mM Tris-HCl, pH 7.5.** Centrifugation was performed at 40.000 rpm and at 20°C. s* indicates sedimentation coefficient. Data analysis was performed using the software DCDT+.

buffer	S - profile	$s_{20,w}$ [S]*	c_0 (OD_{230nm})	speed [k rpm]
A: 25 mM Tris-HCl, pH 7.5				
+ 0 mM NaCl	2 - 5	3.7 ± 0.1 10.7 ± 0.7	0.09 ± 0.00 0.12 ± 0.01	30
+ 10 mM NaCl	2 - 5	4.9 ± 0.1 21.0 ± 0.3	0.17 ± 0.00 0.05 ± 0.00	30
+ 20 mM NaCl	2 - 5	4.6 ± 0.1 19.1 ± 0.3	0.13 ± 0.00 0.09 ± 0.00	30
+ 30 mM NaCl	2 - 5	5.8 ± 0.2 19.6 ± 0.4	0.11 ± 0.00 0.06 ± 0.00	30
+ 40 mM NaCl	2 - 5	6.5 ± 0.1 27.4 ± 0.2	0.07 ± 0.00 0.08 ± 0.00	30
B: increasing Tris-HCl, pH 7.5				
10 mM Tris-HCl	8 - 17	3.0 ± 0.1	0.56 ± 0.03	40
30 mM Tris-HCl	8 - 17	3.3 ± 0.2 13.3 ± 0.1 27.0 ± 0.1	0.11 ± 0.01 0.04 ± 0.00 0.27 ± 0.00	40
50 mM Tris-HCl	8 - 17	13.4 ± 0.3 27.8 ± 0.2 39.9 ± 0.1	0.01 ± 0.00 0.13 ± 0.00 0.15 ± 0.01	40

Table 4 Comparison of the *s*-values of structures formed by synemin-L in 25 mM Tris-HCl, pH 7.5 with different concentrations of NaCl and the *s*-values of structures formed by synemin-L in different Tris-buffers, pH 7.5. All runs in AUC were performed after step-wise renaturation of samples from 8 M urea into the depicted buffers. Sedimentation was measured at 230 nm and 20°C. The concentration of all protein samples was 0.1 g/l. The *s*-values were rounded to one decimal place and the concentration values were rounded to two decimal places.
* Peak value s*(20,w) indicates sedimentation coefficient that has been corrected for the viscosity and density of solvent, relative to that of water at 20°C.

We analyzed the structures formed by synemin-L under different assembly conditions established for *in vitro* assembly of vimentin and desmin (Table 5). Again, distinct *s*-values were measured. The *s*-value of synemin-L (25.1 S) in 25 mM Tris-HCl, 50 mM NaCl, pH 7.5 was similar to the *s*-value in 2 mM NaPi, 100 mM KCl, pH 7.5, with 26.7 S. By increasing the ionic strength to 100 mM NaCl within the buffer containing 25 mM Tris-HCl, pH 7.5, the *s*-value was shifted to 75.9 indicating that bigger structures were formed by synemin-L alone. This effect was repeated by further increasing the concentration of NaCl to 160 mM NaCl, where the *s*-value accounted 94.5 S. These distinct *s*-values suggest ordered aggregates depending on ionic strength.

buffer	S - profile	$s_{20,w}$ [S]*	c_0 (OD_{230nm})
25 mM Tris-HCl, 50 mM NaCl	2 - 5	25.1 ± 2.7	0.43 ± 0.05
25 mM Tris-HCl, 100 mM NaCl	2 - 5	75.9 ± 0.7	0.26 ± 0.00
25 mM Tris-HCl, 160 mM NaCl	2 - 5	94.5 ± 1.2	0.21 ± 0.01
2 mM NaPi, 100 mM KCl	2 - 5	26.7 ± 0.0	0.34 ± 0.00

Table 5 Comparison of the s-values of structures formed by synemin-L in different assembly buffers. All runs in AUC were performed after step-wise renaturation of samples from 8 M urea into the depicted buffers. Sedimentation was measured at 230 nm and at 25.000 rpm, 20°C. The concentration of all protein samples was 0.1 g/l. The *s*-values were rounded to one decimal place and the concentration values were rounded to two decimal places.
* Peak value s*(20,w) indicates sedimentation coefficient that has been corrected for the viscosity and density of solvent, relative to that of water at 20°C.

To visualize the aggregates formed by synemin under different assembly conditions, we fixed them directly in solution and then processed them for electron microscopy. Synemin is not able to form filaments on its own under the different tested buffer conditions. Instead, it forms short proto-filamentous structures under low salt conditions and globular structures under higher salt conditions (Figure 11).

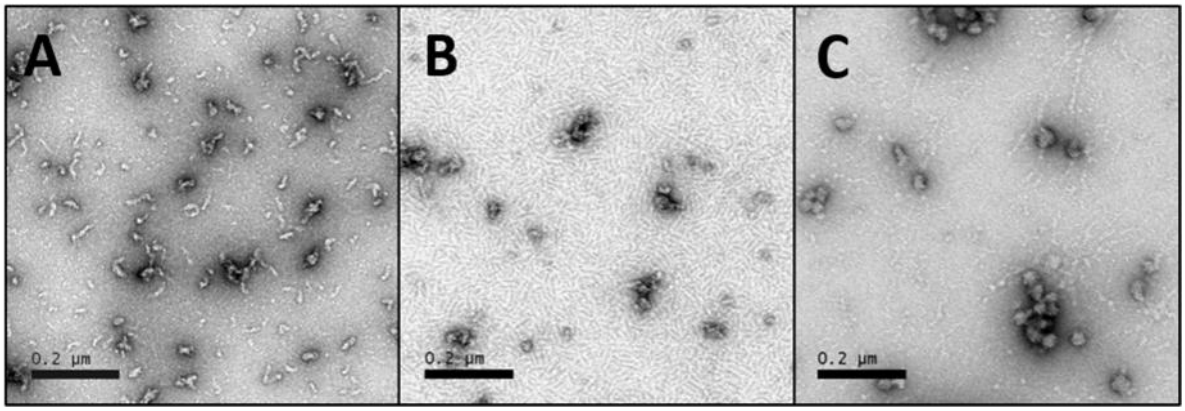

Figure 11: Electron micrographs of negatively stained samples of synemin-L assembled in three different assembly buffers. Assembly was performed at 37°C by addition of an equal amount of "assembly buffer" and stopped by adding 0.1% glutaraldehyde at 1 hour. **(A):** In 25 mM Tris-HCl, 50 mM NaCl, pH 7.5, short protofilamentous structures were seen. **(B):** In 25 mM Tris-HCl, 100 mM NaCl, pH 7.5, the protein structures were globularly. **(C):** In 25 mM Tris-HCl, 160 mM NaCl, pH 7.5, the globular structures had a bigger diameter. Scale bar: 200 nm.

The standard sedimentation assay with 15 minutes at 30 psi was designed to find a filament network formed by desmin after 1 hour of assembly in 25 mM Tris-HCl, 50 mM NaCl, pH 7.5, only within the pellet fraction. For these assembly and centrifugation conditions, synemin mainly remained soluble displaying rather smaller structures than a filamentous network like in the case of desmin (Figure 12). This small structures were visualized by electron microscopy as mentioned above (Figure 11). To characterize possible interactions of synemin with other proteins, a protocol for sucrose gradient centrifugation was established and used for all sucrose gradient centrifugations in this thesis. After 5 hours of centrifugation at 28.000 rpm, 4°C, a clear differentiation of small soluble structures and filamentous proteins as well as a differentiation of interacting and non-interacting partners for synemin is possible. In the standard sucrose gradient centrifugation (see Figure 12-B), synemin-L assembled for 1 hour in 25 mM Tris-HCl, 50 mM NaCl, pH 7.5, was located between the supernatant and the fifth fraction with a peak in fraction number 2.

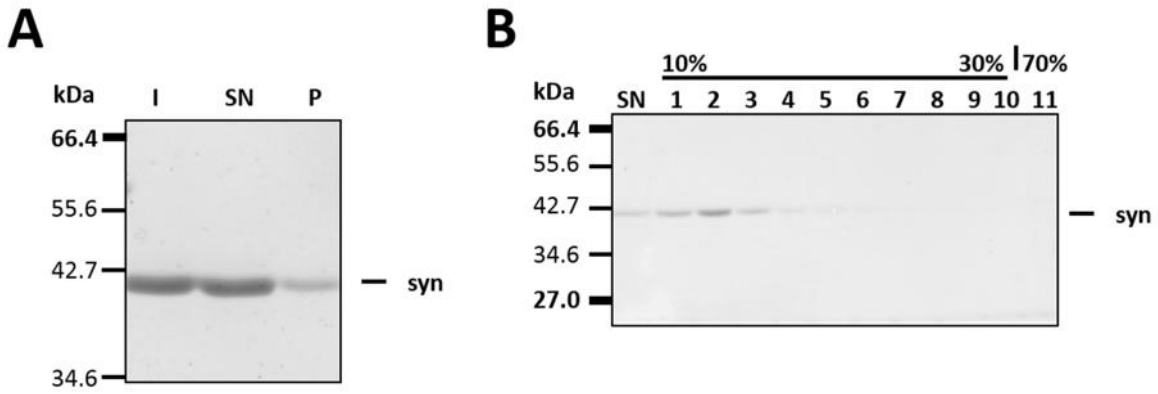

Figure 12: (A): Sedimentation analysis of synemin-L assembled for 1 hour. After one hour of assembly, synemin-L was mainly found within the supernatant corresponding to smaller structures formed by synemin-L alone. The protein was dialyzed into 5 mM Tris-HCl, pH 8.4 and assembly was performed in 25 mM Tris-HCl, 50 mM NaCl, pH 7.5. After assembly, the sample was centrifuged at 30 psi for 15 minutes. An aliquot of each fraction was loaded on a 10% gel and separated by gel electrophoresis (I: input; SN: supernatant; P: pellet). **(B): Sucrose gradient analysis of synemin-L assembled for 60 min at 37°C.** Aggregated Synemin-L occured within the supernatant and faction 1 to 5 with a peak in fraction 2. The protein was dialyzed into 5 mM Tris-HCl, pH 8.4 and assembly was started through increasing the buffer conditions to 25 mM Tris-HCl, 50 mM NaCl, pH 7.5. After assembly, the sample was centrifuged at 28.000 rpm, 4°C for 5 hours. The fractions are shown after separation by gel electrophoresis. (SN: supernatant; Fractions 1 – 10: 10 – 30 % sucrose gradient; 11: 70 % sucrose cushion, syn: synemin-L.)

2.2 Interaction of synemin-L with desmin in renaturation and assembly conditions

The interaction of synemin with desmin and vimentin has not been analysed systematically with respect to the impact of synemin on the renaturation and assembly of desmin and vimentin. In the following section, the data obtained from the *in vitro* analysis are presented.

2.2.1 Characterization of the soluble structures formed by desmin and synemin-L

As previously shown, synemin is unable to form homodimers or homotetramers through standard renaturation. Because most type III and type IV IF proteins are able to form hetero-dimers and hetero-tetramers, the next step was to analyse if synemin is able to interact with desmin through renaturation to tetramers. Therefore, the proteins were mixed before or after renaturation from 8 M urea into 5 mM Tris-HCl, pH 8.4. After dialysis, the buffer conditions were changed to 10 mM Tris-HCl, pH 7.5 to extend the possible s-values of both proteins in sedimentation velocity runs. In 10 mM Tris-HCl, pH 7.5, synemin has a distinct *s*-value of 2.8 S, while desmin has an *s*-value of 9.1 S. When the proteins were renatured together into 10 mM Tris-HCl, pH 7.5, two distinct *s*-values occured. One *s*-value appear at 3.5 S and the other at 12.9 S. This change in *s*-values corresponding to the *s*-values of the single proteins represents an interaction of the proteins mixed before renaturation. The sample mixed after renaturation, but before changing the buffer condition up to 10 mM Tris-HCl, pH 7.5, has two *s*- values at 2.4 and 6.2 S comparable to the *s*-value of synemin in 5 mM Tris-HCl, pH 8.4 (Table 2) and a second *s*-value between the s-value of desmin in 5 mM Tris-HCl, pH 8.4 (Table 2) and desmin in 10 mM Tris-HCl, pH 7.5. This data suggests that synemin is able to interact with desmin during dialysis to create two new species. Moreover, synemin is able to hold tetrameric desmin to some extend back from forming higher structures.

buffer	protein	S-profile	$s_{20,w}$ [S][a]
10 mM Tris-HCl, pH 7.5	synemin	8 - 19	2.8 ± 0.0
	desmin	8 - 19	9.1 ± 0.0
	mixed before renaturation	8 - 19	3.5 ± 0.1 12.9 ± 0.1
	mixed after renaturation	8 - 19	2.4 ± 0.0 6.2 ± 0.0

Table 6: Sedimentation coefficient of synemin-L and desmin in 10 mM Tris-HCl, pH 7.5.
* Peak value s*(20,w) indicates sedimentation coefficient that has been corrected for the viscosity and density of solvent, relative to that of water at 20°C. The sedimentation of proteins was measured at 230 nm and at 40.000 rpm, 20°C. The concentration of the mixed protein samples was 0.2 g/l and for the single protein samples 0.1 g/L. All runs in AUC were performed after step-wise renaturation of samples from 8 M urea into 5 mM Tris-HCl, pH 8.4 followed by changing the buffer conditions to 10 mM Tris-HCl, pH 7.5. The *s*-values were rounded to one decimal place.

2.2.2 The interaction of synemin-L with ULF-like structures formed by mutant desminY122L or vimentinY117L

In order to investigate the interaction of synemin-L with desmin and vimentin on a ULF-like state of assembly, the mutant proteins vimentinY117L and desminY122L were used. VimentinY117L is not able to form filaments under assembly conditions but ULFs with a length of ~ 60 nm and sharpened ends (Figure 13). Therefore, vimentinY117L is a good candidate to analyse the interaction of synemin with vimentin on a ULF-like stage of assembly. Interestingly, the equivalent mutant desmin did not form a filament network, yet longer filaments than ULFs (Figure 13). When vimentinY117L was mixed with synemin before assembly start and the proteins were assembled together for one hour at 37°C, some ULFs stayed unchanged, but about 50% of the visualized proteins appeared as roundish protein aggregates with a diameter of ~ 40 nm.

Following the same treatment, the effect of synemin on desminY122L was a different one. The assembly disturbing effect of synemin-L is more dominant as no ULFs formed by desminY122L were detectable among the protein aggregates with a diameter of ~ 40 nm. The centrifugation assay with the airfuge showed that synemin-L has an effect on the sedimentation behaviour of vimentinY117L (Figure 14). While ULF-like structures formed by vimentinY117L were found both in the supernatant and the pellet, structures formed by synemin-L and vimentinY117L accumulate mainly in the pellet fraction indicating a strong interaction of synemin-L and vimentinY117L. The sedimentation behaviour of desminY122L remained the same. Interestingly, synemin-L was also found in the pellet.

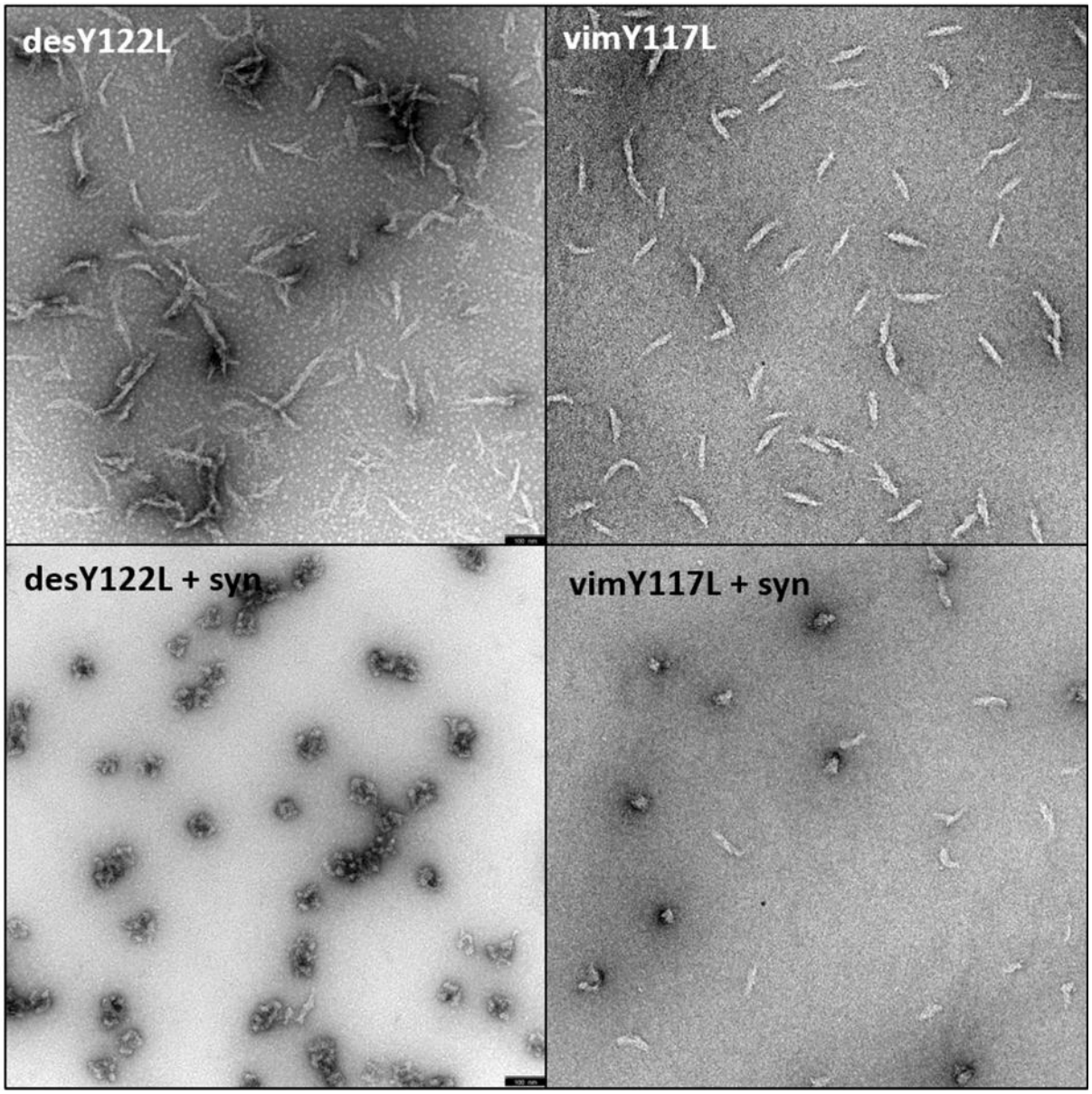

Figure 13: Analysis of negatively stained assembly products of mutant desminY122L and vimentinY117L assembled in the presence of synemin. Synemin had a negative effect on the ULF-forming process of vimentinY117L and the short filament-forming process of desminY122L. The protein concentration of all samples was 0.1 g/l. Assembly was performed in 25 mM Tris-HCl, 50 mM NaCl, pH 7.5, at 37°C for 1 hour. Assembly was stopped at 60 min by addition of 0.1 % glutaraldehyde. (desY122L: desminY122L; vimY117L: vimentinY117L; syn: synemin-L) Bar, 100 nm

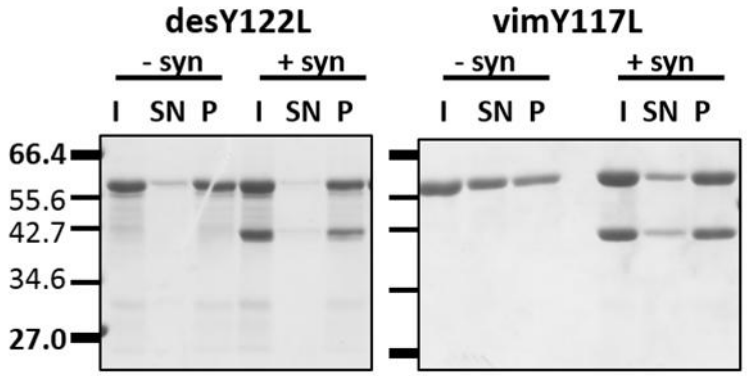

Figure 14: Sedimentation analysis of desminY122L and vimentinY117L assembled in absence and presence of synemin-L. Left panel: In the presence of desminY122L, synemin-L changed its sedimentation behaviour and was found within the pellet fraction together with desminY122L after centrifugation. **Right panel:** VimentinY117L remained like synemin-L mainly in the supernatant, when the protein was assembled alone. The complexes formed by vimentinY117L and synemin-L were mainly found within the pellet instead of the supernatant after centrifugation. The proteins were dialyzed into 5 mM Tris-HCl, pH 8.4 and assembly was started through increasing the buffer conditions to 25 mM Tris-HCl, 50 mM NaCl, pH 7.5. After assembly, the samples were centrifuged at 30 psi for 15 minutes. The occurring fractions were separated by gel electrophoresis. (I: input; SN: supernatant; P: pellet; desY122L: desminY122L; vimY117L: vimentinY117L; syn: synemin-L).

Based on this results, sedimentation velocity runs were performed to determine the sedimentation coefficients of the assembled mutant desminY122L and vimentinY117L mixed with synemin-L at different stages of assembly (Table 7). DesminY122L had an *s*-value of 138.6 S centrifuged after one hour of assembly in 25 mM Tris, 50 mM NaCl, pH 7.5. This might represent the longer filaments visualized with electron microscope. To characterize the interaction of desminY122L with synemin-L, the proteins were mixed before or after renaturation into 5 mM Tris-HCl, pH 8.4. In the following co-assembly situation, one distinct *s*-value occured at 97.9 S in case of the sample mixed before renaturation and at 95.4 S for the sample mixed after renaturation. In both cases, the *s*-value of the mix was smaller than the *s*-value of pure desminY122L but bigger than the *s*-value of assembled synemin protofilamenteous structures.

These data suggests a strong interaction of synemin with desminY122L and is supported by the negatively stained globular structures. In case of vimentinY117L, another phenomenon occured as the ULF-like structures had a distinct *s*-value at 33.4 S. However, when the protein was mixed with synemin-L after renaturation, the sedimentation behaviour of both proteins had changed completely. The single *s*-value was increased up to 54.4 with a shoulder on the right side suggesting larger structures around 110.0 S (Figure 15). Moreover, in the case for vimentinY117L

mixed with synemin-L after one hour of individual assembly and the proteins assembled together for an additional hour, the *s*-value is 54.0. These data suggest that the interaction of synemin with mutant desmin and vimentin is very strong and leads to protein aggregates of distinct size that are independent to the time point of addition of synemin.

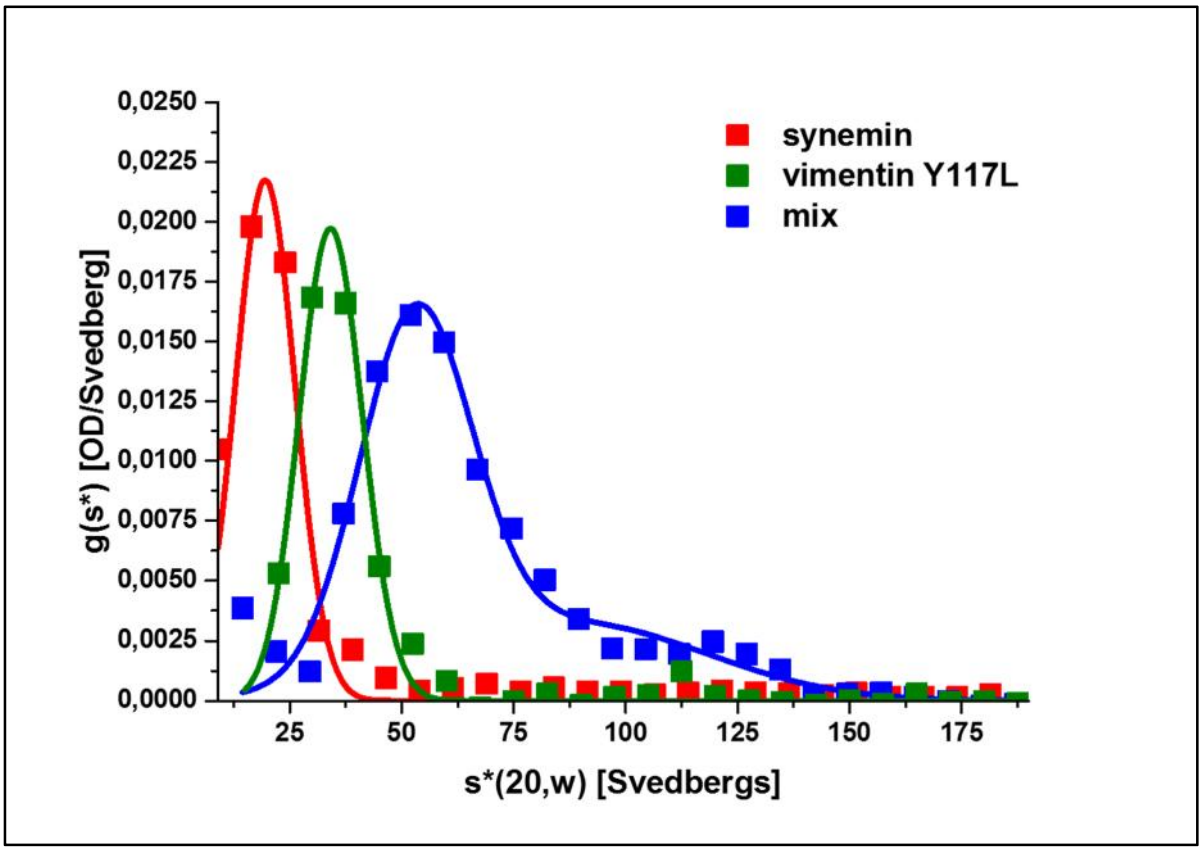

Figure 15: Contribution of the sedimentation coefficients of assembled vimentinY117L and synemin-L. ULFs formed by vimentinY117L in 25 mM Tris-HCl, 50 mM NaCl, pH 7.5, have a distinct *s*-value of 33.4 S. The aggregates formed by synemin-L have an s-value around 20.5 S. When both proteins were co-assembled, a single *s*-value of 54.4 occurred suggesting a strong interaction of the proteins under assembly conditions. Blue line: co-assembly of mutant vimentinY117L and synemin mixed after dialysis. Green line: assembly of vimentinY117L. red line: assembly of synemin-L. All runs in AUC were performed after 1 hour of assembly in 25 mM Tris-HCl, 50 mM NaCl, pH 7.5. Sedimentation was measured at 230 nm and at 40.000 rpm, 20°C. The concentration of all protein samples was 0.1 g/l. s* indicates sedimentation coefficient. Data analysis was performed using the software DCDT+.

protein	S-profile	$s_{20,w}$ [S][a]
desY122L	1 - 4	138.6 ± 1.2
mixed before renaturation	2 - 5	97.9 ± 0.6
Mixed after renaturation	1 - 4	95.4 ± 0.5
protein	**S-profile**	$s_{20,w}$ [S][a]
vimY117L	9 - 12	33.4 ± 0.1
mixed after renaturation	9 - 12	54.4 ± 0.3
mixed after 1 hour of assembly	9 - 12	54.0 ± 0.1
syn	9 - 12	20.5 ± 0.1

Table 7: Comparison of the sedimentation coefficients of assembled desminY122L and vimentinY117L mixed with synemin-L at different stages of assembly. The assembly was performed at 37°C, in 25 mM Tris-HCl, 50 mM NaCl, pH 7.5, for 1 hour. The sedimentation of proteins was measured at 230 nm and at 20°C with 20.000 rpm. The concentration of the mixed protein samples was 0.2 g/l and for the single protein samples 0.1 g/L. The *s*-values were rounded to one decimal place.
* Peak value s*(20,w) indicates sedimentation coefficient that has been corrected for the viscosity and density of solvent, relative to that of water at 20°C.

In addition to the sedimentation velocity runs, sucrose gradient centrifugation was performed to furthermore investigate the interaction of synemin-L with vimentinY117L and desminY122L (Figure 16). DesminY122L assembled alone was mainly found within fraction 11 representing the 70% sucrose cushion. Through co-incubation with synemin-L, the protein did change its sedimentation behaviour as it was found together with synemin-L within fraction 6 to 11 with a peak within fractions 10 and 11. VimentinY117L did change its sedimentation behaviour, too. VimentinY117L assembled alone could be found within fraction 3 to 8 with a peak within fraction 5. The mix of vimentinY117L with synemin-L did result in a changed sedimentation profile of both proteins within fraction 4 – 10 with a peak in fractions 6 to 8. These results confirm the outcome of analytical ultracentrifugation, i.e. the decrease of the *s*-value of desminY122L and the increase of vimentin's *s*-value in presence of synemin-L.

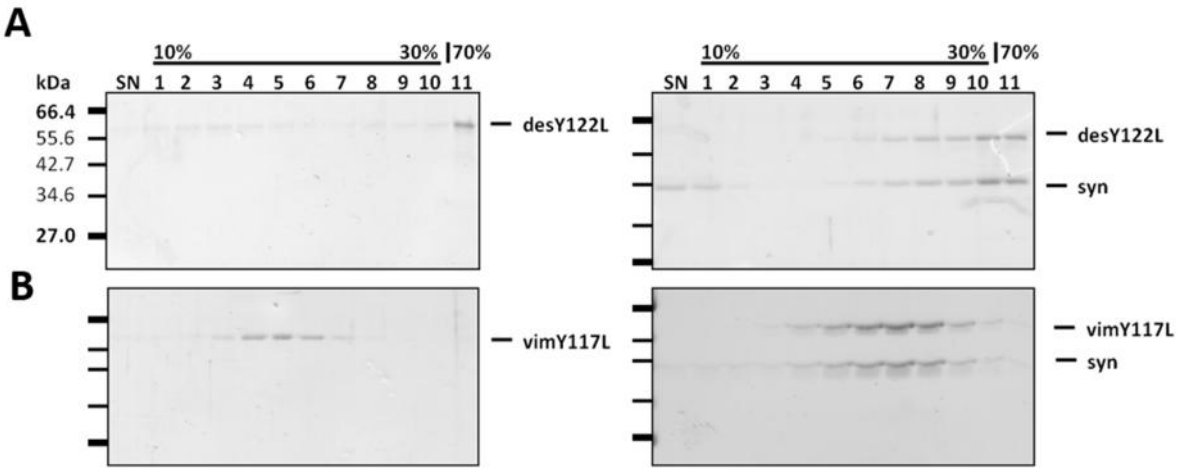

Figure 16: Sucrose gradient analysis of mutant desminY122L and vimentinY117L assembled in the absence or presence of synemin-L. (A): DesY122L assembled in the absence or presence of syn. **(B):** VimY117L assembled in the absence or presence of syn. The proteins were dialyzed into 5 mM Tris-HCl, pH 8.4 and assembly was started through increasing the buffer conditions to 25 mM Tris-HCl, 50 mM NaCl, pH 7.5. After assembly, the samples were centrifuged at 28.000 rpm, 4°C for 5 hours. The fractions are shown after separation by gel electrophoresis. (SN: supernatant; Fractions 1 – 10: 10 – 30 % sucrose gradient; 11: 70 % sucrose cushion; DesY122L: desminY122L; VimY117L: vimentinY117L; syn: synemin-L)

2.2.3 Analysis of assembled desmin and vimentin in the presence of synemin

The interaction shown for synemin-L with ULF-like structures formed by vimentinY117L under assembly conditions predicted an ordered association of synemin with vimentin and desmin under assembly conditions. In order to analyse the influence of synemin-L on the reconstitution and assembly process of wildtype desmin and vimentin, different approaches were used. Desmin formed an intact filamentous network after one hour of assembly in 25 mM Tris-HCl, pH 7.5 (Figure 17). Synemin was added to desmin before renaturation in order to analyse its influence on the assembly process of desmin (Table 6). In another aproach, synemin and tetrameric desmin were mixed after dialysis and co-assembled for one hour.

Figure 17 (Next page): Electron micrographs of negatively stained samples of wildtype desmin mixed with synemin-L at different stages of renaturation and assembly. (A): Assembly of desmin without synemin-L for 1 hour revealed a filamentous network. **(B):** 1 hour of co-assembly of synemin-L and desmin mixed in 8 M urea, pH 8.4, and reconstituted together into 5 mM Tris-HCl, pH 8.4. **(C):** synemin-L mixed with tetrameric desmin after renaturation into 5 mM Tris-HCl, pH 8.4, followed by 1 hour of co-assembly **(D):** Addition of synemin to desmin pre-assembled for 10 seconds and co-assembly for 1 hour in total **(E):** Desmin mixed with synemin 10 minutes after assembly start**. (F)** Addition of synemin to desmin pre-assembled for one hour. All proteins were co-assembled for an additional hour. In all cases of co-assembly of desmin and synemin, shorter filaments with globular protein aggregates at their end and connection points were visible. Assembly was performed at 37°C in 25 mM Tris-HCl, 50 mM NaCl, pH 7.5, and stopped by adding 0.1% glutaraldehyde after 1 hour. Scale bar: 200 nm.

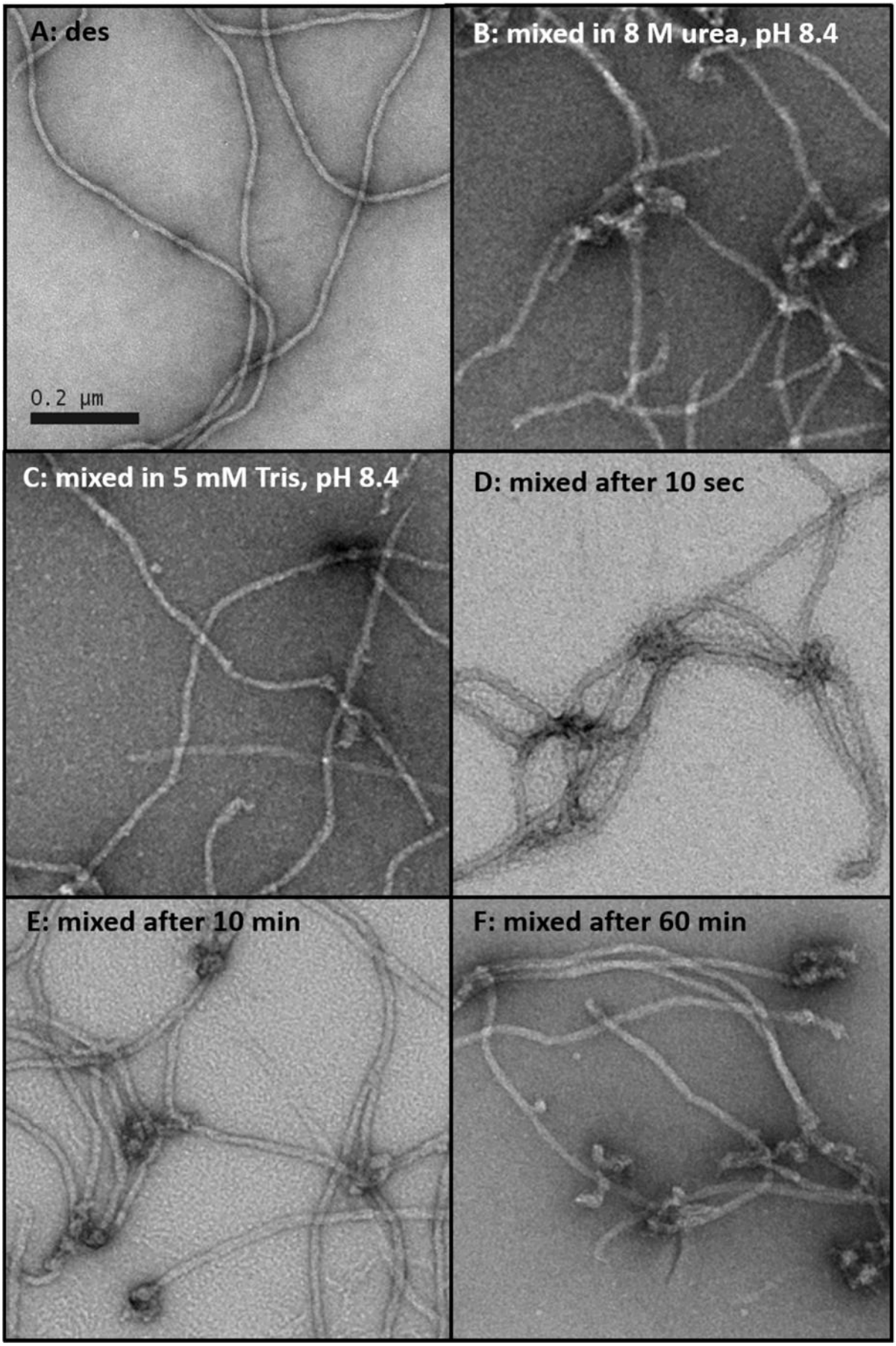
A: des
0.2 µm
B: mixed in 8 M urea, pH 8.4
C: mixed in 5 mM Tris, pH 8.4
D: mixed after 10 sec
E: mixed after 10 min
F: mixed after 60 min

In order to investigate the possible interaction of synemin with pre-assembled desmin, desmin was assembled within different time frames before addition of synemin. Compared to the assembly structure of wildtype desmin, the filaments formed in the presence of synemin were shorter. Often globular structures were found at the ends of filaments as well as at filament “cross over” indicating a stop of the filament forming process through the addition of synemin.

The effect of synemin on the assembly process of vimentin was stronger than its effect on the assembly process of desmin (Figure 18). While vimentin alone formed filament networks within one hour of assembly, it was unable to form filaments in the presence of synemin-L, no matter if vimentin was mixed with synemin-L before and after renaturation. This data suggested a strong negative impact of synemin on the assembly process of vimentin. Moreover, the addition of synemin-L to vimentin pre-assembled for distinct time points led to the decoration of filaments with globular protein aggregates at their ends and connection points. The strong assembly-negative effect of synemin on vimentin and the globular structures found along with the desmin filaments suggest that synemin is not capable to be integrated in the complete intermediate filament network like other type IV IF proteins. Desmin seemed to be able to escape the negative effect of synemin to some extent. This might be based on the assembly kinetics of desmin which are five times higher than those of vimentin.

Figure 18 (next page): Electron micrographs of negatively stained samples of wildtype vimentin mixed with synemin-L at different stages of renaturation and assembly. (A): Assembly of vimentin without synemin-L for 1 hour revealed a filamentous network. **(B):** 1 hour of co-assembly of synemin-L and vimentin mixed in 8 M urea, pH 8.4, and reconstituted together into 5 mM Tris-HCl, pH 8.4. Only protein aggregates were visible. **(C):** When synemin-L and vimentin were mixed after renaturation into 5 mM Tris-HCl, pH 8.4, and co-assembled together, protein aggregates but no filaments were visible. **(D):** When vimentin and synemin were mixed 10 seconds after assembly start and assembled for 1 hour in total, the filaments were shorter and disrupted by globular structures. **(E):** The same was true for vimentin mixed with synemin 10 minutes after assembly start**. (F)** In these case, synemin-L was mixed with vimentin after one hour of assembly followed by an additional hour of co-assembly. Again, the filaments were shorter and packed with protein aggregates. Assembly was performed at 37°C in 25 mM Tris-HCl, 50 mM NaCl, pH 7.5, and stopped by adding 0.1% glutaraldehyde at 1 hour. Scale bar: 200 nm.

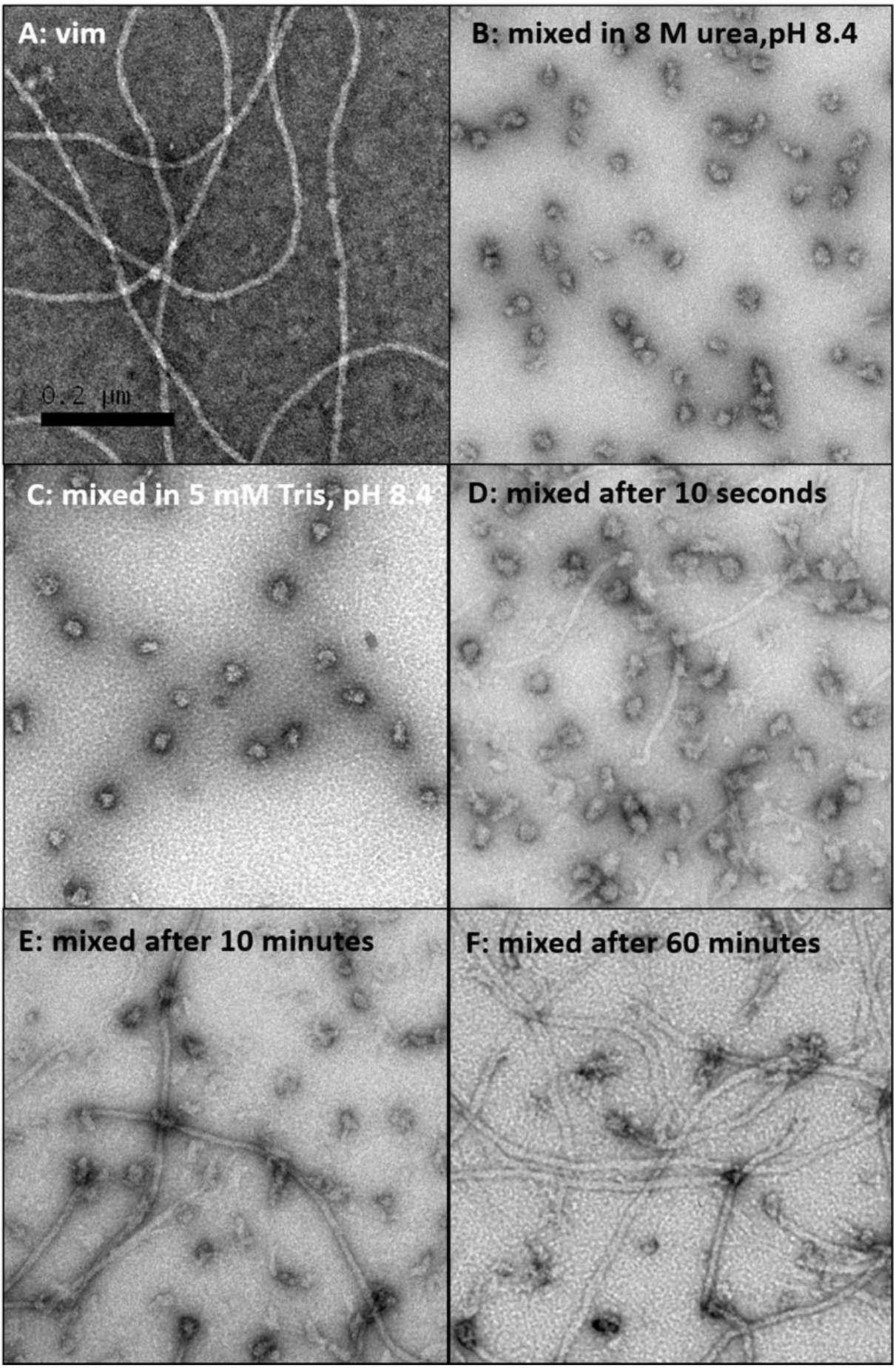
A: vim
0.2 µm
B: mixed in 8 M urea,pH 8.4
C: mixed in 5 mM Tris, pH 8.4
D: mixed after 10 seconds
E: mixed after 10 minutes
F: mixed after 60 minutes

The standard sedimentation assay with the airfuge is calculated with 15 minutes at 30 psi for desmin to be completely sedimentated after one hour of assembly (Figure 19). The change in sedimentation of synemin-L in the standard co-assembly shows the strong interaction of synemin with desmin, when the proteins were mixed after dialysis and co-assembled for 1 hour. Using the standard centrifugation conditions, the assembled network of vimentin did not sedimentate completely, but was primarily found in the pellet. When synemin was mixed with vimentin, synemin changed its sedimentation characteristics too, although it was not found completely in the pellet like in case of the mix with desmin. More vimentin stayed soluble in the supernatant when it was mixed with synemin and co-assembled for 1 hour.

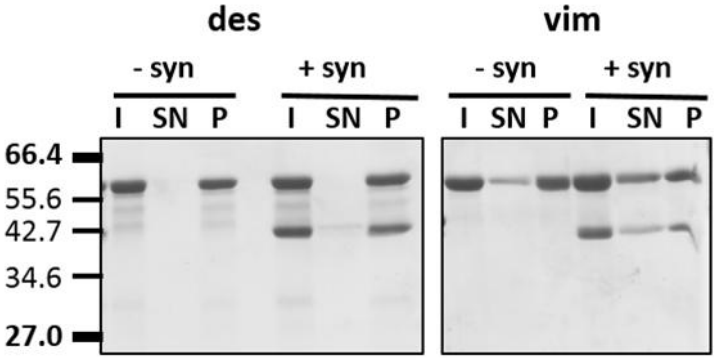

Figure 19: Sedimentation analysis of wildtype desmin and vimentin assembled in the presence of synemin. Synemin-L changed its sedimentation behaviour through mixing with desmin and vimentin and was mainly found within the pellet fraction after 1 hour of assembly. Vimentin have changed its sedimentation behaviour through the mix with synemin-L, too, because more protein remained soluble. The proteins were dialyzed into 5 mM Tris-HCl, pH 8.4 and assembly performed at 37°C in 25 mM Tris-HCl, 50 mM NaCl, pH 7.5, for hour. After assembly, the samples were centrifuged at 30 psi for 15 minutes. The fractions are shown after separation by gel electrophoresis. (I: input; SN: supernatant; P: pellet; des: desmin; vim: vimentin; syn: synemin-L).

For further analysis of the sedimentation behaviour of desmin and vimentin assembled in the presence of synemin, sucrose gradient centrifugations using the established standard protocol have been performed. Desmin assembled alone in 25 mM Tris-HCl, 50 mM NaCl, pH 7.5, was found to be 100% in the 70% sucrose cushion while assembled vimentin had a peak in fraction number 1 to 2 (Figure 20). A shift of the sedimentation profile of the co-assembled vimentin and synemin to fraction 4 to 7 with a peak in fraction 5 occured. Surprisingly, the small globular structures visualized with the electron microscope were found in fractions

corresponding to higher amount of sucrose than the IF network formed by vimentin alone. Moreover, the sucrose gradient centrifugation indicated a strong interaction between synemin-L and desmin as synemin was found after 1 hour of co-assembly within fraction 9 to 11 including a peak in fraction 11. Differences were observed in the sedimentation behaviour of proteins in the sedimentation analysis and the sucrose gradient centrifugation. These differences suggested an influence of the sucrose on the sedimentation behaviour of different IF proteins.

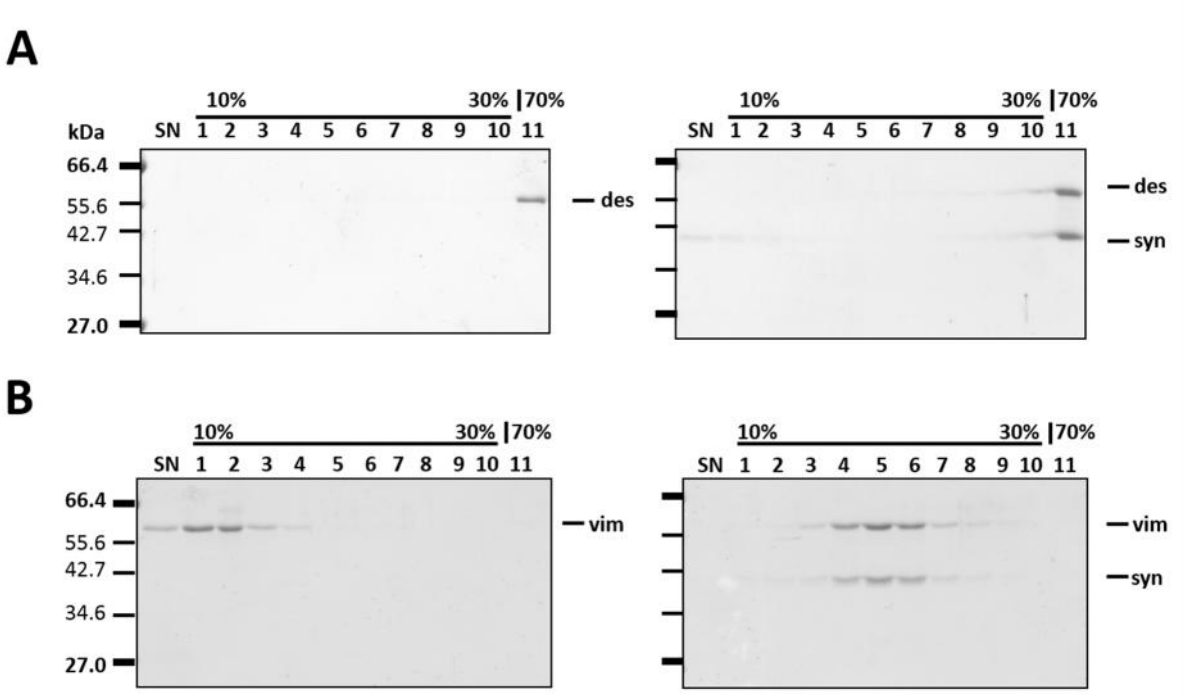

Figure 20: Sucrose gradient analysis of assembled desmin and vimentin in the presence of synemin. (A): Assembly of desmin in absence and presence of synemin-L. Desmin was found within fraction 11 after 1 hour of assembly. In case of the mix of synemin-L with desmin, synemin-L was found within fraction 11 together with desmin **(B): Assembly of vimentin in absence and presence of synemin.** Vimentin was found within the supernatant and fraction 1 to 4 with a peak in fractions 1 and 2. The mix of vimentin with synemin-L did result in a shift of the sedimentation profile of both proteins to the fractions 3 to 7 with a peak between fractions 4 to 6. The protein samples were dialyzed into 5 mM Tris-HCl, pH 8.4 and assembly was started through increasing the buffer to 25 mM Tris-HCl, 50 mM NaCl, pH 7.5. After assembly of 1 hour, the samples were centrifuged at 28.000 rpm, 4°C for 5 hours. The fractions are shown after separation by gel electrophoresis. (SN: supernatant; Fractions 1 – 10: 10 – 30 % sucrose gradient; 11: 70 % sucrose cushion; des: desmin; vim: vimentin; syn: synemin-L.)

2.2.4 Investigation of the possible negative effect of synemin-L on pre-assembled vimentin.

We were able to show that synemin has a negative effect on the filament forming process of vimentin and desmin. In order to analyse the effect of synemin on pre-asembled intermediate filament network in more detail, synemin was added after one hour of preassembly of vimentin. At this time point, vimentin had formed a continuous filament network. At distinct time points after addition of synemin the co-assembly reaction of synemin and vimentin was stopped and the samples were stained negatively and analysed using electron microscopy (Figure 21). As control, instead of synemin, assembly buffer was added and the assembly was stopped after 10 additional seconds. Still, a filamentous network was visible. In all samples containing synemin, shorter filaments were disrupted or connected by globular protein aggregates were visualized. Still, a filamentous network was visible. This data suggested a very strong binding of synemin on the proteins within the filaments and therefore a “severing reaction” as synemin intrudes into the vimentin filament substructure.

Figure 21 (next page): Electron micrographs of negatively stained samples of wildtype vimentin mixed with synemin-L after 1 hour of assembly. (A): Control of wildtype vimentin assembled for 1 hour revealed a filamentous network. **(B):** As a control, an equal amount of assembly buffer was added after 1 hour of assembly. The reaction was stopped 10 seconds after addition. **(C):** Synemin was added after 1 hour of assembly. The reaction was stopped after 10 seconds of incubation with desmin. **(D):** After 30 minutes of incubation of synemin and vimentin, the filaments are shorter and disrupted by globular structures. **(E):** The same was true for vimentin mixed with synemin followed by an incubation step for one hour. **(F)** 72 hours after addition of synemin, a filamentous network packed with globular structures was visible. Vimentin was pre-assembled for 1 hour to gain a completely formed filamentous network. Assembly was performed at 37°C in 25 mM Tris-HCl, 50 mM NaCl, pH 7.5, and stopped at distinct time points by adding 0.1% glutaraldehyde at 1 hour. Scale bar: 200 nm.

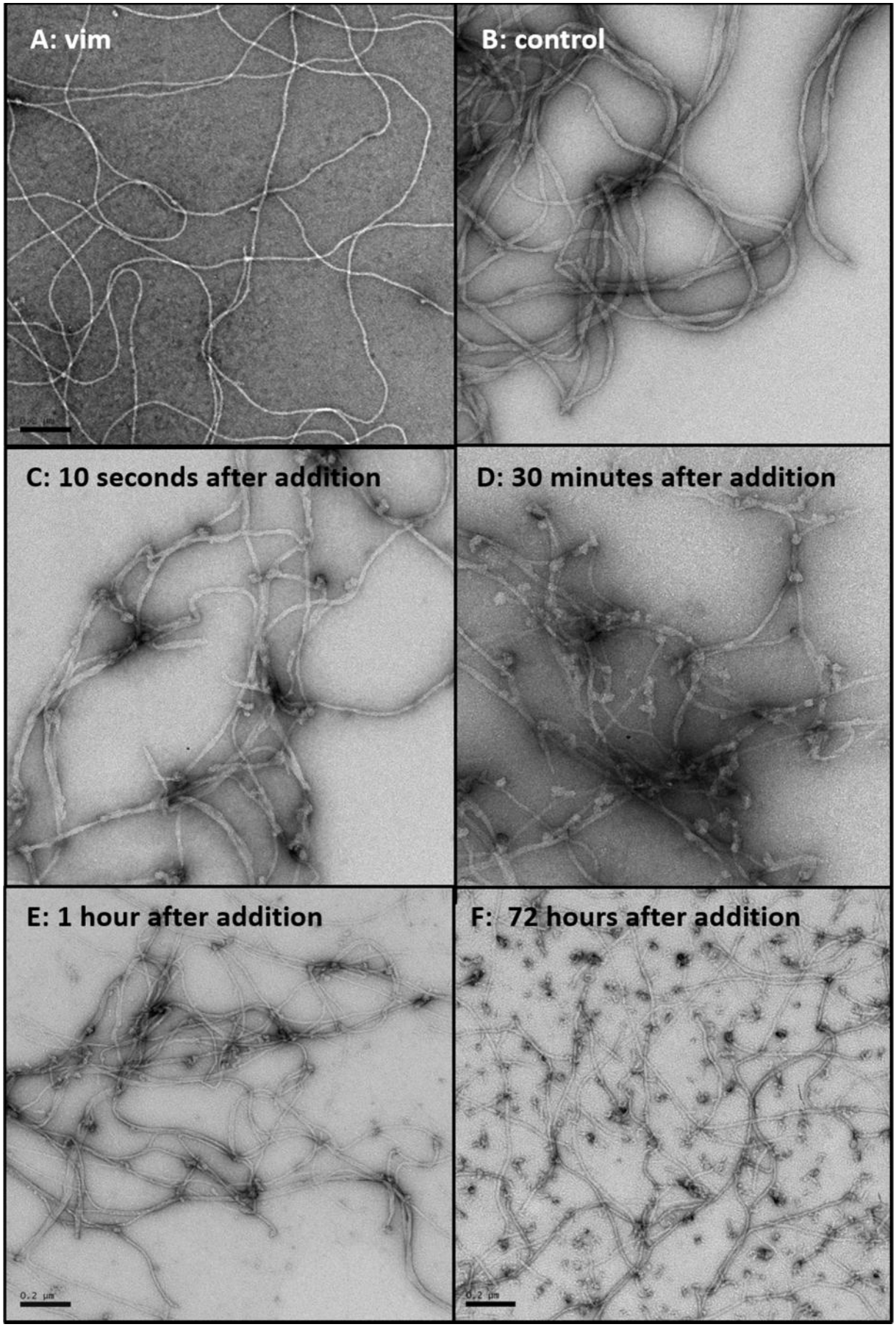
A: vim
B: control
C: 10 seconds after addition
D: 30 minutes after addition
E: 1 hour after addition
F: 72 hours after addition
0.2 µm
0.2 µm

2.3 Characterization of the binding site of human desmin and vimentin for synemin-L

Prior results showed a strong interaction of synemin with desmin and vimentin under *in vitro* assembly conditions. To characterize the binding site of desmin and vimentin for synemin-L, truncated variants of desmin and vimentin were used. The variants lacking the first 85 amino acids of the head domain are called vimentinΔhead and desminΔhead. Both are neither able to form tetramers nor filaments on their own. The same holds true for the variants of desmin and vimentin lacking the head and tail domain, called vimentin rod and desmin rod. As the tail domain is not essential for filament assembly, the tail truncated version of desmin and vimentin are able to form filaments under assembly conditions.

2.3.1 Analysis of truncated versions of vimentin assembled in the presence of synemin-L

The visualization of the co-assembly of synemin-L with the truncated variants of vimentin is shown in Figure 22. In case for vimentinΔhead and vimentin rod, globular protein structures were visible along with the protofilament like structures formed by pure vimentinΔhead and vimentin rod. VimentinΔtail was still able to form single filaments assembled in the presence of synemin. But the filaments were laterally covered by globular protein aggregates suggesting that the binding domain in vimentinΔtail is more accessible than the same domainin full length vimentin.

Figure 22 (next page): Electron micrographs of negatively stained samples of truncated variants of vimentin assembled in the presence of synemin. VimentinΔhead and vimentin rod were not able to form higher structures like filaments. VimentinΔtail was able to form an intact filament network within one hour of pre-assembly. The mix of synemin with vimentinΔhead and vimentin rod unveiled protein aggregates besides smaller soluble structures. A mix of vimentinΔtail and synemin-L resulted in shorter filaments laterally coated with globular protein aggregates. Assembly was performed at 37°C in 25 mM Tris-HCl, 50 mM NaCl, pH 7.5, and stopped by adding 0.1% glutaraldehyde at 1 hour. (VimΔhead: headless vimentin; vim rod: vimentin rod domain; vimΔtail: tailless vimentin; syn: synemin-L.) Bar, 100 nm.

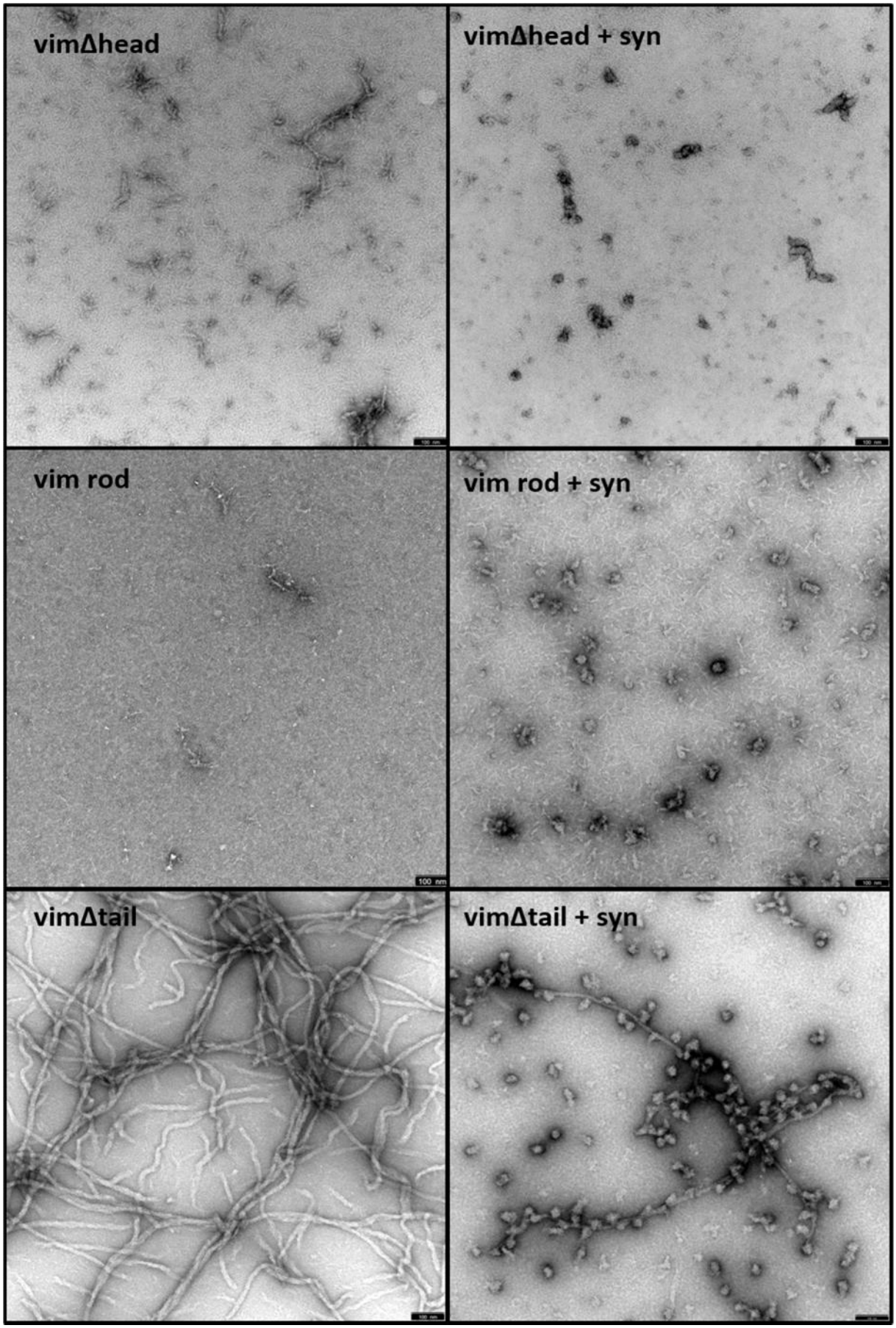
vimΔhead
vimΔhead + syn
vim rod
vim rod + syn
vimΔtail
vimΔtail + syn

Because synemin-L was found mainly within the pellet fraction together with vimentinΔtail (Figure 23) one can assume thatsynemin-L is able to interact with the tail truncated version of vimentin. For the other variants, it was not clearly shown in the standard assembly assay because the sedimentation behaviour of synemin and the truncated variants of vimentin was not changed through co-assembly. Since electron microscope studies and standard sedimentation assays gave no clear evidence of possible interactions of the head and rod domain of vimentin with synemin, a sucrose gradient centrifugation assay was performed to analyse the possible interaction of synemin-L with vimentinΔhead and vimentin rod (Figure 24).

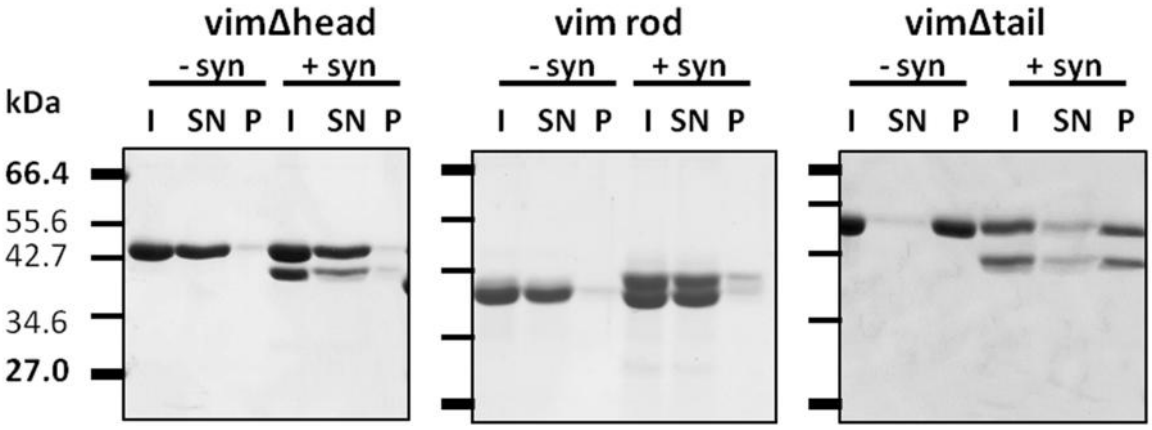

Figure 23: sedimentation analysis of vimentinΔhead, vimentin rod and vimentinΔtail assembled in the presence of synemin-L. Headless vimentin and the rod domain of vimentin were found mainly within the supernatant after centrifugation. Same is true for the mix of synemin-L and the proteins. Tailless vimentin was found within the pellet fraction alone and together with synemin-L suggesting a strong interaction of the proteins. The proteins were dialyzed into 5 mM Tris-HCl, pH 8.4 and assembly was performed at 37°C for 1 hour in 25 mM Tris-HCl, 50 mM NaCl, pH 7.5. After assembly, the samples were centrifuged at 30 psi for 15 minutes. The fractions are shown after separation by gel electrophoresis. (I: input; SN: supernatant; P: pellet; vimΔhead: headless vimentin; vim rod: vimentin rod domain; vimΔtail: tailless vimentin; syn: synemin-L.).

VimentinΔhead was found after standard sucrose gradient centrifugation assay within the supernatant and in fraction number 1 and 2 with a peak in the supernatant. In the case of the sample of vimentinΔhead co-assembled with synemin-L the bands of both proteins were found in the same range, too. Vimentin rod alone showed the same sedimentation behaviour as vimentinΔhead. However, when vimentin rod was combined with synemin-L, the width of the bands of both proteins was increased from the SN fraction up to fraction number 6 with a peak in fraction numbers 1 to 3. While vimentinΔtail was visible within the range of fraction 3 to 11 with a peak in fraction 9

to 10, the co-assembled vimentinΔtail and synemin-L covered a range between fraction numbers 5 to 8 with a peak in fraction 6 to 7. This data indicates a strong interaction of the proteins. Since the sedimentation behaviour of synemin-L had changed though the co-assembly with all truncated variants, it is proven by method of elimination that the binding site for synemin-L is within the rod domain of vimentin.

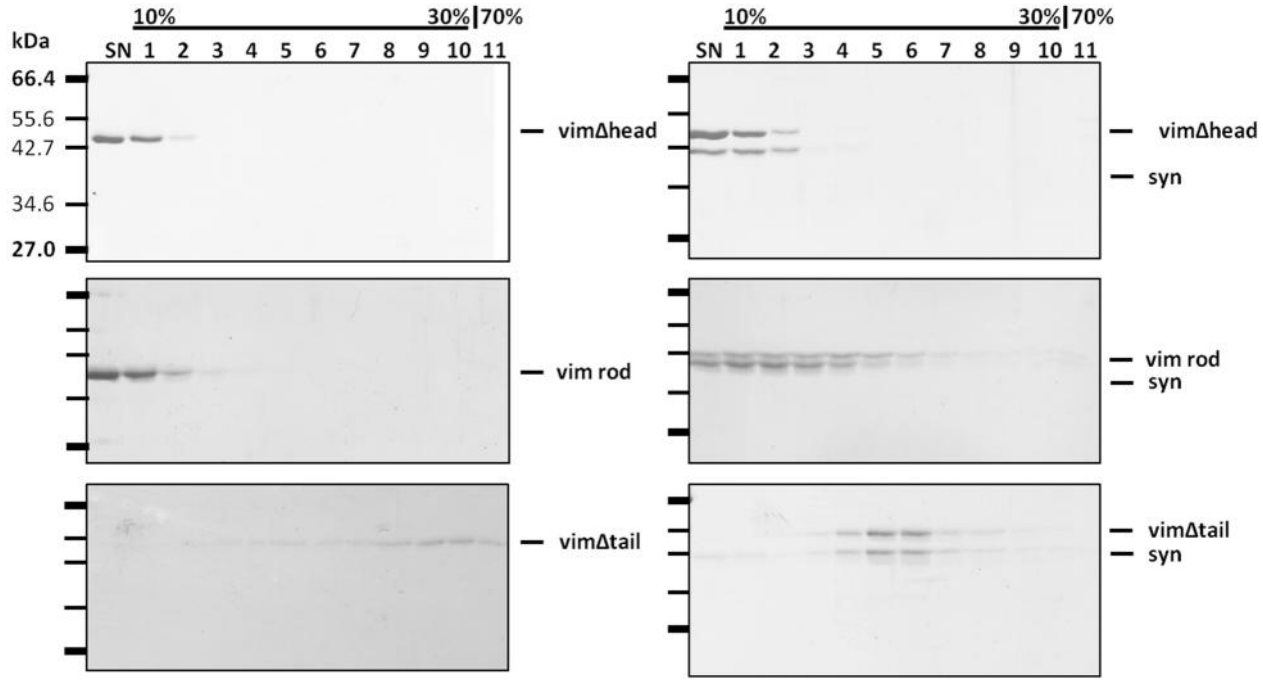

Figure 24: Sucrose gradient analysis of truncated variants of vimentin assembled in the presence of synemin-L. Headless vimentin and vimentin rod were found within the supernatant and fractions 1 to 4 with a peak in the supernatant. Through co-assembly with headless vimentin, synemin-L changed its sedimentation behaviour and was mainly found within the supernatant and fractions 1 and 2. The co-assembly of the rod domain of vimentin with synemin-L increased the range of the sedimentation profile. In this case, synemin-L and vimentin rod were found within the supernatant and fraction 1 to 6 with a peak in fraction 2. Tailless vimentin was found within fraction 5 to 11 with a peak in fraction 10 after one hour of assembly. The co-assembly of tailless vimentin with synemin-L resulted in a shift to fractions 4 to 9 with a peak in fraction 5 and 6. The proteins were dialyzed into 5 mM Tris-HCl, pH 8.4 and assembly was performed in 25 mM Tris-HCl, 50 mM NaCl, pH 7.5. After 1 hour of assembly, the samples were centrifuged at 28.000 rpm, 4°C for 5 hours. The fractions are shown after separation by gel electrophoresis. (SN: supernatant; Fractions 1 – 10: 10 – 30 % sucrose gradient; 11: 70 % sucrose cushion; vimΔhead: headless vimentin; vim rod: vimentin rod domain; vimΔtail: tailless vimentin; syn: synemin-L.)

2.3.2 Analysis of truncated versions of desmin assembled in the presence of synemin-L

The visualization of negatively stained assembly products of desminΔhead, desmin rod and desminΔtail proved the assembly incompetent behaviour of desminΔhead and desmin rod but also the filament forming ability of desminΔtail (Figure 25). Once mixed with synemin-L, globular protein aggregates were visible besides the structures formed by desminΔhead and desmin rod. DesminΔtail might not be able to form filaments anymore, because only globular structures were visible after one hour of assembly together with synemin. Nevertheless, the arrangement of the globular structures and the result of the covered filaments found for vimentinΔtail leaves room for interpretation that short filaments formed by desminΔtail are completely covered by synemin.

Figure 25 (next page): Electron micrographs of negatively stained samples of head truncated variants of desmin assembled in the presence of synemin. Headless desmin and desmin rod were not able to form higher structures like filaments. Tailless desmin was able to form an intact filament network within one hour of assembly. The mix of synemin with desminΔhead and desmin rod unveiled protein aggregates along with smaller soluble structures. The co-assembly of desminΔtail with synemin-L resulted in protein aggeragetes. Assembly was performed at 37°C in 25 mM Tris-HCl, 50 mM NaCl, pH 7.5 and stopped by adding 0.1% glutaraldehyde at 1 hour. (DesΔhead: headless desmin; des rod: desmin rod domain; desΔtail: tailless desmin; syn: synemin-L.) Bar, 100 nm.

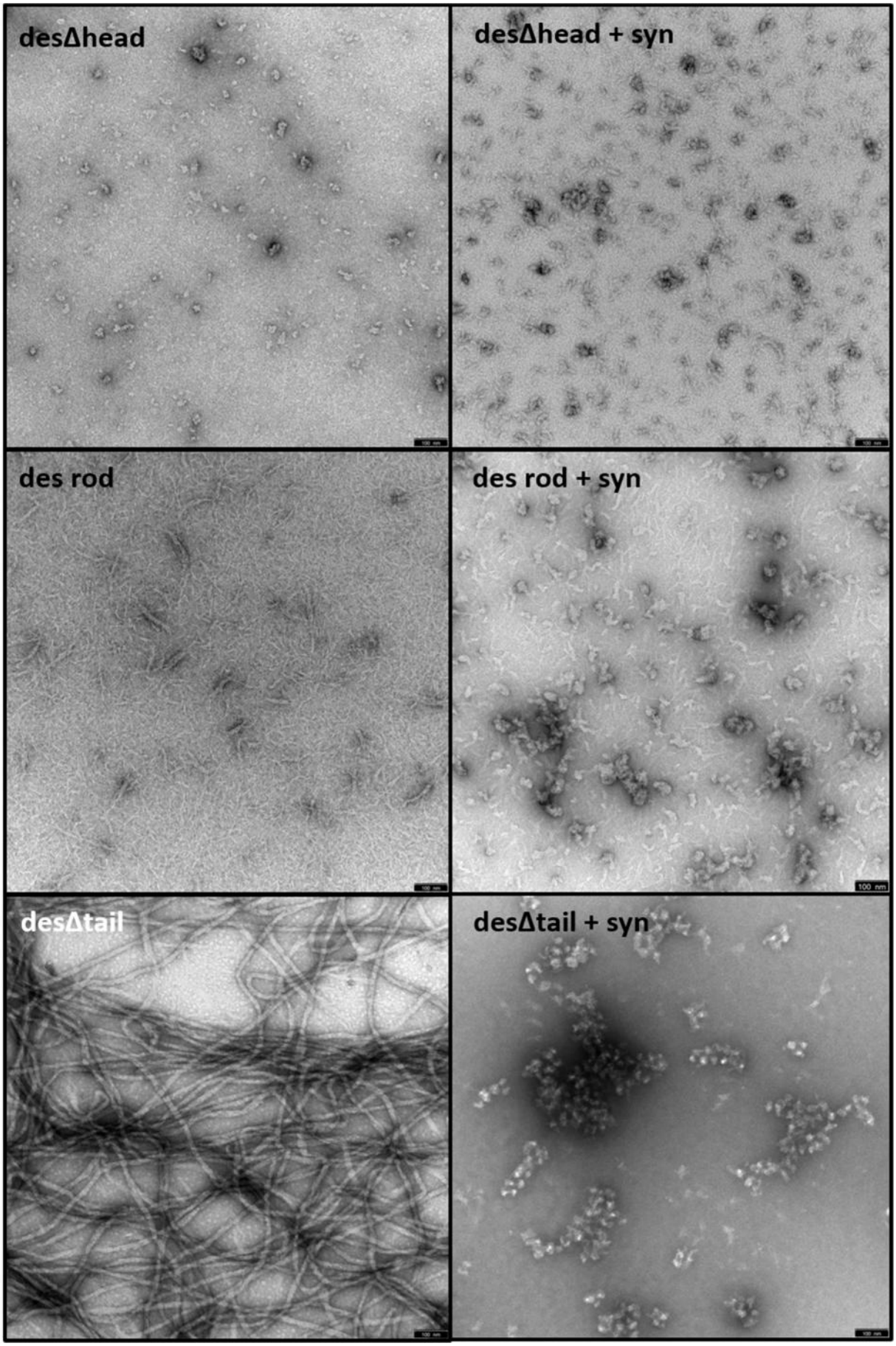
desΔhead
desΔhead + syn
des rod
des rod + syn
100 nm
desΔtail
desΔtail + syn

Standard sedimentation assay in an airfuge showed a strong interaction of synemin with the tail-truncated variant of desmin. Synemin-L was found within the pellet fraction along with desminΔtail (Figure 25). The standard sedimentation assay was not useful to analyse the possible interaction of synemin with desminΔhead and desmin rod, because both proteins were mainly found within the supernatant fractionirrespective if they were mixed or alone.

A sucrose gradient centrifugation of assembled proteins was performed using the established standard protocol (Figure 26). Like vimentinΔhead and vimentin rod, desminΔhead and desmin rod were present within the supernatant and fractions 1 and 2. DesminΔtail was found alone within fraction 11 comparable with assembled wildtype desmin. The mix of synemin with desminΔhead, desmin rod and desminΔtail led to a shift of the sedimentation profile of synemin suggesting a strong interaction between synemin and desmin comparable to the interaction of synemin with vimentin as shown before.

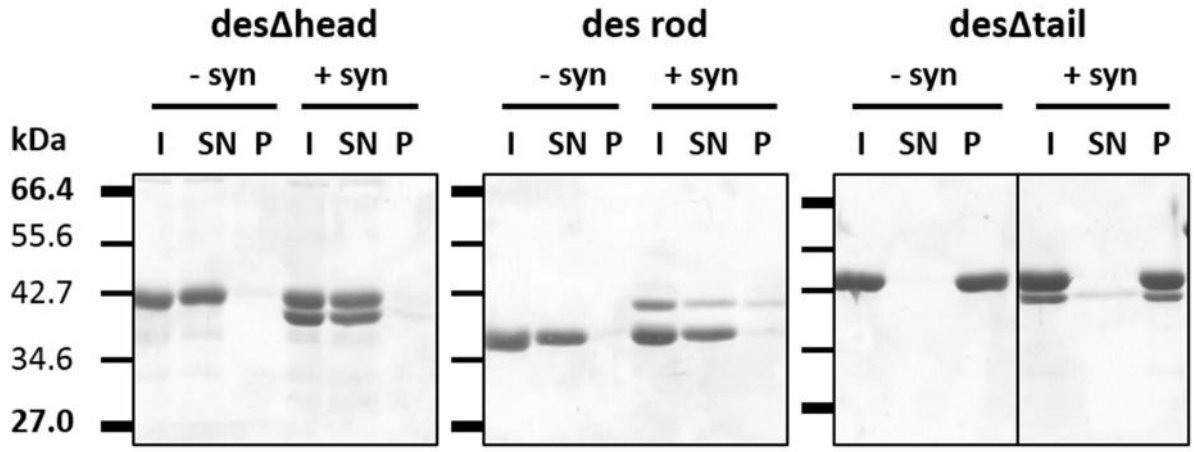

Figure 26: Sedimentation analysis of truncated variants of desmin assembled in the presence of synemin for 60 min. Headless desmin and the rod domain of desmin were mainly found within the supernatant after established standard centrifugation. Same is true for the mix with synemin-L. Tailless desmin was found within the pellet fraction alone and together with synemin-L suggesting a strong interaction of the proteins. The proteins were dialyzed into 5 mM Tris-HCl, pH 8.4 and assembly was performed in 25 mM Tris-HCl, 50 mM NaCl, pH 7.5, for 1 hour at 37°C. After assembly, the samples were centrifuged at 30 psi for 15 minutes. The fractions are shown after separation by gel electrophoresis. (I: input; SN: supernatant; P: pellet; desΔhead: headless desmin; des rod: desmin rod domain; desΔtail: tailless desmin; syn: synemin-L.).

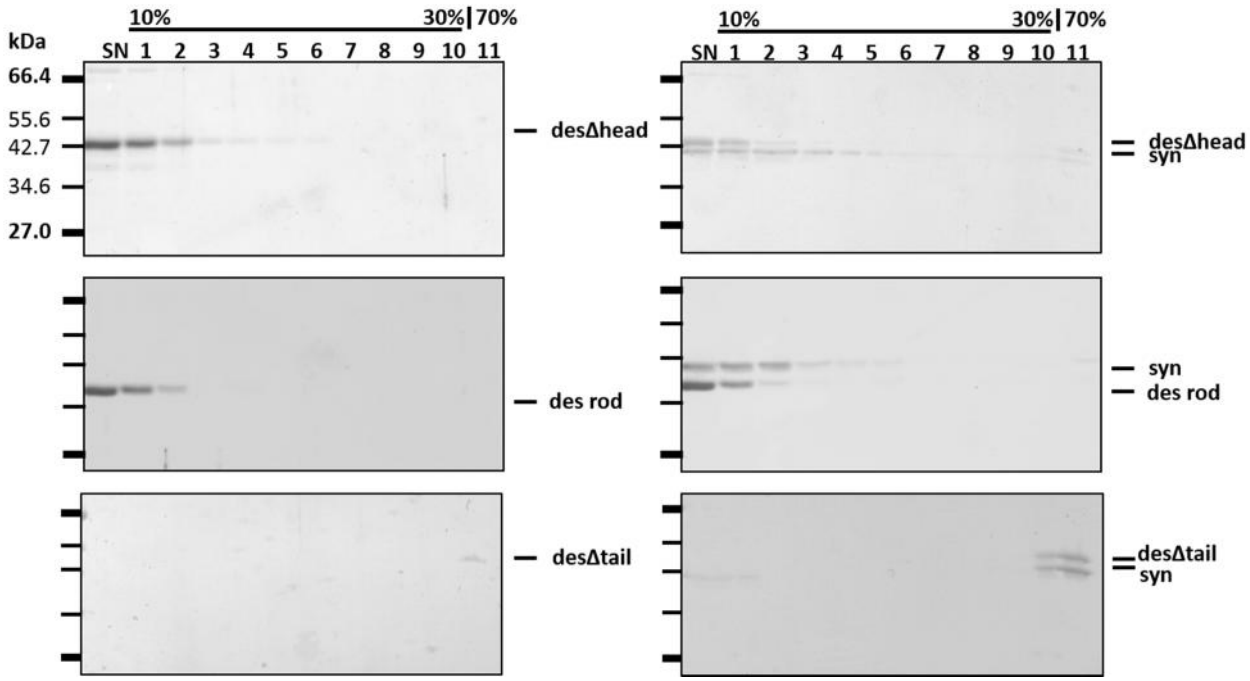

Figure 27: Sucrose gradient analysis of truncated variants of desmin assembled in the presence of synemin-L. Headless desmin and desmin rod were found within the supernatant and fractions 1 to 4 with a peak in the supernatant. Via co-assembly with headless desmin, synemin-L was found within the supernatant and fractions 1 to 7. In fraction 11, a small amount of both, headless desmin and synemin-L, was found. The co-assembly of the rod domain of desmin with synemin-L did change the sedimentation behaviour of synemin-L to the supernatant and fractions 1 to 4 with a peak within the supernatant and fractions 1 and 2. Tailless desmin was found within fraction 11 after one hour of assembly. Through co-assembly of tailless desmin with synemin-L, both proteins were found within fraction 10 to 11 suggesting a strong interaction of both proteins. The protein samples were dialyzed into 5 mM Tris-HCl, pH 8.4 and assembly was performed in 25 mM Tris-HCl, 50 mM NaCl, pH 7.5, for 1 hour at 37°C. After assembly, the samples were centrifuged at 28.000 rpm, 4°C for 5 hours. The fractions are shown after separation by gel electrophoresis. (SN: supernatant; Fractions 1 – 10: 10 – 30 % sucrose gradient; 11: 70 % sucrose cushion; desΔhead: headless desmin; des rod: desmin rod domain; desΔtail: tailless desmin; syn: synemin-L.)**.**

2.3.3 Determination of the binding site for synemin within the rod domain of desmin

Through method of elimination, the rod domain of desmin and vimentin was defined as the binding site for synemin. For further analysis of the binding site of desmin for synemin within the rod domain of desmin, shorter fragments of desmin were used for sucrose gradient centrifugation (Figure 28). The behaviour of this fragments in assembly conditions have been described before (Bär et al. 2009). The fragment desminΔC240 ends within coil 1B, while desminΔC250 terminates at the end of coil 1B and aggregates into proteinaceous masses under assembly conditions. Furthermore, DesminΔC260 ends within the linker L12 domain of desmin and is able to form large aggregates but no filaments after starting the assembly process. DesminΔC300, which ends within coil 2, is able to aggregate into large roundish

structures after the addition of salt. DesminΔN260 skips the first 260 amino acids and therefore contains a small part of linker L12, coil 2 of the rod domain and the complete tail domain. This truncated version have been shown to stay soluble under assembly conditions.

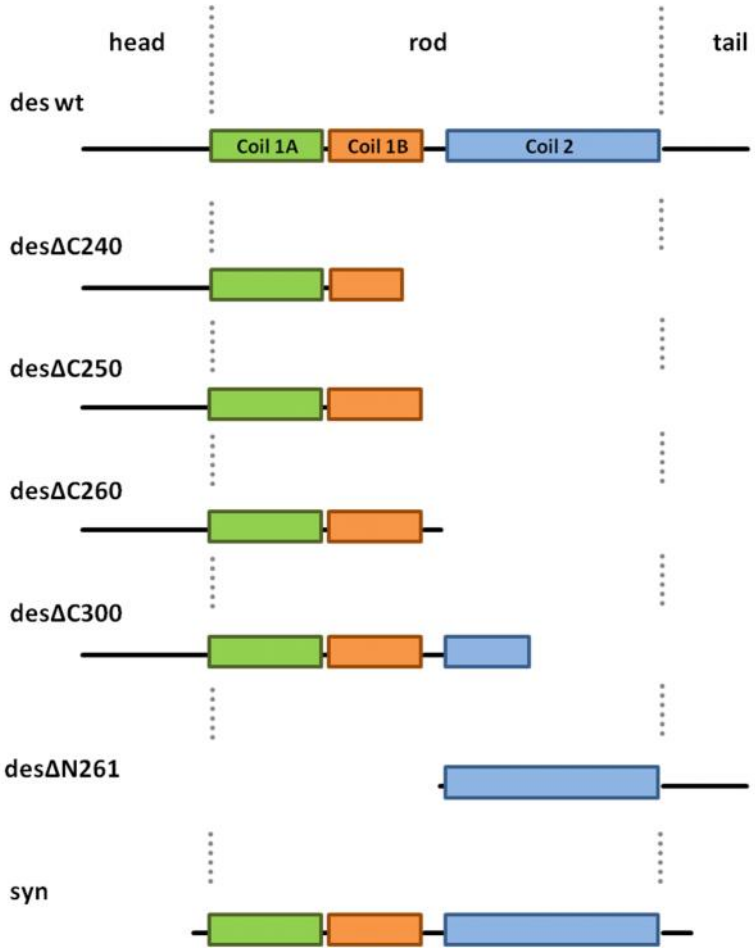

Figure 28: Scheme of the truncated variants of desmin. des wt: full length desmin; desΔC240: the first 240 carboxyterminal amino acids of desmin including the head domain and coil1A, linker1 and a party of coil 1B; desΔC250: the first 250 amino acids of desmin lacking the coil 2 and tail domain; desΔC260: the first 260 amino acids of desmin with the head domain, coil1 and a part of the linker domain between coil1 and coil2; desΔC300: the first 300 amino acids of desmin including the head domain, coil1 and a part of coil2; desΔN261: the second half of desmin including the amino acids from position 261 to 470 representing coil2 and the tail domain.

We now investigated these fragments according to the procedure employed ffor desmin and vimentin as reported above. The results of sucrose gradient centrifugation of the fragments under assembly condition are shown in Figure 29. Interestingly, the fragments of desmin representing the head domain and the first half of the rod domain (desminΔC240 - desminΔC260) were not able to form filaments, but were merely found within fraction 11 corresponding to the 70% sucrose cushion (Figure 28). This suggests a strong effect of the sucrose on the sedimentation behaviour of the first half of desmin. DesminΔN261, representing the second half of

the rod and the tail domain of desmin, was found within the supernatant and fractions 1 to 4 with a peak in the supernatant. Synemin interacted with the fragments desminΔC240 to desminΔC300 and was found within the pellet fraction together with the truncated variants of desmin. But only in case of the combination of synemin-L with desminΔC250, synemin is exclusively found within the pellet fraction indicating a strong binding of synemin-L on this particular fragment of desmin. In combination with desminΔC240, synemin occurred between fraction 3 and 7 indicating a possible weaker binding of synemin on desminΔC240 compared with the interaction of synemin with desminΔC250. In case of the combination of synemin-L with desminΔC260, more synemin is found within the SN and fraction 1 to 3 than in the pellet. For the combination of synemin-L with desminΔC300, additional fractions of synemin are found within the supernatant and fraction 1 besides the protein in fraction 11. Moreover, a shift of the sedimentation profile of synemin-L to fraction 4 to 8 with a peak within fraction 6 in presence of the second half of desmin. As desminΔN261, did not completely change its sedimentation behaviour, one can predict a slight interaction of these proteins. Through addition of synemin, the sedimentation profile of desminΔN261 was changed by increasing the s-profile on the right side from fraction 4 to fraction 8. The results of the interaction study suggest that the binding site for synemin is in the area between amino acid 86 and 240. Hence, the binding site must be within coil1A, in linker L1 and coil1B.

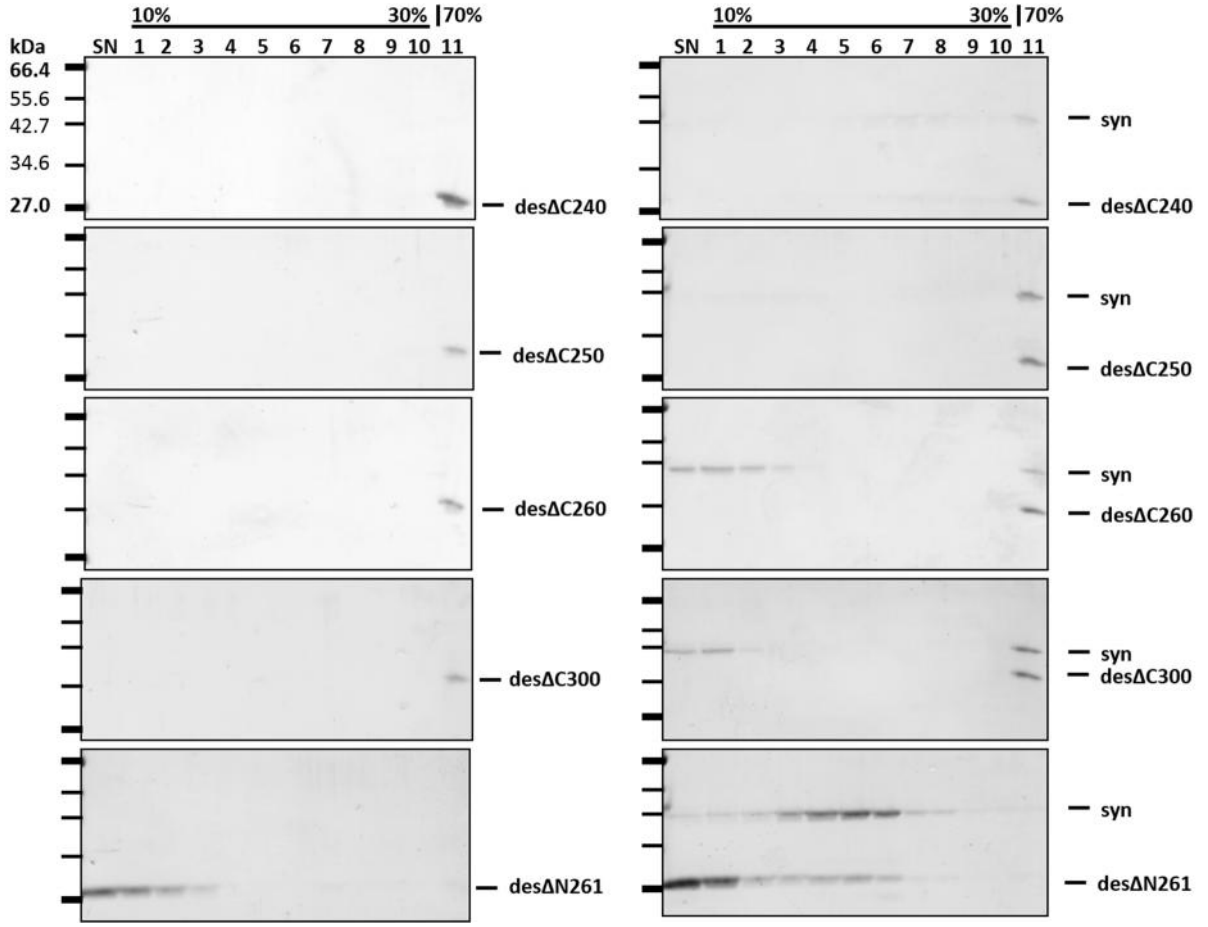

Figure 29: Sucrose gradient analysis of truncated variants of desmin assembled in the presence of synemin for 60 min. The proteins were dialyzed into 5 mM Tris-HCl, pH 8.4 and assembly was started through changing the buffer condition to 25 mM Tris-HCl, 50 mM NaCl, pH 7.5. After assembly, the samples were centrifuged at 28.000 rpm, 4°C for 5 hours. The fractions are shown after separation by gel electrophoresis. (SN: supernatant; Fractions 1 – 10: 10 – 30 % sucrose gradient; 11: 70 % sucrose cushion; desΔC240: amino acids 1 - 240; desΔC250: amino acids 1 – 250; desΔC260: amino acids 1 - 260; desΔC300: amino acids 1 - 300; desΔN261: amino acids 261 - 470.)

Results Part II:

Characterization of the *in vitro* properties of nestin

Part II gives a first impression of a systematic *in vitro* studies of nestin. The characterization of the soluble structures of nestin was performed using sedimentation assays and analytical ultracentrifugation (**2.4.2**). Next, the *in vitro* assembly behavior of nestin was examined with electron microscopy, sedimentation assay and sucrose gradient centrifugation (**2.4.3**). After the characterization of nestin alone, the differences of the interaction of nestin with desmin through renaturating the proteins together or alone were analyzed using sedimentation velocity runs (**2.5.1**). The influence of nestin on the assembly process of mutant vimentinY117L and desminY122L have been investigated using electron microscopy and sedimentation assay (**2.5.2**). To get a first impression of the effect of nestin on assembled vimentin and desmin sucrose gradient centrifugation and electron microscopy have been used (**2.5.3**). The characterization of the binding site of desmin and vimentin for nestin have been performed using electron micrographs as well as sedimentation assays and sucrose gradient centrifugation (**2.6.1** and **2.6.2**).

2.4 Characterization of the structures formed by recombinant human nestin

Based on sequence similarities nestin is characterized as type IV IF protein and is found in proliferating cells together with type III IF proteins like vimentin and desmin. Today, the *in vitro* properties of nestin are not yet well characterized. The next section focuses on the characterization of this protein based on its behaviour under standard dialysis and assembly conditions for type III IF proteins like desmin and vimentin. A tail-truncated variant of nestin was used for these *in vitro* studies to avoid any assembly-disturbing effect of the long tail domain.

2.4.1 Recombinant production of the head and rod domain of human nestin

For protein expression and purification, cDNA of the head and rod domain of nestin were subcloned into the prokaryotic expression vector pET24a. The clone was expressed in E.coli strain BL21 for protein purification. Expression tests with the E.coli strains BL21 DE3 codon+, TG1 and SURE showed less or no produced protein. An inclusion body preparation was the first step of protein purification to purify the exogenously expressed protein (Figure 30). Some protein was lost within the supernatant of two washing steps with buffer GII and the TE buffer.

After inclusion body purification, two ionic exchange columns were used to purify the protein further (Figure 31). The produced tail truncated variant of nestin with an isoelectric point of 5.7 did not bind to the DEAE sepharose at pH 7.5 and was collected within the flow-through (FT) and the washing volume (W). The flow-through and the washing step were blended and used directly for the cationic exchange chromatography using SP sepharose, pH 7.5. Nestin bound to the sepharose and was eluted using a continuous gradient of 0.5 M NaCl. The fractions 13 to 32 were analysed using SDS-PAGE to separate nestin from bacterial proteins within the protein solution. Fraction 14 to 22 were pooled and the protein concentration measured.

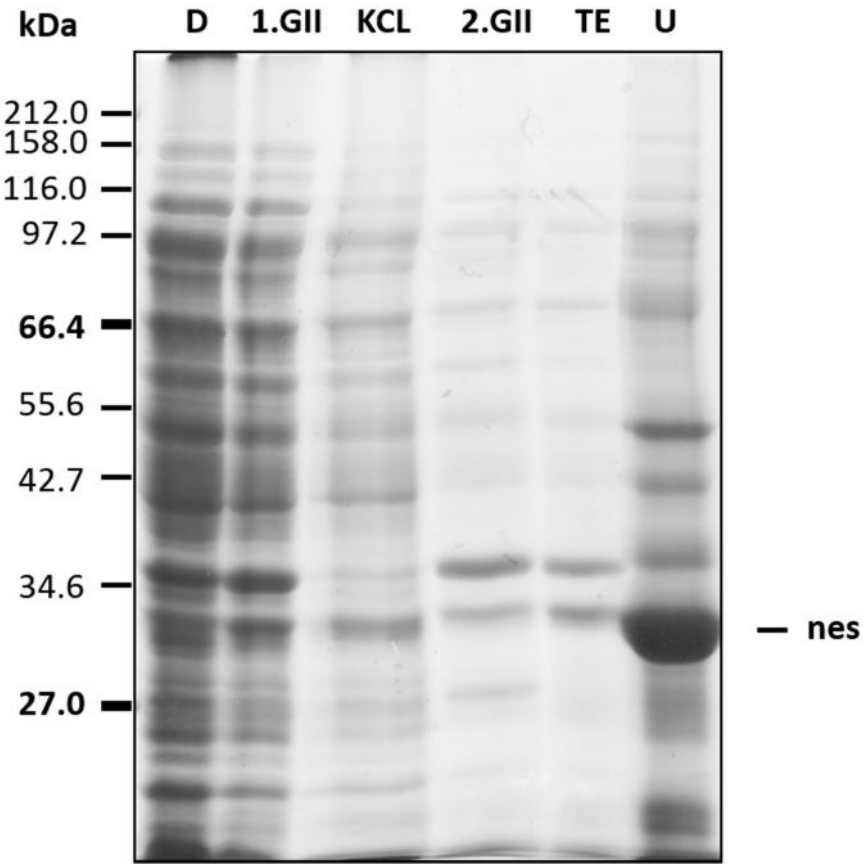

Figure 30: Inclusion body preparation of nestin. D: detergent buffer; 1.GII: first washing step with GII buffer; KCL: GII + 1.5 M KCl buffer; 2.GII: second washing step with GII buffer; TE: TE buffer; U: 9.5 M urea buffer.

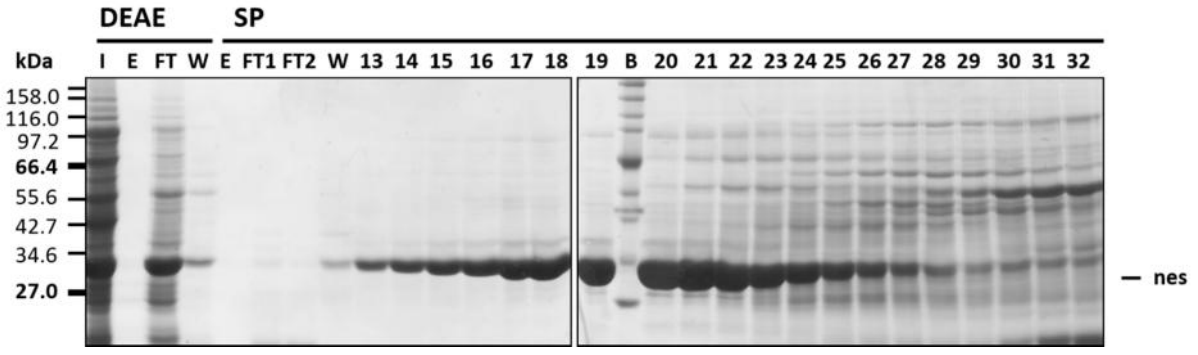

Figure 31: Purification of recombinant human nestin using ionic exchange chromantography. Anionic exchange chromantography was performed using DEAE sepharose, pH 7.5 with a 0.3 M gradient of NaCl. For kationic exchange chromantography, SP sepharose, pH 7.5 with a 0.5 M gradient of NaCl was used. (I: Input; E: Void volume; FT: Flow-through; W: Washing volume; B: Marker)

After purification of the recombinant produced nestin, stability and quality control was performed (Figure 32). The protein remained stable up to six days in 5 mM Tris, pH 8.4. To check quality, defined amounts of protein were loaded and analysed using western blot. No signs of degradation were detected.

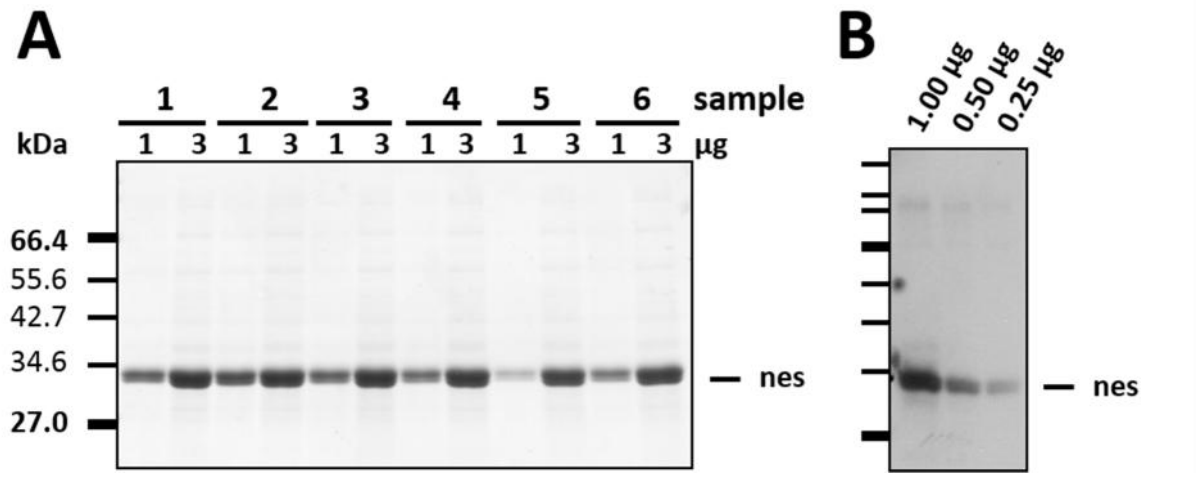

Figure 32: Analysis of purified nestin. (A) Time-dependent stability control of nestin. 1 and 3 µg protein were used to load the SDS-PAGE. (Sample 1: before renaturation; sample 2: after renaturation; sample 3: one day after renaturation; sample 4: 3 days after renaturation; sample 5: 6 days after renaturation; sample 6: 9 days after renaturation). **(B) Quality control of nestin.** To analyse the degradation, 1 µg, 500 ng and 250 ng protein were loaded. First antibody: α-nestin antiserum, produced in rabbits (1:500). Second antibody: HRP-coupled α-rabbit (1:5000).

2.4.2 Analysis of assembly precursor units of nestin after renaturation into different buffer systems

Steinert and colleagues demonstrated that nestin is able to form homodimers and homotetramers *in vitro* (Steinert et al. 1999). We have used established standard renaturation protocols in order to analyse the soluble structures formed by nestin after purification. Furthermore, a sedimentation analysis of the protein renatured into 5 mM Tris with different pH's was performed using the standard centrifugation assay (Figure 33). Nestin, dialyzed into 2 mM NaPi, pH 7.5, has been precipitated completely as determined by protein quantification of the supernatant after centrifugation of the dialyzed sample. While nestin remained soluble in the buffer conditions between 5 mM Tris-HCl, pH 9.5 and pH 8.4, it was mainly found in the pellet fraction in 5 mM Tris-HCl, pH 7.5.

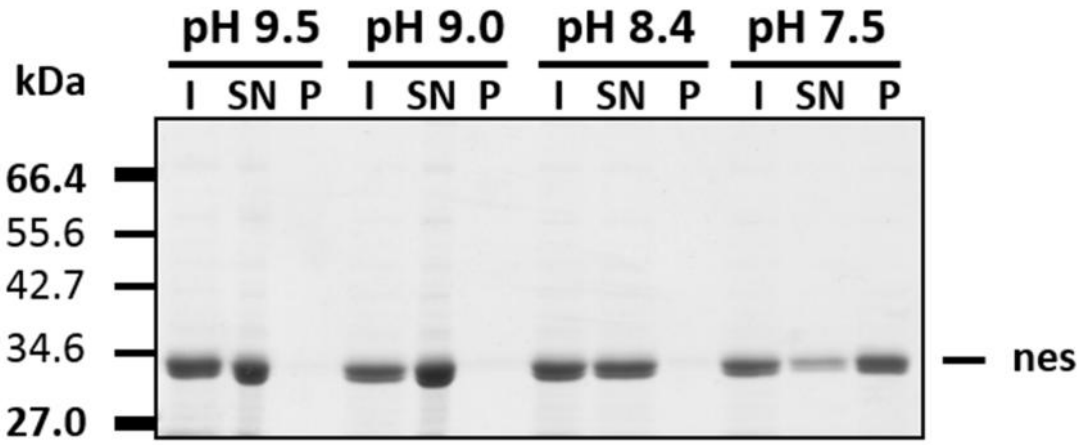

Figure 33: Sedimentation analysis of nestin dialyzed into 5 mM Tris-HCl buffer with different pH overnight. Tailless nestin was found after the centrifugation in the supernatant in 5 mM Tris-HCl with all different pH's except pH 7.5. In 5 mM Tris-HCl, pH 7.5, tailless nestin was mainly found in the pellet fraction suggesting higher aggregates formed by nestin under these conditions. After dialysis, the samples were centrifuged at 30 psi for 15 minutes. The fraction are shown after separation by gel electrophoresis. (I: input; SN: supernatant; P: pellet; nes: tailless nestin).

The result was confirmed using sedimentation velocity runs (Figure 34). The *s*-values of the soluble structures formed by nestin in 5 mM Tris-HCl, pH 9.5 is 20.8 S and in 5 mM Tris, pH 8.4 33.1 S (Table 8). Moreover, the sedimentation profile of nestin in 5 mM Tris-HCl, pH 7.5, showed a heterogeneous contribution with two peaks, one at 29.5 S and one at 138.2 S. Therefore, it has been shown that the pH value has a strong influence on the aggregation process of nestin.

buffer	$s_{20,w}$ [S]*	c_0 (OD_{230nm})	M_{sed} [kDa]
5 mM Tris, pH 9.5	20.8 ± 0.1	0.33 ± 0.00	72.2 ± 3.2
5 mM Tris, pH 8.4	33.1 ± 0.1	0.44 ± 0.00	92.0 ± 1.6
5 mM Tris, pH 7.5	29.5 ± 0.7 138.2 ± 0.4	0.11 ± 0.00 0.48 ± 0.00	-

Table 8: Comparison of the sedimentation coefficients of nestin under different pH conditions.
* Peak value s*(20,w) indicates sedimentation coefficient that has been corrected for the viscosity and density of solvent, relative to that of water at 20°C. The *s*-values and the molecular weigth were rounded to one decimal place and the values of concentration were rounded to two decimal places.
All runs in AUC were performed after step-wise renaturation of samples from 8 M urea into the named buffers.

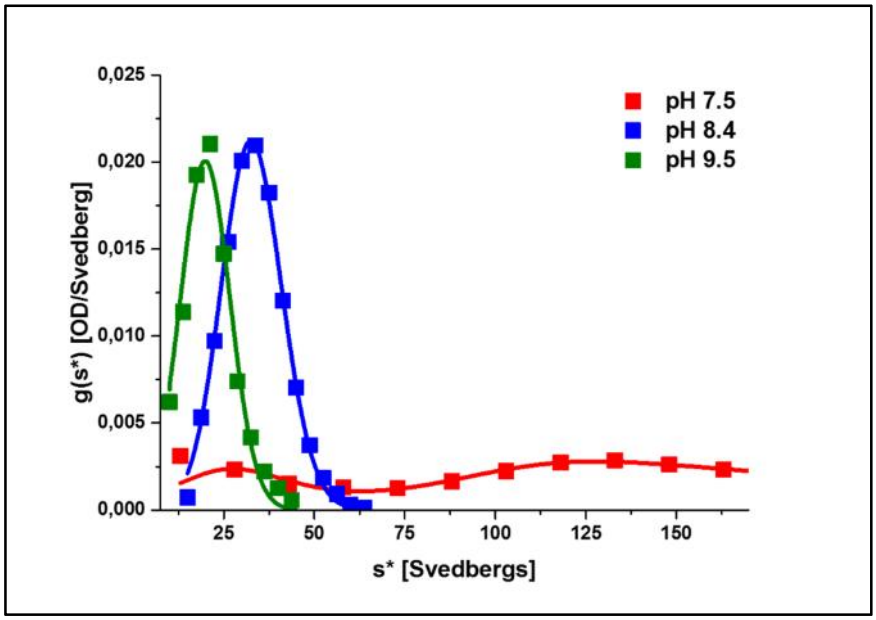

Figure 34: Influence of the pH on the sedimentation characteristics of nestin. Red line: nestin in 5 mM Tris-HCl, pH 7.5 Blue line: nestin in 5 mM Tris-HCl, pH 8.4 Green line: nestin in 5 mM Tris-HCl, pH 9.5. Sedimentation velocity runs were performed at 40.000 rpm, 20°C in 5 mM Tris-HCl with different pH. The sedimentation profile was measured at 230 nm and the protein concentration was 0.1 g/l. The sedimentation coefficient shows a precise dependency of the pH. s* indicates sedimentation coefficient. Data analysis was performed using the software DCDT+.

2.4.3 Structures formed by nestin under different *in vitro* assembly conditions

In order to analyse the assembly, we have chosen the standard assembly conditions established for desmin and vimentin because nestin is thought to heteropolymerize with these proteins. The assembly conditions used for the type III IF proteins should therefore be suitable for nestins *in vitro* characterization. The structures formed by nestin, renatured into the standard dialysis buffer 5 mM Tris, pH 8.4 and assembled for one hour in 25 mM Tris, 50 mM NaCl, pH 7.5, were analysed by negative staining. As described in literature, nestin was not able to form filaments on its own under standard assembly conditions (Figure 35). Instead of filaments, huge unordered, proteinecous masses were visualized with electron microscopy suggesting different aggregation behaviour than seen for synemin under assembly conditions.

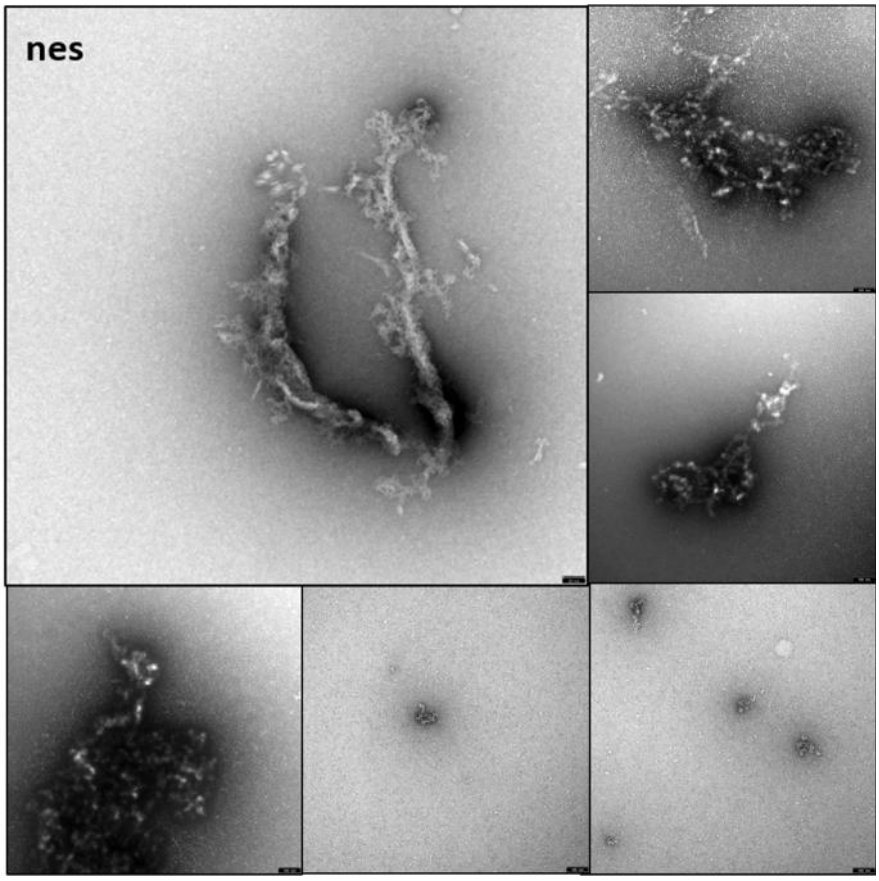

Figure 35: Electron micrographs of negatively stained samples of assembled nestin. Nestin was not able to form filaments, but huge proteineous aggregates under tested conditions. Assembly was performed at 37°C in 25 mM Tris-HCl, 50 mM NaCl, pH 7.5, and stopped by adding 0.1% glutaraldehyde after one hour. Scalebar, 100 nm.

In a standard sedimentation assay, nestin was found completely in the pellet fraction (Figure 36-A). This was also confirmed via sucrose gradient centrifugation as nestin was found in the 70% sucrose cushion (Figure 36-B).

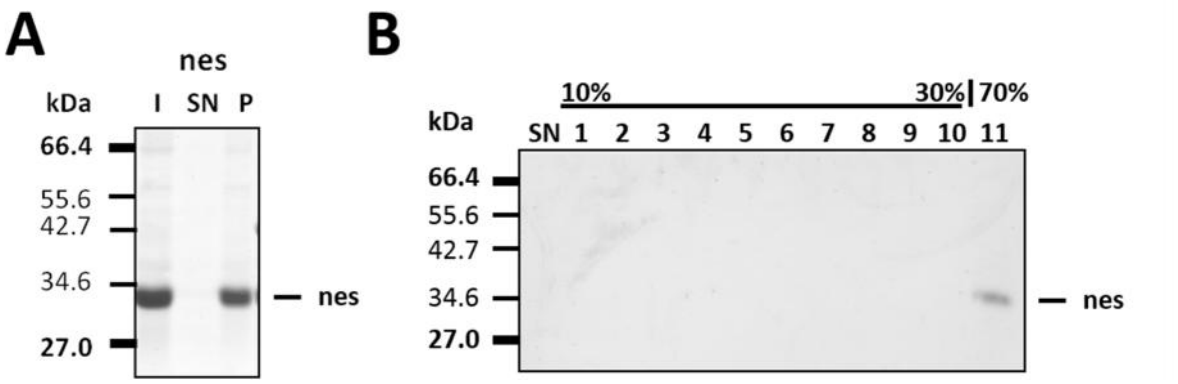

Figure 36: (A): Sedimentation analysis of assembled tailless nestin. Nestin was found within the pellet fraction after performing standard sedimentation assay. The protein was dialyzed into 5 mM Tris-HCl, pH 8.4 and assembly was performed in 25 mM Tris-Hcl, 50 mM NaCl, pH 7.5, for 1 hour at 37°C. After assembly, the sample was centrifuged at 30 PSI for 15 minutes. The fractions are shown after separation by gel electrophoresis. (I: input; SN: supernatant; P: pellet). **(B): Sucrose gradient centrifugation of assembled tailless nestin.** Tailless nestin was found in fraction 11 corresponding to the 70 % sucrose cushion. The protein was dialyzed into 5 mM Tris-HCl, pH 8.4 and assembly was performed in in 25 mM Tris-HCl, 50 mM NaCl, pH 7.5 for 1 hour, 37°C. After assembly, the sample was centrifuged at 28.000 rpm, 4°C for 5 hours. The fractions are shown after separation by gel electrophoresis. (SN: supernatant; Fractions 1 – 10: 10 – 30 % sucrose gradient; 11: 70 % sucrose cushion; nes: tailless nestin.)

2.5 Interaction of nestin with desmin and vimentin in all different stages of assembly

It has been shown that nestin is able to form heterodimers, heterotetramers and heteropolymers with vimentin (Steinert et al. 1999). In order to analyse the structures formed by nestin's head and rod in combination with desmin and vimentin in an established *in vitro* system, we have used recombinant produced protein instead of BHK-21 cells- purified protein.

2.5.1 Analysis of desmin mixed with nestin before or after renaturation into a tetrameric state

To answer the question, whether nestin is able to integrate into forming tetramers of desmin, nestin was mixed with desmin before or after renaturation into 5 mM Tris-HCl, pH 8.4. To eliminate possible source of differences in the renaturation protocol of this work and the results found by Steinert et al, two additional dialysis steps were inserted into the standard renaturation protocol. First, the proteins were dialyzed into 6 M guanidine hydrochloride, pH 8.4, for two hours followed by an additional dialysis step for one hour into 9.5 M urea, pH 8.4. For the samples mixed with nestin before renaturation, proteins were mixed in 9.5 M urea instead of 8 M urea like in case of synemin.

For sedimentation velocity runs, the buffer was changed to 10 mM Tris-HCl, pH 7.5, in order to split the *s*-values of nestin and desmin further (Table 9). The *s*-value of nestin in 10 mM Tris-HCl, pH 7.5, is 42.0 S. The *s*-value of desmin under these conditions constituted 9.7 S. When the proteins were mixed after renaturation, the *s*-values of the mix were 9.6 and 41.0 and thereby similar to the results obtained for the two proteins run independent of each other. Interestingly, the sample of proteins mixed before renaturation behaved slightly different with two *s*-values of 7.6 and 35.5. These results suggest that nestin interacts with desmin if the proteins are mixed in 8 M urea, i.e. in their monomeric form, but they do not interact, if they are mixed in 10 mM Tris-buffer (Figure 37).

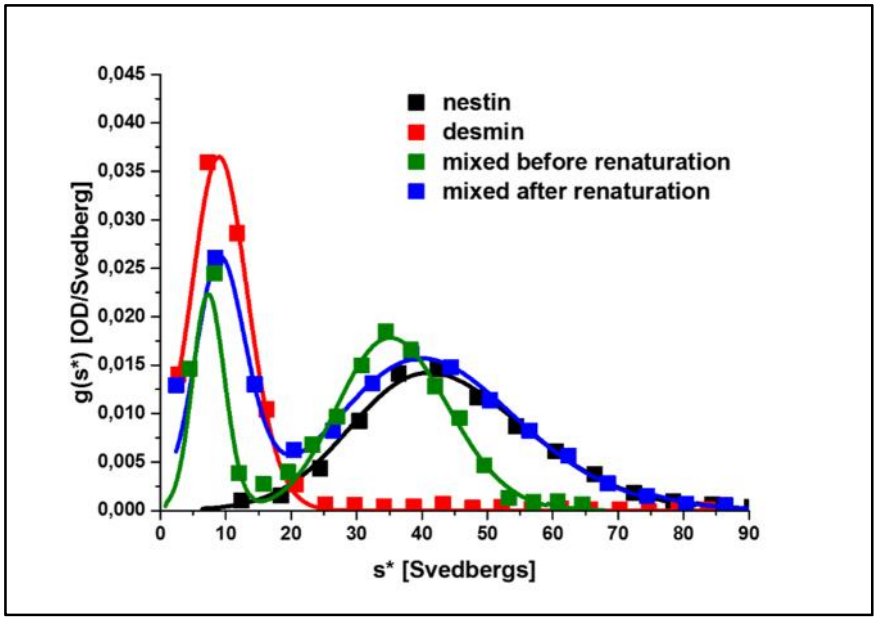

Figure 37: Contribution of the sedimentation coefficients of nestin and desmin in 10 mM Tris-HCl, pH 7.5. Sedimentation velocity runs were performed at 40.000 rpm, 20°C in 10 mM Tris-HCl, pH 7.5. The sedimentation profile was measured at 230 nm and the protein concentration was 0.1 g/l for the single proteins and 0.2 for the mixed protein samples. s* indicates sedimentation coefficient. Data analysis was performed using the software DCDT+. (Nestin: tail truncated variant of nestin; desmin: wildtype desmin; mixed before renaturation: the proteins were mixed in 8 M urea, pH 8.4; mixed after renaturation: the proteins were mixed in 10 mM Tris-HCl, pH 7.5)

buffer	protein	$s_{20,w}$ [S]*	c_0 (OD_{230nm})
10 mM Tris, pH 7.5	nestin	42.0 ± 0.1	0.50 ± 0.00
	desmin	9.7 ± 0.0	0.38 ± 0.00
	mixed before dialysis	7.6 ± 0.2 35.5 ± 0.1	0.14 ± 0.01 0.38 ± 0.00
	mixed after dialysis	9.6 ± 0.1 41.0 ± 0.1	0.25 ± 0.01 0.56 ± 0.00

Table 9: List of s-values of nestin and desmin in 10 mM Tris-HCl, pH 7.5. After step-wise dialysis of the named proteins from 8 M urea into 5 mM Tris-HCl, pH 8.4, the protein samples were dialyzed for 1 hour into 10 mM Tris-HCl, pH 7.5 .The sedimentation of proteins was measured at 230 nm and at 20°C. The concentration of the mixed protein samples was 0.2 g/l and for the single protein samples 0.1 g/L. Samples were centrifuged at 40.000 rpm for 3.5 hours. The *s*-values were rounded to one decimal place and the concentration values were rounded to two decimal places.
* Peak value s*(20,w) indicates sedimentation coefficient that has been corrected for the viscosity and density of solvent, relative to that of water at 20°C.

2.5.2 The interaction of nestin with ULF-like structures formed by desminY122L and vimentinY117L

To analyse the interaction of nestin with ULF-like structures formed by the mutant proteins desminY122L and vimentinY117L, nestin was mixed with desminY122L or vimentinY117L after renaturation into 5 mM Tris-HCl, pH 8.4 and co-assembled for one hour. Negatively stained samples revealed a strong binding of nestin to ULF-like structures (Figure 38). In the case of desminY122L mixed with nestin, the ULF-like structures appeared to be covered completely by a proteinacous mass. As a result, no single ULF was visible. For vimentinY117L, single ULFs were still distinguishable, but the majority of ULFs was retained in a huge proteinecous mass.

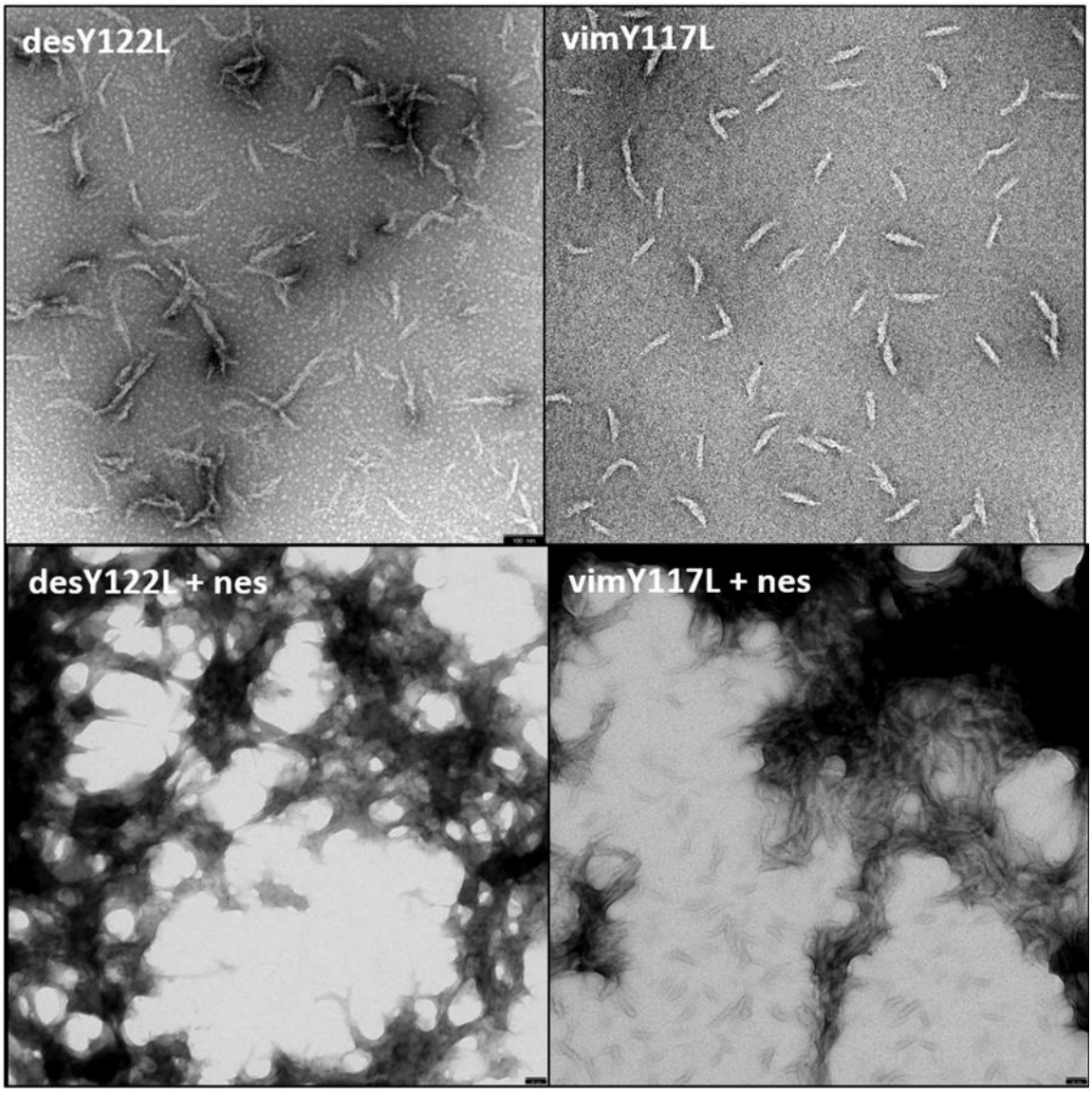

Figure 38 (page 62): Electron micrographs of negatively stained samples of mutant desminY122L and vimentinY117L assembled in the presence of tailless nestin. The addition of nestin resulted in shorter filaments in case of assembled desminY122L and ULFs for vimentinY117L, both coated with a huge proteinecous mass. Assembly was performed in 25 mM Tris-HCl, 50 mM NaCl, pH 7.5, at 37°C and stopped by adding 0.1% glutaraldehyde at 1 hour. The protein concentration for all samples was 0.1 g/l. (desY122L: desminY122L; vimY117L: vimentinY117L, nes: tailless nestin). Scalebar, 100 nm.

The sedimentation assay with the airfuge airfuge has not given a clear result due to the fact that under standard centrifugation conditions nestin was found completely within the pellet and no changes of the sedimentation characteristics of co-assembled mutant desmin or vimentin were visible (Figure 39). This might imply that the visualized coverage of the ULFs and short filaments formed by vimentinY117L and desminY122L was not specific or not very strong.

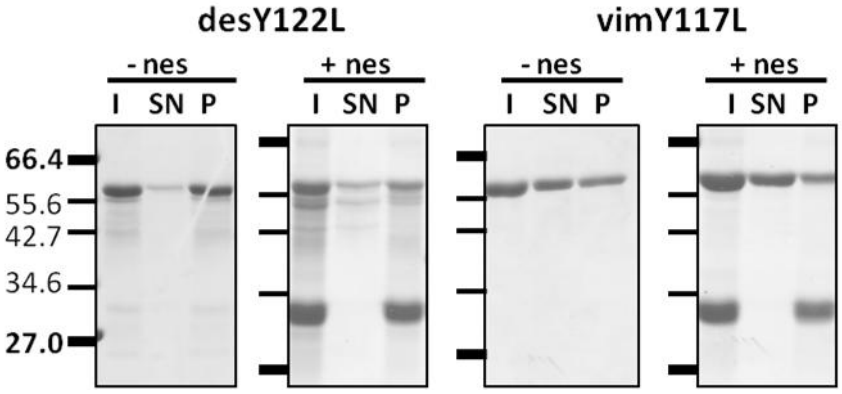

Figure 39: Sedimentation analysis of mutant desminY122L and vimentinY117L assembled in the presence of nestin. Nestin was found in all cases within the pellet without changing the sedimentation behaviour of the other proteins. The proteins were dialyzed into 5 mM Tris-HCl, pH 8.4 and assembly was performed at 37°C for 1 hour in 25 mM Tris-HCl, 50 mM NaCl, pH 7.5. After assembly, the samples were centrifuged at 30 psi for 15 minutes. The fractions are shown after separation by gel electrophoresis. (I: input; SN: supernatant; P: pellet; desY122L: desminY122L; vimY117L: vimentinY117L, nes: tailless nestin.).

Thus it was necessary to clarify the possible interaction shown by the electron microscope with a different technique, for example sucrose gradient centrifugation of the co-assembled proteins (Figure 40). The sedimentation profile of desminY122L was not changed through co-assembly with nestin. The proteins were found within fraction 11 corresponding to the 70% sucrose cushion like in the single protein assembly situation. The combination of vimentinY117L with nestin unveiled a slight interaction as a small amount of vimentinY117L was found within fraction 11 together with nestin. These vimentin/nestin complexes were clearly separated from the main peak of vimentinY117L which was recovered in fraction 4.

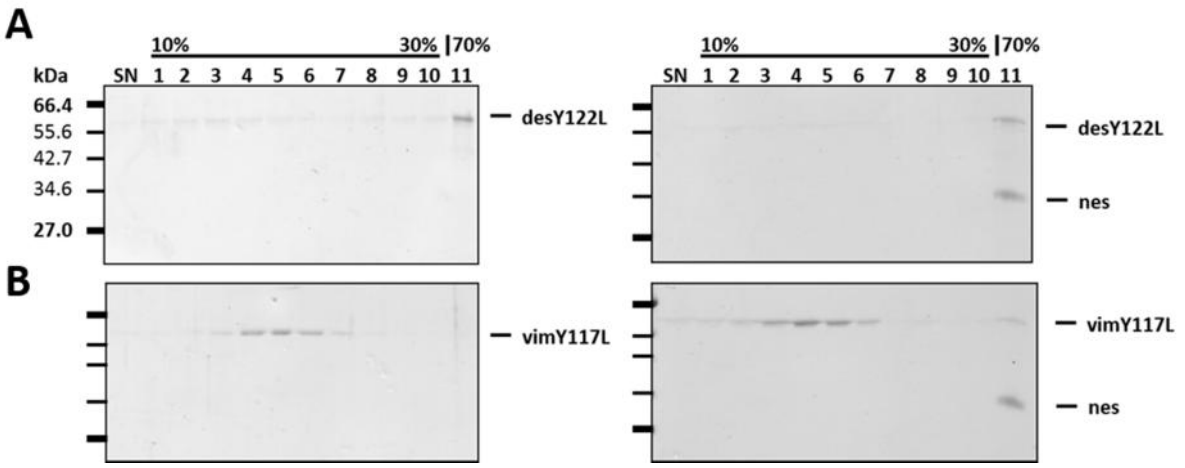

Figure 40: Sucrose gradient analysis of mutant desmin and vimentin assembled in the presence of nestin for 60 min. A: left side: DesY122L assembled for 1 hour; right side: DesY122L assembled for 1 hour in the presence of syn. **B:** left side: VimY117L assembled alone; right side: VimY117L assembled in the presence of synemin. The proteins were dialyzed into 5 mM Tris-HCl, pH 8.4 and assembly was performed in 25 mM Tris-HCl, 50 mM NaCl, pH 7.5, for 1 hour at 37°C. After assembly, the samples were centrifuged at 28.000 rpm, 4°C for 5 hours. The fractions are shown after separation by gel electrophoresis. (SN: supernatant; Fractions 1 – 10: 10 – 30 % sucrose gradient; 11: 70 % sucrose cushion; desY122L: desminY122L; vimY117L: vimentinY117L, nes: tailless nestin.)

2.5.3 Analysis of human desmin and vimentin assembled in the presence of tail-truncated nestin

For further investigation of the effect of nestin on the assembly process of desmin, we have analysed the *in vitro* assembly of desmin and vimentin renatured in a tetrameric state with or without nestin (Figure 41). Nestin was mixed with desmin in 9.5 M urea and the proteins were renatured together before they were co-assembled at 25 mM Tris-HCl, 50 mM NaCl, pH 7.5. Instead of filaments huge protein aggregates occurred, suggesting a strong interaction between nestin and desmin. The mix of nestin with tetrameric desmin after renaturation into 5 mM Tris-HCl, pH 8.4, followed by co-assembly, unveiled a filamentous network coated with protein aggregates. This finding indicates that desmin was able to form filaments with nestin on a tetrameric state. Vimentin mixed with nestin in the monomeric state and co-assembled for one hour was still able to form short filaments suggesting that the effect of nestin on the filament forming process of vimetin was not as strong as the effect on desmin. The protein aggregates found within the sample were smaller than the huge aggregates formed by nestin in co-assembly with desmin. When tetrameric vimentin was co-assembled with nestin for one hour, the protein aggregates were bigger but short filaments were still visible.

To verify the results of the electron microscopy, a sucrose gradient centrifugation was performed (Figure 42). Huge aggregates formed by co-assembled desmin and nestin mixed before renaturation were found within fraction 11. Therefore, no differences between the sedimentation profile of the mix and the solitary nestin or desmin were visible. When nestin was mixed with tetrameric desmin letting the proteins co-assemble for one hour, no differences in the sedimentation profile were detectable. The sedimentation profile of vimentin preassembled for one hour was changed through mixing it with nestin before renaturation. Co-assembled vimentin was found within all fractions with peaks, between fraction 10 and 11 and between fraction 2 and 3. Nestin was found within fractions 10 to 11, too. When nestin was mixed with vimentin on a tetrameric state, just before co-assembly, vimentin was found in all fractions with a peak between fractions 2 and 5, but less protein within fraction 11. Nestin on the other hand was found mainly within fraction 11. These results confirm the strong interaction between nestin and vimentin.

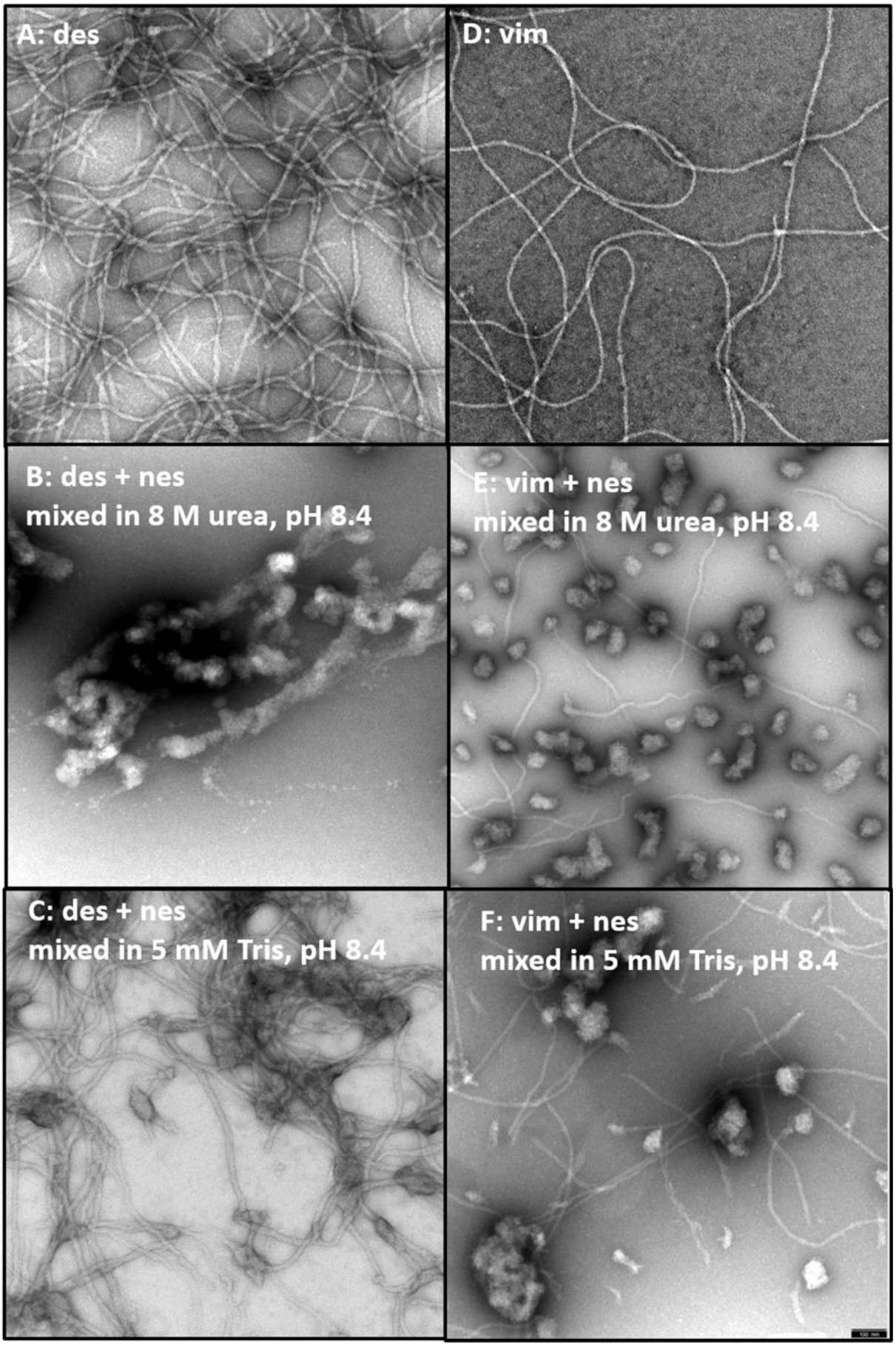
A: des
D: vim
B: des + nes
mixed in 8 M urea, pH 8.4
E: vim + nes
mixed in 8 M urea, pH 8.4
C: des + nes
mixed in 5 mM Tris, pH 8.4
F: vim + nes
mixed in 5 mM Tris, pH 8.4

Figure 41 (page 66): Electron micrographs of negatively stained samples of desmin and vimentin mixed with nestin before or after renaturation into 5 mM Tris-HCl, pH 8.5 and assembled together. (A): Desmin assembled for 1 hour revealed a filamentous network. **(B):** Desmin mixed with tailless nestin before renaturation resulted in huge proteinecous aggregates. **(C):** The co-assembly of desmin mixed with tailless nestin showed filaments covered with proteinecous masses **(D):** The assembly of vimentin for 1 hour created a filamentous network. **(E):** Vimentin mixed with tailless nestin before renaturation and co-assembled for 1 hour resulted in shorter filaments and roundish protein aggregates in between. **(F**) In case of the co-assembly of tailless nestin with vimentin mixed after renaturation, short filaments besides bigger protein aggregates were visible. Assembly was performed in 25 mM Tris-HCl, 50 mM NaCl, pH 7.5, at 37°C and stopped by adding 0.1% glutaraldehyde at 1 hour. (Des: desmin; vim: vimentin). Bar, 100 nm.

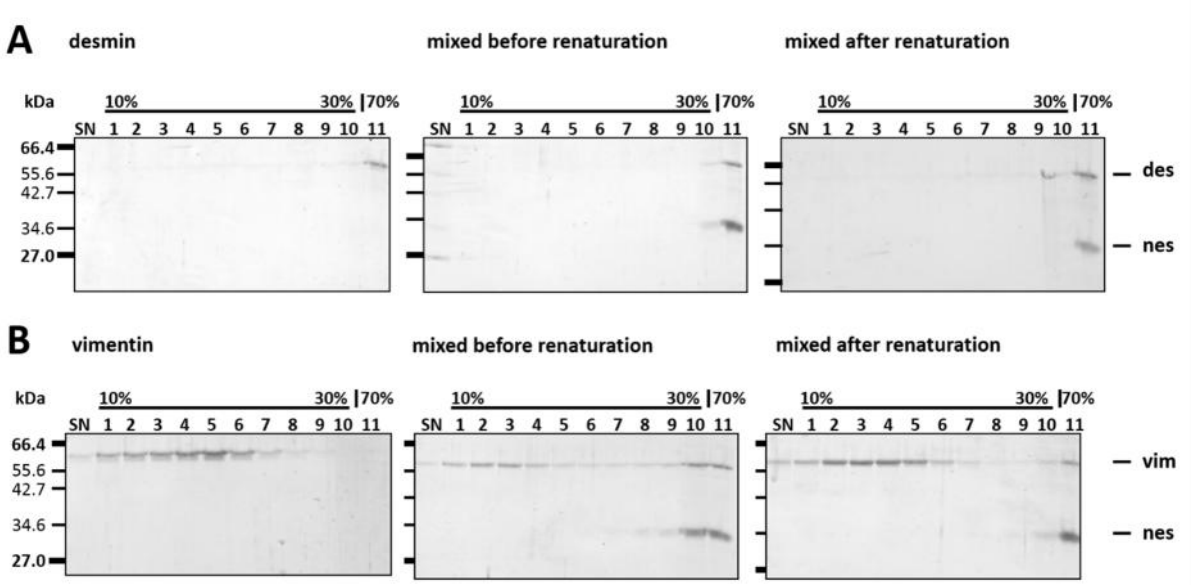

Figure 42: Sucrose gradient centrifugation of assembled desmin and vimentin mixed with nestin before or after renaturation. (A): Desmin mixed with tailless nestin before or after renaturation. (B): Vimentin mixed with tailless nestin before or after renaturation. The protein samples were dialyzed alone or together into 5 mM Tris-HCl, pH 8.4 and assembly was performed in 25 mM Tris-HCl, 50 mM NaCl, pH 7.5, at 37°C for 1 hour. After assembly, the samples were centrifuged at 28.000 rpm, 4°C for 5 hours. The fractions are shown after separation by gel electrophoresis. (SN: supernatant; Fractions 1 – 10: 10 – 30 % sucrose gradient; 11: 70 % sucrose cushion; des: desmin; vim: vimentin; nes: tailless nestin.)

2.6 Characterization of the binding site of desmin and vimentin for nestin

To characterise the binding site of desmin and vimentin for nestin, head- and tail-truncated variants of desmin and vimentin were used as shown above for synemin-L.

2.6.1 Co-assembly of truncated versions of human vimentin with tail-truncated nestin

To characterize the interaction of nestin with the truncated variants of vimentin, electron microscopy, sedimentation analysis as well as sucrose gradient centrifugation have been used. Under assembly conditions the typical nestin protein aggregates were found in the mix of nestin with vimentinΔhead and vimentin rod as visualized with the electron microscope (Figure 43). VimentinΔtail was able to form filament network in the presence of nestin, but the filaments were decorated with dense protein aggregates.

The cosedimentation analysis of the truncated variants of vimentin indicated no interaction of nestin with headless vimentin and the vimentin rod as the proteins were separated by centrifugation (Figure 44). Nestin was found in the pellet fraction while vimentinΔhead and vimentin rod were found in the supernatant due to their inability to form higher structures. In case of the cosedimentation of vimentinΔtail, it was not possible to predict if the visualized protein aggregates interacted with the filamentous network formed by vimentinΔtail. Both proteins were found in in the pellet fraction after centrifugation independent of being centrifuged themselves or in the mixture.

Figure 43 (next page): Electron micrographs of negatively stained samples of truncated variants of vimentin assembled in the presence of nestin. VimentinΔhead and vimentin rod were not able to form higher structures like filaments. VimentinΔtail was able to form an intact filament network within one hour of assembly. The mix of tailless nestin with vimentinΔhead and vimentin rod unveiled huge unordered protein aggregates besides smaller soluble structures. Mixing of vimentinΔtail with tail-truncated nestin did result in a filamentous network decorated with huge globular protein aggregates. Assembly was performed at 37°C in 25 mM Tris-HCl, 50 mM NaCl, pH 7.5, and stopped by adding 0.1% glutaraldehyde at 1 hour (vimΔhead: headless vimentin; vim rod: vimentin rod domain; vimΔtail: tailless vimentin; nes: tail-truncated nestin.). Bar, 100 nm.

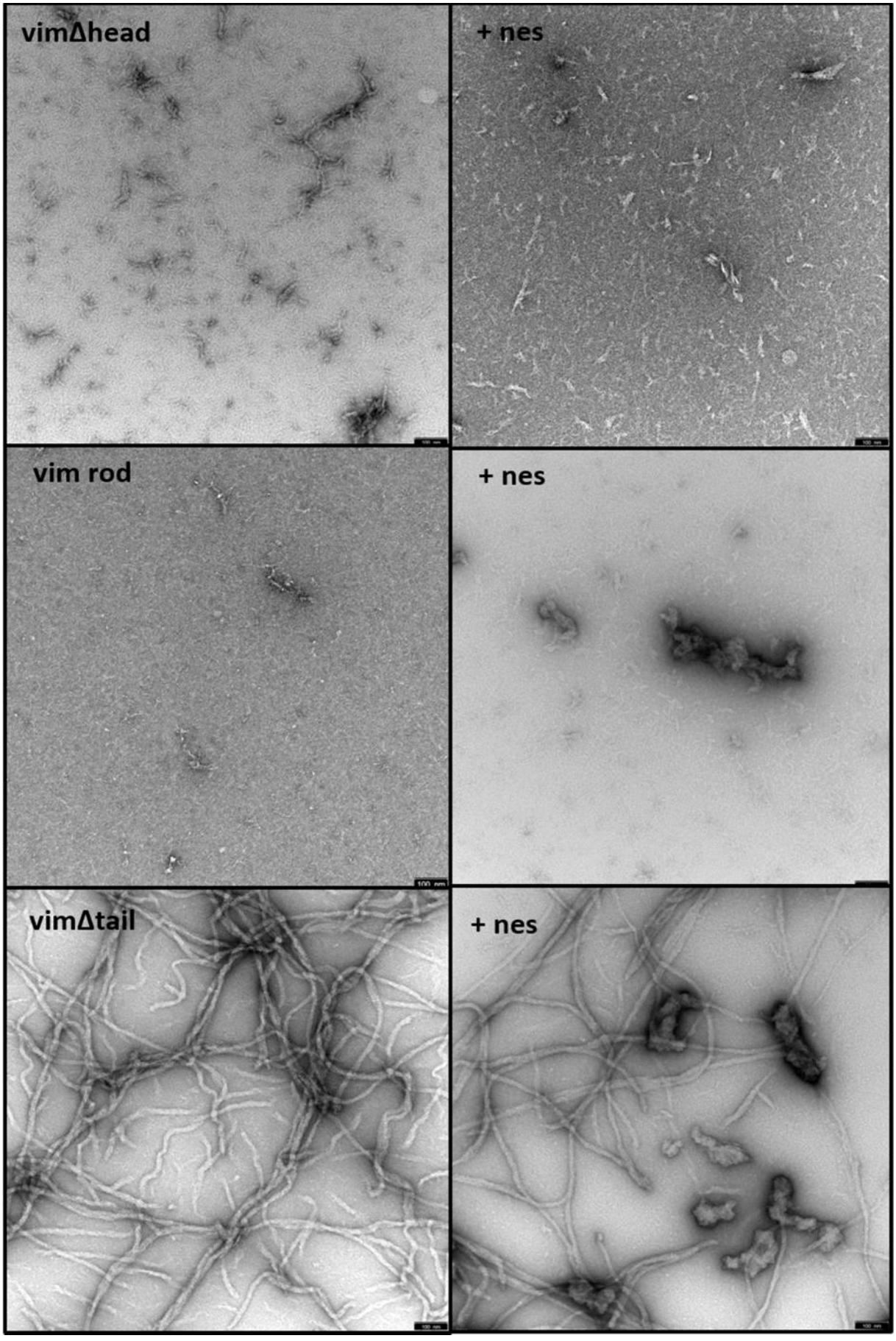
vimΔhead
+ nes
vim rod
+ nes
vimΔtail
+ nes

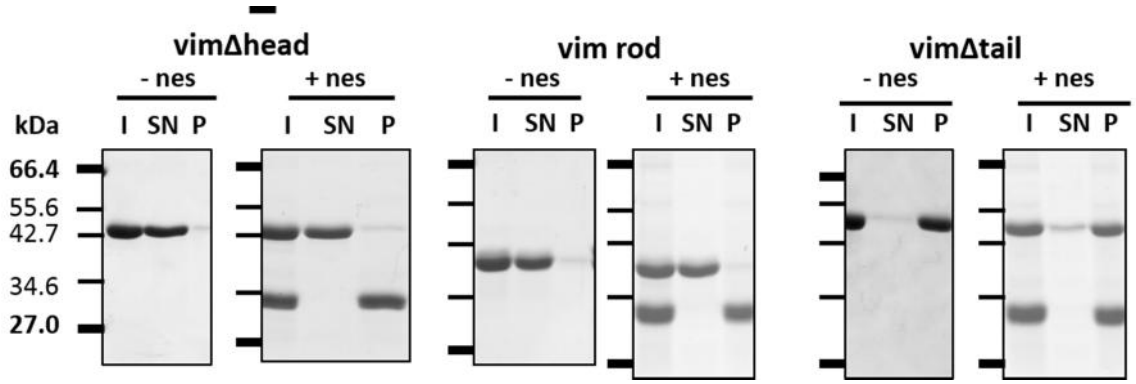

Figure 44: Sedimentation analysis of truncated variants of vimentin assembled in the presence of nestin. The sedimentation behaviour of all proteins was not changed through mixing nestin with the truncated variants of vimentin. The protein samples were dialyzed into 5 mM Tris-HCl, pH 8.4 and assembly was performed at 37°C in 25 mM Tris-HCl, 50 mM naCl, pH 7.5, for 1 hour. After assembly, the sample was centrifuged at 30 psi for 15 minutes. The fraction are shown after separation by gel electrophoresis. (I: input; SN: supernatant; P: pellet; vimΔhead: headless vimentin; vim rod: vimentin rod domain; vimΔtail: tailless vimentin; nes: tail-truncated nestin.).

The analysis of the sucrose gradient centrifugation (Figure 45) confirmed the separation of vimentinΔhead and vimentin rod from nestin, which was found within fraction 11 while the truncated variants of vimentin were found within the supernatant and fractions 1 to 2. In the case of vimentinΔtail, no interaction was detectable because the sedimentation profile of vimentinΔtail was not changed in presence of nestin.

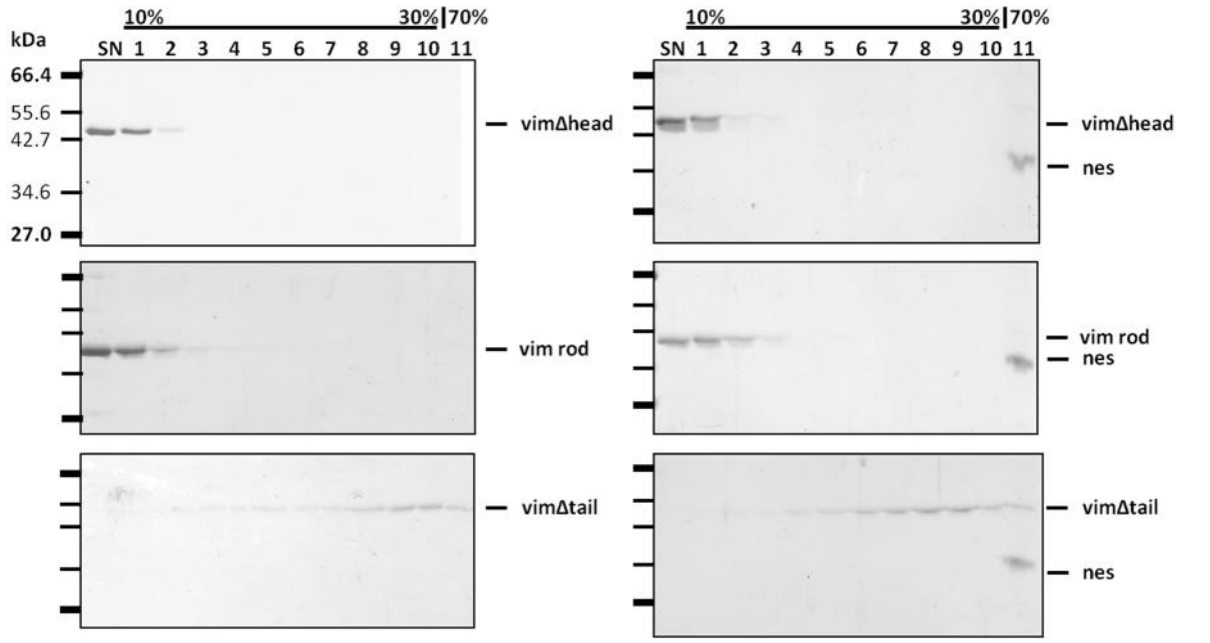

Figure 45: Sucrose gradient analysis of truncated variants of vimentin assembled in the presence of nestin for 60 min. The sedimentation behaviour of all proteins remained the same in the mixed situation compared with the single protein assembly. The proteins were dialyzed alone or together into 5 mM Tris-HCl, pH 8.4 and assembly was performed at 37°C, in 25 mM Tris-HCl, 50 mM NaCl, pH 7.5, for 1 hour. After assembly, the samples were centrifuged at 28.000 rpm, 4°C for 5 hours. The fractions are shown after separation by gel electrophoresis. (SN: supernatant; Fractions 1 – 10: 10 – 30 % sucrose gradient; 11: 70 % sucrose cushion; vimΔhead: headless vimentin; vim rod: vimentin rod domain; vimΔtail: tailless vimentin; nes: tail-truncated nestin.).

2.6.2 Co-assembly of truncated versions of human desmin with the head and rod domain of nestin

The characterization of the binding site of desmin for nestin showed a few differences in comparison to the characterization of vimentin. In electron microscopic analysis, the co-assembled sample of desmin rod and nestin showed proto-filamentous structures (Figure 46). But in the sedimentation assay and sucrose gradient centrifugation, no interaction of desmin rod with nestin was detectable (Figure 47 and Figure 48). Similar to vimentinΔtail, the filament network of desminΔtail was decorated with globular structures. But the interaction was not detectable with standard centrifugation assays as desminΔtail was accumulated in the pellet in sedimentation assay and to the fraction 11 in the sucrose gradient centrifugation with or without nestin.

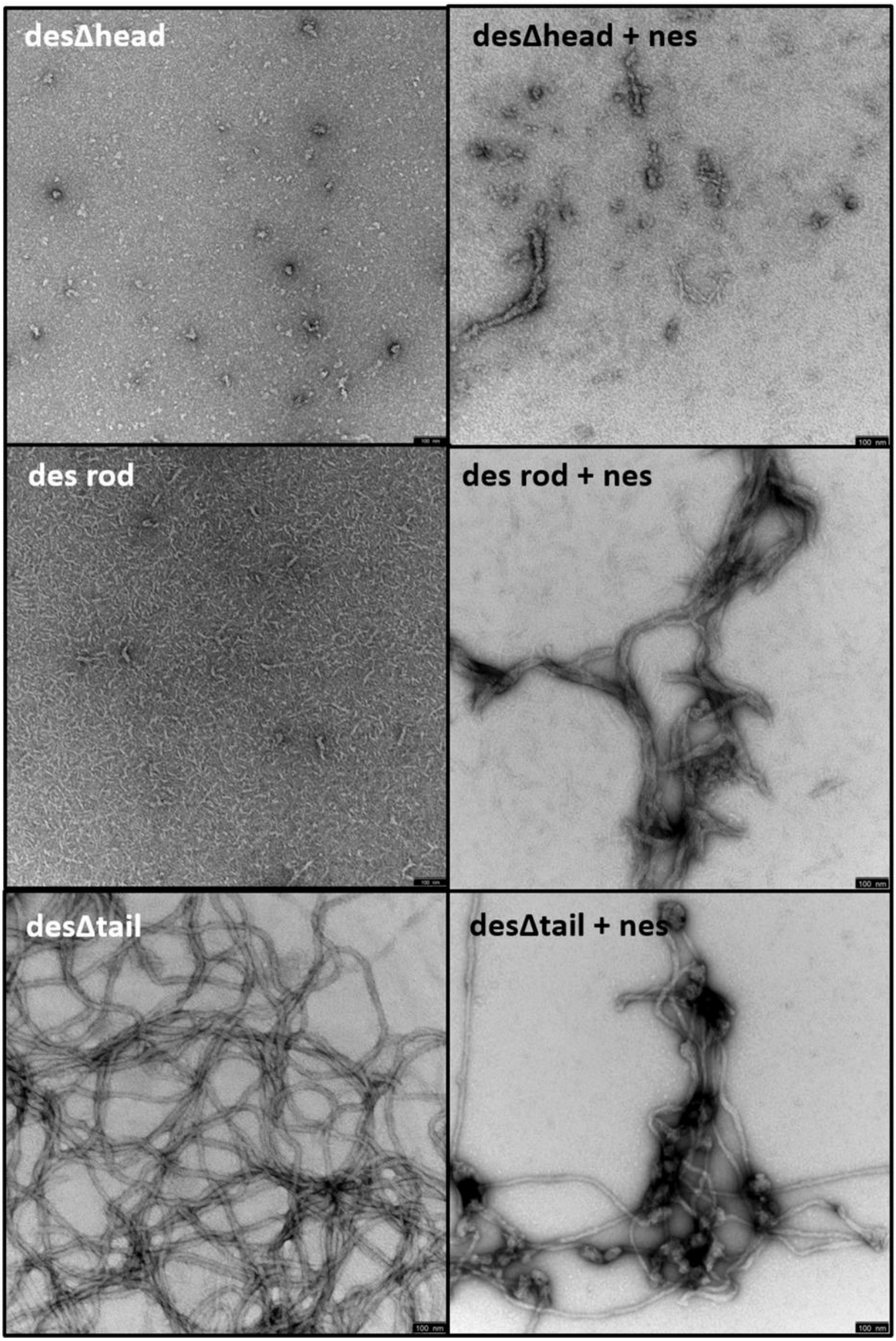
desΔhead
desΔhead + nes
des rod
des rod + nes
desΔtail
desΔtail + nes
100 nm

Figure 46 (page 72): Electron micrographs of negatively stained samples of truncated variants of desmin assembled in the presence of nestin. Headless desmin and desmin rod were not able to form higher structures like filaments. Tailless desmin was able to form an intact filament network within one hour of assembly. The mix of nestin with desminΔhead unveiled protein aggregates besides smaller soluble structures. The co-assembly of tailless nestin and desmin rod showed pseudofilamentous strcutures besides soluble protein. DesminΔtail co-assembled with nestin did result in fialments covered with small protein aggeragetes. Assembly was performed at 37°C in 25 mM Tris-HCl, 50 mM NaCl, pH 7.5 and stopped at 60 min by addition of 0.1 % glutaraldehyde. (desΔhead: headless desmin; des rod: desmin rod domain; desΔtail: tailless desmin; nes: tailless nestin.). Bar, 100 nm.

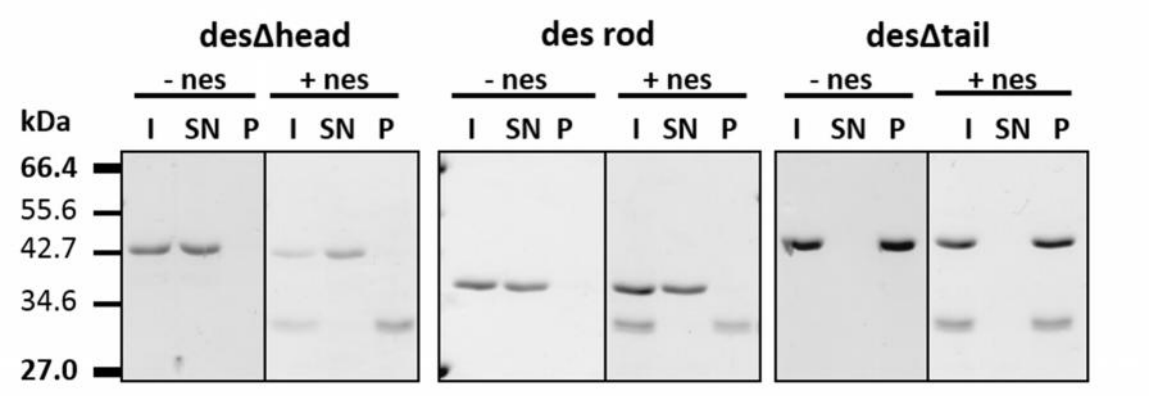

Figure 47: Sedimentation analysis of truncated variants of desmin assembled in the presence of nestin. The proteins did not change their sedimentation behaviour through mixing with nestin. The proteins were dialyzed into 5 mM Tris-HCl, pH 8.4 and assembly was performed in 25 mM Tris-HCl, 50 mM NaCl, pH 7.5, for 1 hour at 37°C. After assembly, the samples were centrifuged at 30 psi for 15 minutes. The fractions are shown after separation by gel electrophoresis. (I: input; SN: supernatant; P: pellet; desΔhead: headless desmin; des rod: desmin rod domain; desΔtail: tailless desmin; nes: tailless nestin.).

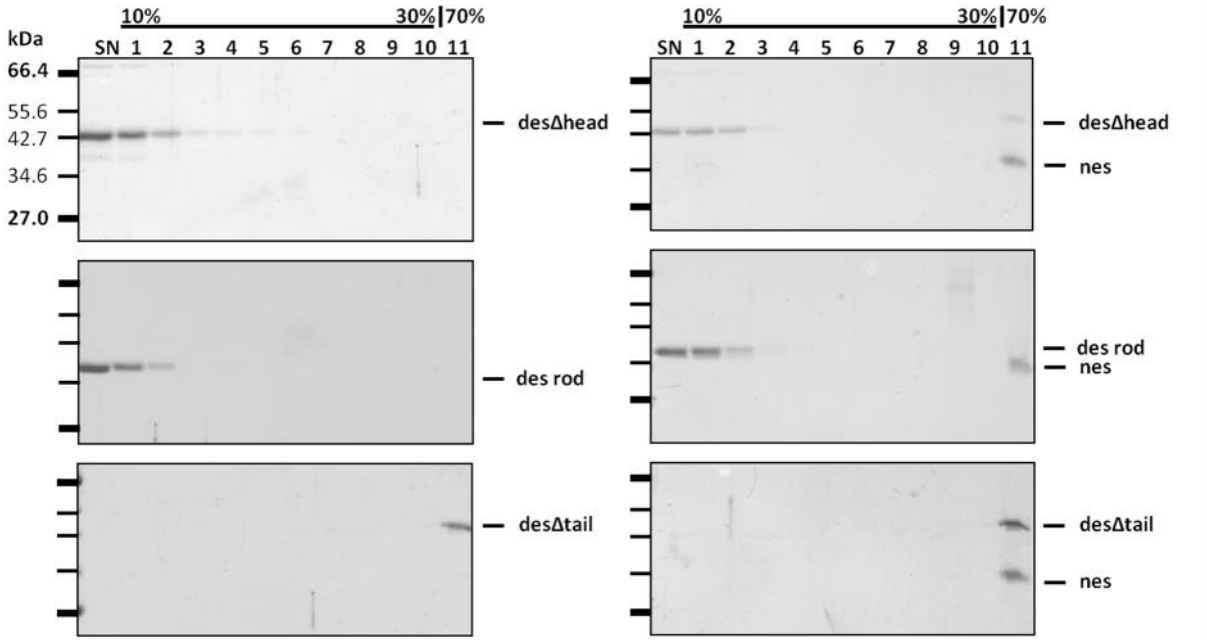

Figure 48: Sucrose gradient analysis of truncated variants of desmin assembled in the presence of nestin for 60 min. The proteins did not change their sedimentation behaviour through co-assembly with nestin. The protein samples were dialyzed into 5 mM Tris-HCl, pH 8.4 and assembly was performed in 25 mM Tris-HCl, 50 mM NaCl, pH 7.5, for 1 hour at 37°C. After assembly, the samples were centrifuged at 28.000 rpm, 4°C for 5 hours. The fractions are shown after separation by gel electrophoresis. (SN: supernatant; Fractions 1 – 10: 10 – 30 % sucrose gradient; 11: 70 % sucrose cushion; desΔhead: headless desmin; des rod: desmin rod domain; desΔtail: tailless desmin; nes: tail-truncated nestin.).

3 Discussion

The major differences of intermediate filaments (IFs) to the other two major cytoskeletal systems of vertebrate cells microtubules and microfilaments are besides the development- and tissue- specific expression of the 70 different IF proteins the nucleotide-independent assembly into apolar fibrous structures (Harald Herrmann et al. 2009). The IF network of muscle cells is located at the z-discs and links internal organelles like the mitochondria and nuclei to the contractile apparatus. Vimentin and desmin are the major type III IF proteins besides type IV IF proteins like synemin-H, -M, nestin and syncoilin. The proteins are expressed differential in muscle development and maintenance. Some point mutations within desmin lead to a distinct subgroup of myofibrillar myopathies, called desminopathies connected with morphological and functional damage. Desminopathies are characterized by protein aggregates found within the muscle fibres. In these aggregates, other proteins like synemin and nestin are found besides desmin. The possible role of these proteins in the aggregation process is not yet understood. Moreover, the interaction of wildtype desmin with synemin and nestin is not systematically characterized. Therefore, this thesis is a step in understanding the interaction of synemin and nestin with desmin and vimentin.

3.1 Synemin and nestin, real IF proteins or IF associated proteins?

The tail domain of synemin offers a broad interaction basis for non-IF proteins. Synemin is supposed to be an A-kinase anchoring protein in the heart and therefore connects protein kinase A (PKA) to the cytoskeleton. Moreover, an overexpression of synemin together with an increase in PKA targeting has been shown in failing hearts (Russell et al. 2006). An abnormal accumulation of synemin together with desmin was demonstrated in patients with myofibrillar myopathies, inclusion body myositis, dermatomyositis, oculopharyngeal muscular dystrophy and denervation atrophy

(Olivé et al. 2003). During muscle atrophy, desmin's head domain is phosphorylated at Ser28, Ser32 and Ser68. The phosphorylation of desmin leads to its association with TRIM32 and therefore to the disassembly of desmin and its degradation (Cohen et al. 2012). The downregulation of synemin in hepatocellular carcinoma has been shown to have no destabilizing effect on the cytoskeleton *in vivo* (Liu et al. 2011). Moreover, synemin is thought to be an antagonist of protein phosphatase A (PP2A) and therefore a promoter of AKT-dependent glioblastoma cell proliferation (Pitre et al. 2012). PP2A has been shown to be directly connected to dephosphorylation of vimentin (Turowski et al. 1999). This data suggests that synemin is important for the assembly and disassembly process of desmin and vimentin. Interestingly, metavinculin, a binding partner of synemin, is able to sever actin filaments through its tail domain (Janssen et al. 2012). Therefore, it might be possible that synemin is involved in connection and disconnection of the intermediate filament network to the sarcolemma and therefore to the assembly, structural organization and disposition of the IF network and cytoskeletal cross-talk in muscle cells (Sihag et al. 2007).

Nestin plays an important role in early stages of myogenesis as it regulates the cleavage of the Cdk5 activator protein p35 to its degradation-resistant form, p25. Therefore, nestin is able to inhibit the activation of Cdk5 by p25, which is critical for the progress of differentiation (Pallari et al. 2011). Moreover, Cdk5 regulates the organization of the nestin scaffold. In the bidirectional relationship between nestin and Cdk5, Cdk5 regulates the organization and stability of its own nestin scaffold and therefore the association with p35 (Sahlgren et al. 2003). Besides its role in myogenesis, nestin promotes the phosphorylation-dependent disassembly of vimentin filaments into aggregates during mitosis (Chou et al. 2003). This disassembly is induced through the phosphorylation of ser55 within the head domain of vimentin by the M-phase-promoting factor. Interestingly, nestin's functionality is not coupled to its incorporation into the cytoskeleton shown in NES-/- neural stem cells (Park et al. 2010).

3.1.1 Comparison of the amino acid sequences of synemin and nestin with desmin and vimentin.

As a first step of this thesis, we have investigated the specific sequence alignment features desmin and vimentin in comparison to synemin and nestin and used the visualization system designed to compare the differences of the proteins (Strelkov et al. 2002). The amino acid sequences of synemin and nestin have some characteristics untypical for intermediate filament proteins. The head domain of nestin is only eight amino acids long, the head of synemin at least ten amino acids. The importance of the positive charges of the head domain for tetramer formation has been shown before for vimentin. The short head domain of nestin lacks any arginine and therefore any binding site, while synemin has one arginine.

The alpha helical structure of the rod domain of intermediate filament proteins bases on the typical heptadic with hydrophobic amino acids at position *a* and *d*. The highly conserved LNDR motif within the beginning of coil 1A is altered in nestin and synemin (Figure 49-(1)). The typical heptadic pattern is partly changed by acidic and basic amino acids at position *a* and *d*. On the other hand, highly conserved motives of basic and acidic amino acids within the coil domain are partly replaced by unpolar amino acids (Figure 49-(2) and -(3)). Within the beginning of coil 2, the typical DLTAALRDIRAQ (ghijkabcdef) sequence is found in desmin and vimentin (Figure 49-(4)). In case of synemin and nestin, the beginning of the coil 2 domain is dominated by a heavy introduction of prolines, which are considered as alpha helic breaking motif. Moreover, for synemin an abnormal accumulation of hydrophobic amino acids within coil 2 (YALLVA) is visible (Figure 49-(5)). The highly conserved TYRKLEGEE motif at the border to the tail domain is disrupted in nestin and synemin-L as both lack the lysine and the third glutamic acid (Figure 49- (6)). Moreover, it has been shown that the head domain, the TAAL motif and the TYRKLLEGEE motif of vimentin are needed for synemin to gain the ability to assemble (Khanamiryan et al. 2008).

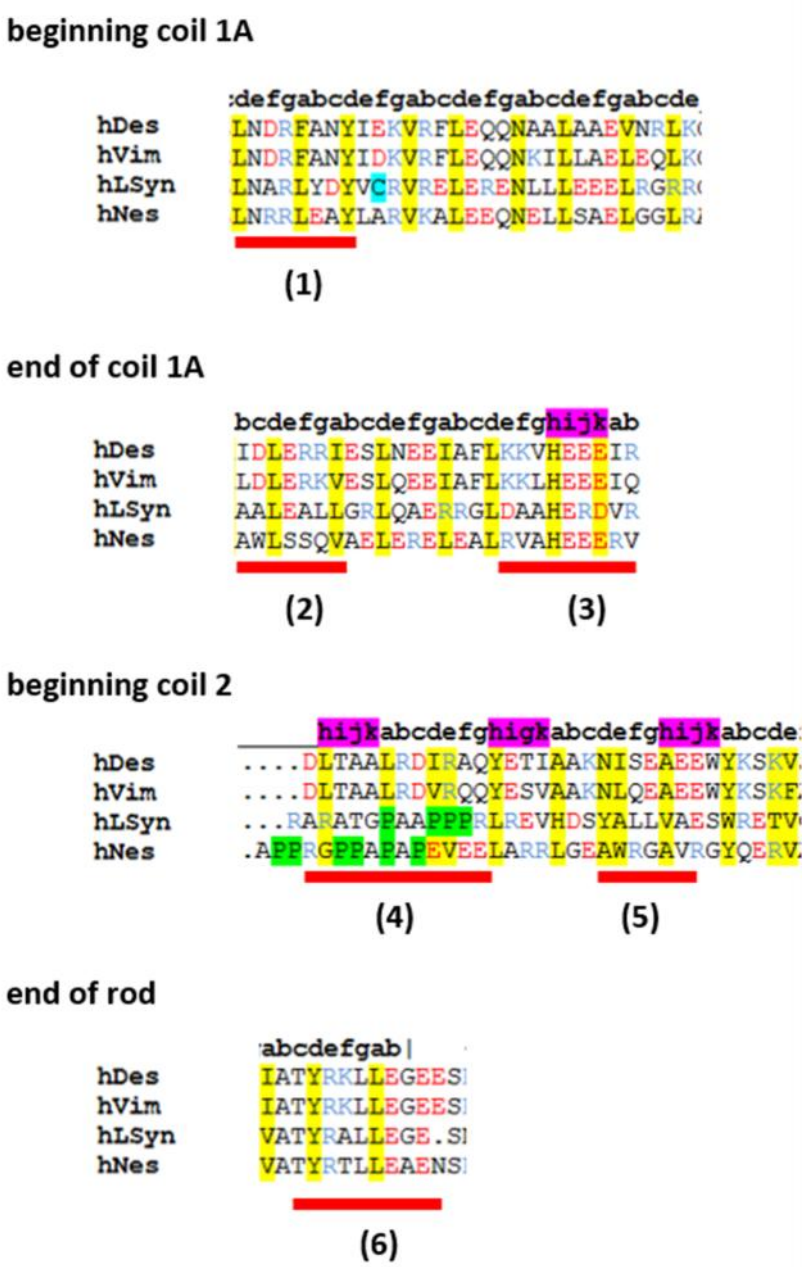

Figure 49: Differences in protein sequence of synemin and nestin compared with desmin and vimentin. **(1)** Thie highly conserved IF specific motiv at the beginning of the rod domain LNDRFANY differ in case of synemin and nestin. **(2/3)** The conserved hydrophobic amino acids at *a* and *d* position within the rod domain are flanked by less charged amino acids in case of synemin and nestin. **(4)** The beginning of coil 2 is dominated by a proline –rich motif in case of synemin and nestin in comparison to vimentin and desmin. **(5)** Within Coil 2, a hydrophobic accumulation in case of synemin-L and an oppositional charge in case of nestin were detectable. **(6)** The highly conserved TYRKLLEGEE-motif is disrupted in synemin and nestin. Both lack the lysine and the third glutamic acid. Amino acids are written in the one-letter-code. Above the sequence repeat pattern were indicated. **(**hDes: human desmin; hVim: human vimentin; hLSyn: human synemin-L; hNes: human Nestin)

3.1.2 The renaturation behaviour of synemin-L and nestin.

To prevent any interference of the long tail-domains of nestin and synemin-H or synemin-M, we have produced and purified a tail truncated variant of nestin and the shortest isoform of synemin, synemin-L. As the tail domain of IF proteins is not needed for *in vitro* assembly and in the case of K8/K18 and vimentin as well as desmin in transfected cells (Bader et al. 1991; H Herrmann, Hofmann, and Franke 1992), an interpretation of the IF typical behaviour of the muscle specific isoforms of synemin should be possible with the shorter natural variant, synemin-L and with the tail-truncated variant of nestin. The three isoforms of synemin only differ in the tail domain while the head and the rod domain are the same.

After renaturation from 8 M urea into 5 mM Tris-HCl, pH 8.4, an opposing behaviour of synemin and nestin was observed using analytical ultracentrifugation. Synemin-L remained monomeric with an *s*-value of 2.4 S. Also, this is true for the other tested renaturation buffers except HEPES buffers. This data suggests that synemin is unlike vimentin or desmin unable to form tetramers in the standard renaturation buffers. A similar observation was made for keratin 18, which is unable to form homodimers during dialysis while its obligatory co-assembly partner K8 is able to (Lichtenstern et al. 2012). The same has been shown for NF-M and NF-H which are unable to form homodimers and need NF-L to form heterodimers (Leung and Liem 1996).

In contrast, nestin was able to form higher structures with an *s*-value of 33.1 s in 5 mM Tris-HCl, pH 8.4. Moreover, nestin showed a strong pH sensitive behaviour by decreasing the *s*-value to 20.9 S at high pH (5 mM Tris-HCl, pH 9.5) and increasing the *s*-value to 138.2 S at physilogical pH (5 mM Tris-HCl, pH 7.5). Using the software *DCDT+*, the predicted molecular mass was with 72.12 kDa connected to a dimeric structure for nestin in 5 mM Tris-HCl, pH 9.5. This result is comparable with the work of Steinert suggesting that nestin is able to form homodimers (Steinert et al. 1999).

3.1.3 Assembly properties of synemin-L and nestin

It has been shown before that synemin is not able to form filaments on its own but globular structures under different *in vitro* assembly conditions (Bilak et al. 1998). In an environment where NF-H is able to form short, tortuous filaments, synemin has shown the same behaviour (Gardner, Dahl, and Bignami 1984).

One of our aims was to characterize the self-assembly incompetent behaviour of synemin-L in detail. As a first result, synemin showed a less salt dependent behavior than desmin or vimentin. The increasing of the ionic strength up to 50 mM NaCl in a buffer containing 5 mM Tris-HCl, pH 7.5, led to a less remarkable increase of the *s*-value to 3.4 S. Meanwhile, sedimentation velocity runs of synemin observed in buffers with increased amount of Tris-HCl, pH 7.5, showed an ordered three-step-process of aggregation. In 10 mM Tris-HCl, pH 7.5, only the smallest *s*-value of 3.0 S occured. In 30 mM Tris-HCl, pH 7.5, two additional *s*-values at 13.3 S and 27.0 S were detectable. The second *s*-value was about 4 times higher than the first and the third *s*-value was two times higher than the second s-value. In case of 50 mM Tris-HCl, pH 7.5, the three s-values were around 15.2 S, 27.8S and 39.9 S. Again, the step between 15.2 S and 27.8 S was about two times higher and the last *s*-value 39.9 S was one and a half times higher than the second *s*-value.

In 25 mM Tris-HCl, pH 7.5, an ordered process has also been observed but in this conditional setting only two s-values occured and the second s-value was about four times higher than the first *s*-value. In 25 mM Tris-HCl, 50 mM NaCl, pH 7.5, synemin had a distinct *s*-value with 24.2 S. This *s*-value is comparable to the s-value of 26.7 S in more physiological buffer 2 mM NaPi, 100 mM KCl, pH 7.5. In 25 mM Tris-HCl, 100 mM NaCl, pH 7.5, the distinct *s*-value occured at 75.9 S. It was three times higher than for 25 mM Tris-HCl, 50 mM NaCl, pH 7.5. In the tested buffer with the highest ionic strength, the increase of the distinct *s*-value was about four times higher than in 25 mM Tris-HCl, 50 mM NaCl, pH 7.5. In electron microscopic analysis, the assembly of synemin in 25 mM Tris-HCl, 50 mM NaCl, pH 7.5, resulted in protofilament-like structures but with increasing the ionic strength the aggregated protein sample turned into more globular structures.

Again, synemin and nestin differ in their individual behaviour in 25 mM Tris-HCl, 50 mM NaCl, pH 7.5. Through an ordered process synemin formed aggregates of

distinct size and *s*-values depending on the ionic strength. On the other hand, nestin formed bigger, unordered heterogeneous aggregates as visualized with electron microscope. This aggregates were found within the 70% sucrose fraction and in the pellet of sedimentation analysis.

3.1.4 Impact of synemin and nestin on the filament forming process of vimentin and desmin.

To analyse the potential interaction of synemin and nestin with desmin during its renaturation into tetramers, the proteins were mixed with desmin in the monomeric and a tetrameric state. Both proteins interact with desmin during renaturation as the two distinct s-values of both mixes were changed compared with the *s*-values of the single proteins.

In case of synemin, a shift from 2.8 S and 9.1 S of single proteins to 3.5 S and 12.9 S occured. The second *s*-value at 12.9 S of the mixed protein sample accorded to the addition of the *s*-values of the structure formed by desmin alone and the first *s*-value of the mix before renaturation in 10 mM Tris-HCl, pH 7.5. For nestin and desmin, the mix of the proteins led to a decrease of boh *s*-values of the single proteins from 9.7 S and 42.5 S to 7.6 S and 35.5 S, indicating an interaction. The shift in both cases represented the fact that the interaction of nestin and synemin with desmin creates two new species. When the proteins were mixed after dialysis, synemin had a negative effect on the tetrameric desmin to form higher structures within 10 mM Tris-HCl, pH 7.5, as the mix had two distinct *s*-values around 2.4 S and 6.2 S. Moreover, nestin did not interact with desmin on a tetrameric state because the s-values of the mix were comparable to the *s*-values of the single proteins. The fact, that nestin had the same *s*-value within 10 mM Tris-HCl, pH 7.5, and 5 mM Tris-HCl, pH 8.4, showed that the higher amount of buffering Tris-HCl prevented the aggregation seen in 5 mM Tris-HCl, pH 7.5.

To analyse the interaction of synemin and nestin with type III IF proteins in a ULF-like state, the mutant vimentin Y117L and desmin with a mutation on the equivalent position Y122L were used. VimentinY117L stayed in a ULF-like state with an *s*-value of 33.4 S time-independent. DesminY122L was able to form longer filaments within an hour of assembly, but they were shorter than for wildtype desmin and with a

distinct *s*-value around 138.6 S. The combination of syemin with desminY122L and vimentinY117L on different stages of renaturation and assembly revealed one single *s*-value around 96.7 S for desminY122L and 54.2 S for vimentin Y117L after one hour of co-assembly with synemin. This specific *s*-value showed that the interaction of synemin with desmin and vimentin is very specific, leading to one species of aggregated proteins visible with the electron microscope. On the other hand, the mix of nestin with desminY122L and vimentinY117L after dialysis followed by an assembly in 25 mM Tris-HCl, 50 mM NaCl, pH 7.5, showed no interaction detectable with the standard sucrose gradient centrifugation. Anyway, the elctron microscopic analysis unveiled clotted ULFs in case of vimentinY117L and clotted longer filaments in case of desminY122L indicating at least a lateral interaction of nestin with desmin and vimentin on a ULF-like state.

The co-assembly of synemin with desmin led to shorter filaments connected by globular structures in all cases of co-assembly representing a very specific binding of synemin on the forming desmin filaments. In the case of vimentin, co-assembly with synemin caused the strong binding of synemin to vimentin and thus prevented further assembly of vimentin after addition of synemin. Desmin retains some residual ability to form filaments through its higher speed of assembly which is five time higher than that of vimentin. The electron micrographs of the co-assembly of nestin with desmin and vimentin unveiled a different behaviour of nestin. In the case of nestin mixed with desmin before dialysis, huge non-ordered protein aggregates without filaments were visible while in the case of vimentin mixed with nestin before dialysis, short filaments besides smaller roundish protein aggregates were observed. These aggregates were bigger than those observed with synemin. Moreover, the co-assembly experiment of nestin with vimentin confirmed that nestin is only to some extent interacting with vimentin as shown with sucrose gradient centrifugation (Steinert et al. 1999).

3.1.5 Characterization of the binding site of desmin and vimentin for nestin and synemin

In order to characterize the binding domain of type III IF proteins for synemin, we have used short fragments of desmin as described before (Bär et al. 2009). The sedimentation behaviour of the truncated desmin variants containing the first half of desmin (desminΔC240 - desminΔC300) differed from the sedimentation behaviour in standard sedimentation assay shown by Bär suggesting an impact of the sucrose on the sedimentation behaviour of the first half of desmin. It has been shown that actin as well as microtubules are also able to assemble without nucleotides in presence of sucrose (Kasai, Nakano, and Oosawa 1965; Shelanski, Gaskin, and Cantor 1973). Therefore it might be possible that all assembled variants of desmin containing the first half were able to form huge structures through sucrose and sedimentate into the pellet fraction.

With this approach, we were able to locate the binding domain within an area of 155 amino acids of the first part of the rod domain as synemin changed its sedimentation behaviour in presence of the trunctated variants of desmin containing the first half. The binding site is between amino acids from 85 to 240. It was suggested before that desmin mutations in the terminal consensus motif TYRKLLEGEE prevent synemin - desmin heteropolymer filament assembly correlated to the abnormal salt bridges of desmin- dimers (Chourbagi et al. 2011). Plectin, a known cytolinker, interacts with desmin via binding motifs within the region from aa 109 to aa 288 of their rod domain (Favre et al. 2011). Moreover, plectin is thought to link IFs to costameric sarcolemma through synemin-M, α-dytrobrevin and actin (Hijikata et al. 2008). On the other hand, Nestin interacts with full length vimentin as shown by sucrose gradient centrifugation. But no interactions of the truncated variants of vimentin (vimentinΔhead, vimentin rod and vimentinΔtail) were detectable as the proteins did not change their sedimentation behaviour in presence of nestin. This result might indicate that for the interaction full length vimentin is needed or that the interaction is not specific as thought before. In case of desmin, the standard sucrose gradient centrifugation was not usable to distinguish wether the interaction of nestin with desmin is mediated by the head and rod domain of desmin due to the fact that desminΔtail sedimentated down to the pellet with or without nestin. In electron microscopic analysis of desminΔtail mixed with nestin, huge protein aggregates are visible besides an intact filamentous

network. It has been shown that desminΔhead and desmin rod do not change their sedimentation behaviour in presence of nestin. But in case of desmin rod assembled with nestin, peudo-filamenteous strcutures are visualized with electron microscopy. This finding needs further investigation.

4 Conclusion & Outlook

There is general consensus that synemin and nestin are IF proteins proper. However, our functional studies do question this conception. Due to the differences in amino acid sequence and domain organization, it was necessary to analyse synemin and nestin systematically for IF protein typical interactions and the ability to form heteropolymers together with their thought interaction partners desmin and vimentin *in vitro*.

Like NF-H, NF-M and keratin 18, synemin is unable to form dimers or tetramers on its own as shown in sedimentation velocity runs. But synemin is able to interact with desmin during dialysis in order to form higher structures. The combination of synemin with desmin after renaturation of desmin into tetrameric state shows a negative interaction without starting the *in vitro* assembly established for desmin and vimentin. Under assembly conditions, synemin interacts strongly with vimentin and desmin. This interaction has a negative impact on the assembly process of desmin and vimentin. The binding is mediated by a binding domain within the first 155 amino acids of the rod domain of the type III IF proteins as shown with truncated variants of desmin. This data suggests that synemin is an IF associated protein which connects the IF network to the sarcomere.

Nestin showed a very pH-sensitive behaviour. By decreasing the pH to 7.5, more protein has been found in the pellet fraction in 5 mM Tris-HCl. The huge protein aggregates formed by single nestin showed an unstructured form in assembly conditions established for desmin and vimentin. The co-assembly situation of vimentin and desmin mixed with nestin after renaturation unveiled an intact filamentous network covered with huge protein aggregates. The sucrose gradient centrifugation have shown an interaction of nestin with vimentin to some extend. Meanwhile, the mutant type III IF proteins unable to form higher structures than ULFs in case of vimentinY117L or short filaments in case of desminY122L show the same

phenomenon in presence of nestin under assembly conditions by being covered with a huge proteineous carpet. The characterization of the binding domain remained unclear due to the fact that no change in the mixes with truncated variants was observed in sucrose gradient centrifugation. This could mean that nestin needs full-length type III IF proteins or the used assembly conditions are not the right approach to analyse the interaction of nestin with desmin and vimentin. These data suggest that nestin interact with vimentin and desmin in a more lateral way and therefore act as an IF associated protein. To characterize the molecular interaction of nestin with vimentin and desmin, further *in vitro* and *in vivo* investigations are needed.

Eventually, a better understanding of the interaction of the IF associated proteins synemin-L and nestin with type III IF proteins desmin and vimentin may contribute to the comprehension of the development and tissue specific connection of the IF network to other cell compartiments.

5 Material

Enzymes were obtained from Roche Diagnostics (Mannheim). Chemicals were obtained from the following companies: Fluka (Neu-Ulm), Gerbu (Gaiberg), GIBCO BRL (german department in Berlin and Eggenstein), Merck (Darmstadt), Pharmacia (Freiburg in Breisgau), Qiagen (Hilden), Riedel-de Haen (Seelze), Roth (Karlsruhe), Serva (Heidelberg), Sigma (Munich)

5.1 Media & Solutions

5.1.1 Molecular biological methods

5.1.1.1 Amplification of cDNA by PCR

5x Phusion buffer:	20 mM Tris-HCl, pH 7.4
	0.1 mM EDTA
	1 mM DTT
	100 mM KCl
	0.5 % Tween20
	0.5 Nonident P 40
	200 µg/ml BSA
	50 % Glycerol

100% DMSO

5.1.1.2 Mutagenesis

10x Pfu buffer:	100 mM KCl
	100 mM $(NH_4)2SO_4$
	200 mM Tris-HCl; pH 8.8
	20 mM $MgSO_4$
	1 % Triton X-100
	1 mg/ml nuclease-free BSA
NZY^+ broth (autoclaved)	10 g NZ amin (casein hydrolysate)
	5 g yeast extract
	5 g NaCl
	20 g agar
	add dd H_2O to 1 litre
	pH 7.5, calibrated with 5 N NaOH

5.1.1.3 Agarose gel electrophoresis

1xTAE	40 mM Tris-HCl; pH 8.0
	0.12 % conc. acetic acid
	1 mM EDTA
6xDNA agarose gel	100 mM Tris-HCl; pH 7.5
	200 mM EDTA
	0.01 % bromophenol blue (w/v)
	30 % Ficoll (W/v) type 400
	0.01 % xylene cyanol (w/v)

5.1.1.4 QIAquick PCR purification kit

For the composition of the buffers PB, PE and EB see handbook of Qiagen (Hilden)

Ligation of DNA fragments

10x ligation buffer	300 mM Tris-HCl, pH 7.4
	100 mM $MgCl_2$
	100 mM DTT
	10 mM ATP

5.1.1.5 Plasmid preparation

For the composition of the buffers P1, P2, P3, PB, PE, EB, QBT, QC and QF see the handbook of Qiagen (Hilden)

100% Isopropanol

TE	10 mM Tris
	1 mM EDTA, pH 8.0

5.1.2 Proteinbiochemical methods

5.1.2.1 SDS-PAGE

3x Laemmli sample buffer	187.5 mM Tris-HCl; pH 6.8
	150 mM DTT
	0.2 % bromophhenol blue (w/v)
	30 % glycerol
	9 % SDS (w/v)

Stacking gel [upper Tris (4x)]	0.5 M Tris-HCl; pH 6.8
	0.4 % SDS (w/v)
Separating gel [lower Tris (4x)]	1.5 M Tris-HCl
	0.4 % SDS (w/v)
1x running buffer	192 mM Glycin
	25 mM Tris-HCl; pH 8.8
	0.1 % SDS
Acrylamide solution	30 % acrylamide (w/v)
	0.8 % bisacrylamide
APS:	10 % stock solution in dd H_2O
TEMED:	10 % stock solution in dd H_2O

	Separating gel (10 %)	**Separating gel (12.5 %)**	**Stacking gel**
Acrylamide	2.2ml	2.75ml	293µl
ddH_2O	2.9ml	2.35ml	1.38ml
Upper Tris	/	/	556µl
Lower Tris	1.7ml	1.7ml	/
10%APS	67µl	67µl	22.2µl
10% TEMED	67µl	67µl	22.2µl

Table 10: Pipet scheme for preparation of a 10% or 12.5 % laemmli gel

5.1.2.2 Coomassie®-brilliant blue – staining of laemmli gels

Staining solution	40 % tech. Isopropanol
	7 % acetic acid
	0.2 % Coomassie brilliant blue R-250
Destaining solution	20 % tech. Isopropanol
	7.5 % acetic acid
	72.5 % dd H_2O

5.1.2.3 Transfer of proteins

1x Borat transfer buffer	20 mM Boric acid-NaOH; pH 8.8
	1 mM EDTA
	4 mM 2-mercaptoethanol
	add 1l dd H_2O

5.1.2.4 Ponceau S- staining of Proteins on PVDF-membranes

1x TBST	10 mM Tris-HCl; pH 8.0
	150 mM NaCl
	0.05 % Tween 20
Ponceau S stock solution	2 % Ponceau-S
	30 % TCA
	30 % sulfosalicylic acid

5.1.2.5 Preparation of inclusion bodies from E.coli

Lysis buffer	50 mM Tris-HCl; pH 8.0
	25 % Saccharose
	1 mM EDTA
10 % NP40 in dd H_2O	
Detergent buffer	20 mM Tris-HCl, pH 7.5
	200 mM NaCl
	2 mM EDTA
	1 % sodium desoxycholate
	1 % NP40
9.5 M buffered urea	10 mM Tris-HCl; pH 7.5
	9.5 M urea
	5 mM EDTA
	50 µM Pefabloc SC
	1 mM DTT
methyl ammonium chloride	10 mM

5.1.2.6 Protein concentration measurement

The biorad protein assay kit of biorad laboratories (Ricjmond, CA) was used to measure protein concentrations in solution

Ion exchange chromatography

Urea buffer	8 M urea
	1 mM DTT
	1 M column buffer

DEAE spharose

CM sepharose

5.1.2.7 Dialysis

Urea buffer	10 M urea in dd H_2O
	Mixed bed resins beads

Dialysis buffer, pH 8.4	5 mM Tris-HCl; pH 8.6
	1 mM EDTA
	0.1 mM EGTA
	1 mM DTT

5.1.2.8 Assembly

10x Low assembly buffer	200 mM Tris-HCl, pH 7.0
	500 mM NaCl
10x Medium assembly buffer	200 mM Tris-HCl, pH 7.0
	1 M NaCl
10x high assembly buffer	200 mM Tris- HCl, pH 7.0
	1.6 M NaCl
0.2% glutaraldehyde solution	8 % (v/v) glutaraldehyde 2.5 %
	82 % (v/v) dialysis buffer
	10 % (v/v) of the current 10x assembly buffer
2% uranyl actetate solution	

5.1.3 Media

LB medium	86 mM NaCl
	10 mM $MgSO_4$
	1% bactotrypton (w/v)
	0.5 % yeast extract; pH 7.2 (w/v)
TB medium	4 mM KH_2PO_4
	91 mM K_2HPO_4
	1.2 % Trypton (w/v)
	2.4 % yeast extract (w/v)
	0.4 % glycerol (w/v)
LB agar	1.5 % agar (w/v) in LB medium
LB Amp agar	LB agar with 100 µg/ml ampicillin
LB Kan agar	LB agar with 20 µg/ml kanamycine

For induction, a 100 mM IPTG- stock solution was used.

5.1.3.1 Kits

QIA quick PCR purification kit (256) (Qiagen, Hilden)

QIA prep Spin Miniprep kit (250) (Qiagen, Hilden)

QIAGEN plasmid Maxi kit kit (25) (Qiagen, Hilden)

QuickChange® XL site-directed mutagenesis Kit (Stratagene, La Jolla)

5.2 Biological material

5.2.1.1 External material

glycerol stock solution of XL-10Gold® bacteria with ptrcHis2 (invitrogene) containing humane alpha-; beta- and L- synemin obtained from Omar Skalli (LSU Health Sciences Center, New Orleans)

Procaryotric cells

E.coli DH5 alpha: for amplification and preparation of plasmid-DNA

E.coli TG1: for expression of recombinant proteins

E.coli BL21 (DE3) codonPlus: for expression of recombinant proteins

5.2.1.2 Expression vectors for transformation of bacteria

Vector	Size	Resistance	Reference
pET-24a(+)	5310 bp	Kanamycin	Novagen (Madison, USA)
pDS5 (NCoI, SD2)	3953 bp	Ampicillin	(H Herrmann et al. 1999)

Table 11: Expression vectors for transformation of bacteria

5.2.1.3 Expression plasmid for transformation of bacteria

construct	Bacteria tribe
Human Nestin head and rod in pET-24a(+)	BL21
Human L-synemin in pDS5	pDS5

Table 12: Expression plasmid for transformation of bacteria

5.2.1.4 DNA oligonucleotides

Name	type	sequence	usage
PZ7	Forward	5’ GAG AGA CAT ATG CTG TCC TTG CGG CTG C 3’	Cloning synemin-L/ NdeI
PZ8	Reverse	5’ GAG AGA AAG CTT TTA CTC ACA TCC ATC TGA CG 3’	Cloning synemin-L/ HindIII
	Forward	5’ GAG AGA CAT ATG GAG GGC TGC ATG GGG 3’	Cloning nestin head and rod/ NdeI
	Reverse	5’ GAG AGA CTT TTA CAG CCG GGA GTT CT 3’	Cloning nestin head and rod /HindIII

Table 13: List of DNA oligonucleotides

5.2.1.5 Antibodies

antibody	type	antigene	dilution	reference
α-synemin, N-terminal	guinea pig	Human synemin	1:5000	Herrmann’s lab
α-Nestin, rod	rabbit	Human nestin	1: 500	Sigma-Aldrich

Table 14: List of primary antibodies

antibody	dilution	reference
Peroxidase-conjugated AffiniPure goat α-guinea pig IgG	1:5000	Dianova
Peroxidase-conjugated AffiniPure goat α-rabbit IgG	1: 5000	Jackson ImmunoResearch Laboratories Inc.

Table 15: List of secondary antibodies

5.2.1.6 Size standards

5.2.1.7 DNA standards

For Agarose gel electrophoresis, EcoRI/HindIII and BamHI digested λ-DNA have been used to get fragments of defined size.

5.2.1.8 Protein size standard

For SDS-Page, the protein standard “Broad Range-7702L” (New England Biolabs, Bad Schwalbach) have been used.

5.2.1.9 Equipment

Machine	Company
Analytical ultracentrifuge: Optima XL-A	Beckman (USA)
Airfuge	Beckman (USA)
Incubator	Heraeus (Osterode)
Ultracentrifuge: XL-70	Beckman (USA)
Documentation system for gels: E.A.S.Y RH-3	Herolab
Balance PM 460	Mettler (Geissen/ Switzerland)
Balance PJ 6000	Mettler (Geissen/ Switzerland)
Magnetic stirrer	Jankel and Kunkel (Staufen i.Br.)
Power supply	Biotech-Fischer (Heidelberg)
PCR minicycler TM	MJ Research BIOzym diagnostics (Hess. Oldendorf)
pH meter	Metrohm (Switzerland)
photometer	Keison (England)
table centrifuge “biofuge pico”	Heraeus (Osterode)
drop counter	Gibson (Langenfeld)
vortex	Bender and Hobein (Zürich)
water bath	B.Braun (Melsungen)
centrifuge for falcons	Heraeus (Osterode)

Table 16: List of equipment used

5.2.1.10 Other material

Material	Company
AGFA PAN AP X25 films	Agfa-Gevaert (Leverkusen)
dialysis tube	Serva (Heidelberg)
Falcon centrifuge tubes (15 ml and 50ml)	Becton Dickinson (USA)
filter paper	Schleicher and Schuell (Dassel)
microtubes (1.5 ml and 2.0 ml)	Eppendorf (Hamburg)
microscope slides	Langenbrinck (Teningen)
tips	star lab (Ahrensburg)
PVDF membrane	Immobilion-P Millipore (Bedford)

Table 17: Other material

6 Methods

6.1 DNA techniques

6.1.1 Amplification of cDNA fragments (PCR)

The polymerase chain reaction (Mullis and Faloona 1987) was used for amplification of specific DNA fragments. The selectivity of this method is based on the specific choice of primers, which bind the DNA on its 3'- or 5'-end complimentary. A specific DNA polymerase starts the duplication of the DNA in this defined area of DNA. Table 18 shows the pipette scheme of used reagents for this work.

reagent	volume [µl]			
	control	0 % DMSO	3 % DMSO	6 % DMSO
ddH_2O	29.5	32.5	31.0	29.5
5x phusion buffer	10	10	10	10
dNTPS	5	5	5	5
DMSO	3	0	1.5	3
Primer 1[100 ng/µl]	1	1	1	1
Primer 2[100 ng/µl]	1	1	1	1
template [1 ng/µl]	0	1	1	1
phusion polymerase	0.5	0.5	0.5	0.5
final volume	50	50	50	50

Table 18: pipet scheme used for PCR

All PCRs were performed using a minicycler (Biozym, Oldendorf) with following program.

step	temperature [°C]	time	cycle
primary DNA denaturation	98	3 minutes	
denaturation	98	20 seconds	
hybridization	72	20 seconds	35
synthesis	72	1minute per kb	
elongation	72	10 minutes	
cooling	4	∞	

Table 19: program used for PCR

After PCR, 3 µl of the sample were mixed with 7 µl dd H_2O and 2 µl 6xDNA agarosegel buffer and controlled on an agarosegel.

6.1.2 Mutagenesis

Quick Change® XL site-directed mutagenesis kit (Stratagene) was used to mutate the position of the gene encoding synemin using gene specific primers.

6.1.3 Agarose gel electrophoresis

DNA fragments were separated corresponding to their size in an electric field with agarose gel electrophoresis. The speed of migration is within a specific range of size inverse to the fragment size (bp). For the separation of fragments 1% agarose gels have been produced with SeaKem® LE agarose (Biozym diagnostics, Hess. Oldendorf) in bouling 1xTAE. When the agarose solution was cooled down to 40°C, ethidium bromide in a final concentration of 1 µg/µL was added. Ethidum bromide intercalates into the DNA and therefore, fragments are visible in ultraviolet light. The fluid agarose gel was poured into a gel apparature for mini gels. The DNA-samples were mixed with 1/6 volume of DNA agarose sample buffer. Through the basicity of the running buffer (1xTAE), the DNA has a negative net charge and goes to the anode. To estimate the molecular weight of the separated DNA fragments, 15 µL of molecular weight standard were put on. As size standard with EcoR I, Hind III and BamH I restricted lambda-DNA was used. Electrophorese was done in 30 to m45 minutes at 70V. The gels were analyzed using the Gel-Imager DNR bio imaging system.

6.1.4 Purification of PCR products

PCR products were purified using the QIAquick PCR purification kit (256) and eluted in 35 µl.

6.1.5 Restriction digestion of DNA

With specific restriction enzymes, the DNA is cleaved within a specific restriction site, building a 5'phosphate group and a 3' hydroxyl group.

Preparativ restriction digestion and dephosphorylation of the 5'phosphate group of DNA fragments

The vector DNA was parallel in two single restriction reactions cleaved. Therefore, 1.5 µl vector DNA (1µg/µL) were digested with 5 U of the restriction enzyme within a volume of 20 µL in the recommended buffer system for 2 hours at 37°C. To control the successful linearization of the vectror DNA, 1 µL of each sample were loaded on a 1% agorose gel. After the combination of both restriction reactions, 0.5 µL enzyme was added and again digested for 2 h. The vector DNA was dephosphorylated with the Fast dephospho& ligation kit

For the preparative restriction digestion of the PCR products 35 µL of purified PCR products were digested with 10U of both restriction enzymes in a final volume o 40 µ in the recommended buffer system for 2 h at 37°C. The enzymatic reaction was stopped at 70°C for 10 minutes. Afterwards, the digested PCR products were purified with the PCR purification kit (Qiagen) and diluted in 40 µl EB buffer.

6.1.6 Ligation of DNA fragments

The digested vector DNA and PCR fragments were ligated using the Fast Dephospho & Ligation kit.

Transformation of competent E.coli bacteria with heat shock

To insert foreign DNA in bacteria, we used the transformation with heat shock. Therefor, 100 µL competent bacteria with an approximate transformation efficiency of 10^6 colonies/µg DNA were melt on ice for 5 minutes, before they were mixed with 10 µL of ligase product and incubated for 20 minutes on ice. Through the following heat shock for 3 minutes at 37°C, pores in the cell wall are opening and the foreign DNA

can enter the cell. After 1 minute incubation on ice, the cell pores are closed again. After addition of 400 µL antibody-free LB media, cells were incubated for 1 h at 37°C. To ensure a selection, 200 µL cell suspension were plate on agar plates containing the plasmid corresponding antibody and incubated over night at 37°C.

6.1.7 Preparation of DNA

For isolation and purification of plasmid DNA, the method described by Birnboim and Doly (Birnboim and Doly 1979) was used, which is based on alkalic lysis.

6.1.8 Plasmid preparation in small scale

2 mL LB media with the corresponding antibody were inoculated with a steril picked bacteria colony and over night at 37° C on a shaker (~230rpm) incubated. On the following day, the overnight culture was purified using the QIAQuick Mini plasmid purification kit. Through a restriction digestion the plasmid DNA was controlled.

6.1.9 Plasmid preparation in large scale

100 mL LB media with the corresponding antibody were inoculated with a steril picked bacteria colony and over night at 37° C on a shaker (~230rpm) incubated. On the following day, the overnight culture was purified using the QIAQuick Maxi plasmid purification kit. Through a restriction digestion the plasmid DNA was controlled.

6.1.10 DNA sequencing

The DNA was sequenced based on the principle of Sanger (Sanger, Nicklen, and Coulson 1977) with usage of fluoreszence-labeled didesoxynucleotides. The sequencing was performed by the company GATC.

6.1.11 Measurement of DNA concentration

The DNA concentration of the plasmid preparations in small and large scale were analyzed through measurement of the absorbance at 260 nm. With following formula, the DNA concentration was calculated:

$c = Abs_{260nm} \times 50\ mg/\mu L$

With the quotient Abs 260nm/Abs 280 nm the purity of the DNA was determined. With a merit around 1.8 is the DNA pure.

6.2 Proteinbiochemical methods

6.2.1 Bacteriolysis

In case of the E.coli strain TG1, the bacteriolysis was performed after 17 hours incubation at 3/°C and 225 rpm in the incubator. 2 mL of culture were dosed, centrifuged and the pellet resuspended in 100 µl media. After that treatment the pellet was boiled with 3xLaemmlie sample buffer for 10 minutes at 95°C in the heater.

In case of the E.coli strain BL21 (DE3) codon plus, two different preparations were performed. One was induced through 10 mM IPTG, while the other was not induced. After three and 17 hours of incubation at 37°C and 225 rpm in the incubator, samples of 2 ml were taken of both and centrifuged and boiled. 15 µL of each sample were analyzed through SDS-PAGE

6.2.2 Discontinuous polyacrylamide gel electrophoresis

For separation of protein samples, the method of discontinuous polyacrylamide gel electrophoresis described by Laemmli (Laemmli 1970) was used. Proteins are separated corresponding to their molecular weight under denaturing conditions. Stacking and separation gel were prepared through copolymerization of acrylamide, N,N' – bisacrylamide (BIS) with different concentration of acrylamide and adjusted pH. Initiator of the radical Copolymerization was ammonium persulfate (APS), which act as a source of free radicals. N, N, N', N' – tetramethylethylenediamine (TEMED) stabilizes the radicals. The size of the pores is connected to the ratio of acrylamide to BIS. For the separation of proteins, 10% - polyacrylamide gels were used. The sodium dodecyl sulfate (SDS) within the Laemmli sample buffer is a anionic detergent, which denatures the proteins and masks the protein charges with a negative charge. The proteins migrate to the anode and are separated by their molecular weight because of the negative charge. Protein samples were mixed with Laemmli sample buffer and boiled for 5 minutes at 95°C before loading on the gel. Gel electrophoresis run for 1 hour at 70 V.

6.2.3 Coomassie®-staining of polyacrylamid geles

After finishing the gel electrophoresis, the polyacrylamide gel was incubated in coomassie brilliant blue R-250 – staining solution for 1 hour at room temperature. The staining solution was removed and remaining staining solution washed out with destain solution. Therefore, only distinct stained protein bands occur on the gel.

6.2.4 Protein transfer (Western Blot)

Following the Western Blot - protocols of Towbin (Towbin, Staehelin, and Gordon 1979), the separated proteins were transfered in a wet blotting process from the acrylamide gel to an PVDF-membrane. First the PVDF membranes were activated in ethanol abs. After electrophoresis, the gel, needed sponges, whatman paper and the PVDF membrane in borat buffer equilibrated. Before starting the transfer, blot chamber was filled with borat transfer buffer. The transfer starts with 100mA for five minutes and is increased every five minutes in 50mA-steps to the finale strength of 500mA. After one hour at 500mA, transfer was stopped and the PVDF membrane was stained for 15 minutes at room temperature in Ponceau S solution (1:10 in destilled water). By washing with aqua bidest the red stained protein bands became visible. The membranes were dried or used for the immunological detection of proteins.

6.2.5 Immunological detektion of proteins

For the immunological detection, ECL (enhanced chemiluminescence)-system of Amersham LIFE SCIENCE (Braunschweig) was used for a not – radioactive, chemiluminescentiv detection method. First, PVDF membrane was incubated in 5% milk/TBST for 30 minutes at room temperature for blocking. The following incubation with the first antibody (diluted in 5% milk/TBST) was performed for one hour at room temperature. Afterwards, the PVDF membrane was cleaned for 10 minutes three to five times before adding the second antibody (diluted in 5% milk/TBST) for 30 minutes. After washing the membranes in TBST five times for five minutes, the secondary antibody was added and was incubated for 30 minutes at room temperature. After washing, the coupled HRP has transformed the cooled ECL-detection reagent. Therefore, light was emitted and the PVDF-membrane exponated on a radiographic film (Kodak X-OMAT AR5)

6.2.6 Protein expression

Competent cells (*E.coli* - stock TG1 or BL21) were transformed with DNA following the protocol for protein expression. One colony was picked and incubated stirring over night at 37°C in 400 mL TB medium with corresponding antibiotics. At the following day, the culture was centrifuged for ten minutes at 5.000 rpm.

6.2.7 Inclusion body preparation

The Preparation of proteins following the protocol of Nagai et al. (Nagai and Thøgersen 1987) is based on the fact, that bactria pack strong expressed proteins in insoluble inclusion bodies. With this purification we are able to isolate and concentrate the proteins. All steps of protein preparation were performed on ice. The bacteria pellet of the centrifugation (see chapter) was resuspended in 8 mL precooled lysis buffer and with a douncer homogenized. After adding 2 mL lysis buffer with 10 mg/mL lysozyme and douncing, the suspension was incubated for 30 minutes for lysis. Afterwards, 100 µL $MgCl_2$ (1M), RNase A (10 mg/mL), 10 µL DNaseI (50 µg/µL), 100µL PMSF (in ethanol abs.) and 200 µL 10% NP40 added und again homogenized. In this step, the proteases are inhibited, the DNA digested und cytoplasmic as well as membrane bounded proteins solubilized. After adding 20 mL detergent buffer, 200 µL DTT (1M), 300µL PMSF (in ethanol abs.) and 100 µL Pefabloc SC (50mM), the suspension was again dounced and centrifuged at 4°C with 8000 rpm for 20 minutes. In the pellet of this centrifugation were the outer cell walls, not lysed bacteria, peptidoglycan components and the inclusion bodies. In the supernatant are soluble membrane and cytoplasmic protein and DNA- and RNA fragments. In all following washing steps with 1x GII, 1xGII + 1.5M KCl, 1x GII und 1xTE were DTT (1mM), 100 µl PMSF (2mM) and 50 µL Pefabloc SC (50 µM) added. The incubation time was for all washing steps except for the washing step with 1xGII + 1.5M KCl 10 minutes. For the washing step with 1xGII + 1.5M KCl, the incubation time was 30 minutes. After incubation the suspension was centrifuged for 10 minutes at 4°C with 8.000 rpm. The pellet of the last washing step was resuspended in 8 mL 9.5 M buffered urea and centrifuged with the ultracentrifuge ((Beckman XL-70 20739; 50 Ti-Rotor; RT) for one hour at 35.000 rpm. The supernatant was collected and 10 mM methyl ammonium chloride (MAC) added before storage at -20°C.

6.2.8 Protein purification through ionic exchange chromatography

Following the inclusion body preparation, two purification steps through ionic exchange chromatography were performed. In this method, the used column matrix is derivated with loaded groups and absorbs the added components selectively.

6.2.8.1 Anionic exchange chromatography

DEAE sepharosis (Fast Flow, GE Healthcare Bio-Science AB) was used as column matrix. The Diethylaminoethyl-groups are weak anionic exchange groups. For anion exchange chromatography, 25 mL DEAE sepharosis was mixed with an equivalent amount of degazed column buffer and for 10 minutes degazed, before the column was loaded and washed with column buffer two times. The protein sample of the inclusion body preparation was mixed with an equivalent amount of column buffer and loaded on the column. 5 µL of the protein – column buffer- mix were aliquoted for a later SDS-PAGE. A volume corresponding to half of sepharose (empty volume; EV) and a volume corresponding to the volume of loaded protein – column buffer- mix (flow-through; FL) were collected in 50 mL falcons. The column was washed with column buffer corresponding to the double volume of sepharose and collected as wash solution (WS). The protein was eluated with a 100 mL gradient of NaCl (0 – 0.5 M NaCl in column buffer). Of single fractions were the Protein concentration analyzed via Bradford and the fraction with high protein amount further analyzed with SDS-PAGE and following coomassie® staining. As reference, samples of empty volume, flow-through and wash solution were on the gel, too. The samples with high amount of protein and purity were pooled and collected for the cationic exchange chromatography.

6.2.8.2 Cationic exchange chromatography

For cationic exchange chromatography, cm sepharose (Fast Flow, GE Healthcare Bio-Science AB) was used. The carboxymethyl groups work as weak cationic exchange group. The procedure is the same as for the anionic exchange chromatography, but the protein sample were dialyzed in the column buffer for one hour before loading on the column. After dialysis, the protein sample was mixed with the column buffer one to one and loaded on the column. The pooled samples was mixed with 10mM methyl ammonium chloride (MAC), in 1.5 mL eppendorf tubes aliquoted and stored at -80°C.

6.2.9 Dialysis

Before dialysis, the dialysis tubes (exchange up to 12 kDa) were incubated for 15 minutes in dialysis buffer to remove rest of the ethanol containing storage solution. Afterwards, the dialysis tubes were cleaned with dd H_2O, filled with protein and dialyzed against the corresponding dialysis buffer to renature the protein in a step-wise dialysis from 8 M urea over 6 M, 4 M, 2 M and 1 M urea down to non-urea buffer. The buffer was exchanged every twenty minutes. After the last dialysis step, the dialysis tubes were put in a bigger amount of dialysis buffer and dialyzed against it over night at 4°C. The next day, proteins were removed of the dialysis tubes and protein concentration measured with the Bradford-method.

In case of the dialysis of nestin in order to analyse it's interaction with desmin and vimentin in all different stages of assembly, the proteins were first dialyized into 6 M guanidine hydrochloride, pH 8.4 for two hours. Afterwards, an additional dialysis step into 9.5 M urea was performed. In case of mixing the proteins with nestin before renaturation, the proteins were mixed in 9.5 M urea before starting the standard dialysis mentioned above.

6.2.10 Protein concentration measurement

For quantitative Protein concentration measurement, the method of Bradford (Bradford, 1976) was used. This method is based on the absorption shift from 465 nm to 595 nm of an acidic solution of the Coomassie Brilliant Blue G-250 stain through binding on proteins. The reagent (BIO Rad, München) was diluted one to five with dd H_2O. For exact protein concentration measurement, a BSA straight calibration line with different amounts of BSA (stock solution: 1.03 g/L) was performed. As zero value, one to five diluted reagent without protein was used. After a short incubation of five minutes, the OF at 595 nm was measured. The protein concentration was derived by the BSA - straight calibration line and the measured OD of the protein.

BSA - straight calibration line	0	1	2	3	4	5
BIO - Rad Reagent (1:5 diluted)	1ml	1ml	1ml	1ml	1ml	1ml
BSA - stock solution (1,03 µg/µl)	/	1µl	2µl	3µl	4µl	5µl

Table 20: Used amounts of BSA for straight calibration line

6.3 Electron microscopy

6.3.1 Preparation of cupper grids

20 VE cupper grids (3.05 mm, 300 mesh, BALTEC preparation) were coated with formvar (Polyvinylformal) and carbon. For formvar-coating, object slides were dunk for 30 seconds in 0.5% formvar solution (resolved in chloroform) and dried at room temperature. With a scalpel, the edges of the object slides were grinded. The formvar sheets were transported on the surface of dd H_2O by dipping the object slide. The VE cupper grids were put on the formvar sheet with the side to be coated down. With a freshly object slide, the VE cupper grids on the formvar sheet were fished out of the water with the formvar coated side of the grids looked upside. After drying the object slides overnight, the carbon film was added with a Baltec SCD 005 sputtering machine. The coated cupper grids were stored at room temperature in the dark. A few minutes before usage, the cupper grids were glow discharged with the Baltec SCD 005 sputtering machine.

6.3.2 *In vitro* filament assembly

The protein samples were dialyzed following the described protocol and the protein concentration measured with Bradford and setted toa protein concentration of 0.2 g/l. Through addition of assembly buffer, the pH changed from 8.4 to 7.5 and the ionic strength from 5 mM Tris-HCl up to 25 mM Tris-HCl and the corresponding concentration of NaCl (50 mM, 100 mM or 160 mM). Therefore, the filament forming process is started.

At distinct time points was the filament forming process stopped through addition of 0.2% glutaraldehyde in the corresponding assembly buffer. As negative control for the filament forming process, proteins in dialysis buffer were fixed with the same amount of 0.2 % glutaraldehyde. 15 µL of fixed assembly reaction were put on the prepared cupper grids and settled for 15 seconds before washing the grids for 10 seconds in dd H_2O. For negative contrast, the grids were stained with uranyl acetate for 15 seconds. Between the three steps, the solution were carefully removed with a filter paper. The cupper grids with the fixed and stained protein sample were stored at room temperature in the dark.

6.3.3 Electron microscopy

With an electrone microscope it is possible to investigate protein structures on molecular level. The cupper grids with the samples were visualized with a Philips EM410. Through the acceleration voltage of 80kV, an electron stream (λ = 4.3 pm; $\lambda = h/ m * v$; $\lambda = 1.23/ \sqrt{k}$) is formed. Images were acquired at different magnifications on a CCD-camera. These images were further processed in ImageJ.

6.3.4 Centrifugation assays

150 µl protein samples were centrifuged with the airfuge and 30 psi after distinct times of assembly. The centrifugation time was 15 minutes. The supernatant was collected and with laemmli sample buffer boiled at 95°C for 5 minutes. The pellet was diluted with 3x laemmli sample buffer and incubated for a few minutes. Afterwards, the pellet was filled up with dialysis buffer to get the equal amount and boiled for 5 minutes at 95°C. The samples were analyzed using a 10% SDS gel. Assembled protein sample without centrifugation was used as input control.

6.4 Rotary shadowing

In order to absorb particles of interest onto a surface with singnificant structure (mica) without disturbtion by surface-forces, glycerol-sparying low-angle rotary metal shadowing was performed in cooperation with Dr. Richter (DKFZ) following established protocols (C. M. Cohen, Tyler, and Branton 1980). The metal-shadowing in high-vacuum provides a surface image at ultrastructural resolution.

The in glycerol dissolved proteins were sprayed as an aerosol onto the surface of freshly cleaved mica. The following retraction of the aerosol-drops results of a front of structures depleted from solvent.

6.5 Sucrose gradient centrifugation

For sucrose gradient centrifugation 10 mL of continued sucrose gradient from 10 to 30% were prepared on top of 1 ml of 70% sucrose cushion. The samples were loaded on top of the gradient and centrifuged for 5 hours at 4°C and 28.000 rpm with the ultracentrifuge. After centrifugation, fractions of 1 ml were collected from the top

of the tube down to the bottom with the 70% sucrose cushion and analyzed with SDS PAGE.

6.6 Analytical ultracentrifugation (AUC)

Through sedimentation velocity runs, a methodical analysis of soluble complexes in the native state is possible. Through the gravitation field produced by centrifugation, particles sedimentate different in dependency of their molecule charcteristics like protein-protein-interactions. On every molecule is affected by three forces during centrifugation; the sedimentation force F_z, the buoyancy force F_b and the friction force. Therefore, a concentration gradient occurs on the border between sedimentating sample and solution. The gradient (boundary) moves in dependency of the time to the bottom. Because of the diffusion of the particles, a broadering of the boundary occurs. The boundary speed was measured using the g(s*)-method established by Stafford (Stafford 1992). The *s*-values as sedimentation coefficient of a macromolecule are reported in Svedberg [S] units, which are corresponded to 10^{-13} seconds.

All AUC experiments were performed using an Optima™ XL- A analytical ultracentrifuge at 20°C and different speed in dependency of the size of the analyzed particles. The distribution of centrifugally accelerated particels was measured by absorption at 230 nm with a high-intensity xenon flash lamp.

The distribution was analyzed using the program DCDT+ developed by J. Philo (http://www.jphilo.mailway.com/dcdt+.htm; (Lebowitz, Lewis, and Schuck 2002). Data analysis was performed as described (Mücke et al. 2004).

6.7 Data analysis

DNA- and protein sequences were analyzed with HUSAR version 4.1 (http://husar.dkfz-heidelberg.de/).

The databank search was performed using the homepage of the national centre for biotechnology imformations (http://www.ncbi.nlm.nih.gov/)

The Image processing was performed using Adobe Photoshop CS4; Adobe Illustrator CS$ and ImageJ 1.34s.

7 References

Aebi, U, J Cohn, L Buhle, und L Gerace. 1986. „The nuclear lamina is a meshwork of intermediate-type filaments“. *Nature* 323 (6088): 560–64. doi:10.1038/323560a0.

Bader, B. L., T. M. Magin, M. Freudenmann, S. Stumpp, und W. W. Franke. 1991. „Intermediate Filaments Formed de Novo from Tail-Less Cytokeratins in the Cytoplasm and in the Nucleus“. *The Journal of Cell Biology* 115 (5): 1293–1307.

Bär, Harald, Dirk Fischer, Bertrand Goudeau, Rudolf A. Kley, Christoph S. Clemen, Patrick Vicart, Harald Herrmann, Matthias Vorgerd, und Rolf Schröder. 2005. „Pathogenic Effects of a Novel Heterozygous R350P Desmin Mutation on the Assembly of Desmin Intermediate Filaments in Vivo and in Vitro“. *Human Molecular Genetics* 14 (10): 1251–60. doi:10.1093/hmg/ddi136.

Bär, Harald, Norbert Mücke, Anna Kostareva, Gunnar Sjöberg, Ueli Aebi, und Harald Herrmann. 2005. „Severe muscle disease-causing desmin mutations interfere with in vitro filament assembly at distinct stages“. *Proceedings of the National Academy of Sciences of the United States of America* 102 (42): 15099–104. doi:10.1073/pnas.0504568102.

Bär, Harald, Sarika Sharma, Helga Kleiner, Norbert Mücke, Hanswalter Zentgraf, Hugo A. Katus, Ueli Aebi, und Harald Herrmann. 2009. „Interference of Amino-Terminal Desmin Fragments with Desmin Filament Formation“. *Cell Motility and the Cytoskeleton* 66 (11): 986–99. doi:10.1002/cm.20396.

Bellin, R M, T W Huiatt, D R Critchley, und R M Robson. 2001. „Synemin may function to directly link muscle cell intermediate filaments to both myofibrillar Z-lines and costameres“. *The Journal of Biological Chemistry* 276 (34): 32330–37. doi:10.1074/jbc.M104005200.

Bellin, R M, S W Sernett, B Becker, W Ip, T W Huiatt, und R M Robson. 1999. „Molecular characteristics and interactions of the intermediate filament protein synemin. Interactions with alpha-actinin may anchor synemin-containing heterofilaments“. *The Journal of Biological Chemistry* 274 (41): 29493–99.

Bhosle, Rahul C, Daniel E Michele, Kevin P Campbell, Zhenlin Li, und Richard M Robson. 2006. „Interactions of intermediate filament protein synemin with dystrophin and utrophin“. *Biochemical and Biophysical Research Communications* 346 (3): 768–77. doi:10.1016/j.bbrc.2006.05.192.

Bilak, S R, S W Sernett, M M Bilak, R M Bellin, M H Stromer, T W Huiatt, und R M Robson. 1998. „Properties of the novel intermediate filament protein synemin and its identification in mammalian muscle“. *Archives of Biochemistry and Biophysics* 355 (1): 63–76. doi:10.1006/abbi.1998.0702.

Birnboim, H C, und J Doly. 1979. „A rapid alkaline extraction procedure for screening recombinant plasmid DNA“. *Nucleic Acids Research* 7 (6): 1513–23.

Capetanaki, Y., und D. J. Milner. 1998. „Desmin Cytoskeleton in Muscle Integrity and Function“. *Sub-Cellular Biochemistry* 31: 463–95.

Chernyatina, Anastasia A., Stefan Nicolet, Ueli Aebi, Harald Herrmann, und Sergei V. Strelkov. 2012. „Atomic Structure of the Vimentin Central A-Helical Domain and Its Implications for Intermediate Filament Assembly“. *Proceedings of the National Academy of Sciences of the United States of America* 109 (34): 13620–25. doi:10.1073/pnas.1206836109.

Chourbagi, Oussama, Francine Bruston, Marianna Carinci, Zhigang Xue, Patrick Vicart, Denise Paulin, und Onnik Agbulut. 2011. „Desmin Mutations in the Terminal Consensus Motif Prevent Synemin-Desmin Heteropolymer Filament Assembly“. *Experimental Cell Research* 317 (6): 886–97. doi:10.1016/j.yexcr.2011.01.013.

Chou, Ying-Hao, Satya Khuon, Harald Herrmann, und Robert D. Goldman. 2003. „Nestin Promotes the Phosphorylation-Dependent Disassembly of Vimentin Intermediate Filaments during Mitosis“. *Molecular Biology of the Cell* 14 (4): 1468–78. doi:10.1091/mbc.E02-08-0545.

Claeys, Kristl G., Peter F. M. van der Ven, Anthony Behin, Tanya Stojkovic, Bruno Eymard, Odile Dubourg, Pascal Laforêt, u. a. 2009. „Differential Involvement of Sarcomeric Proteins in Myofibrillar Myopathies: A Morphological and Immunohistochemical Study“. *Acta Neuropathologica* 117 (3): 293–307. doi:10.1007/s00401-008-0479-7.

Cohen, C. M., J. M. Tyler, und D. Branton. 1980. „Spectrin-Actin Associations Studied by Electron Microscopy of Shadowed Preparations“. *Cell* 21 (3): 875–83.

Cohen, Shenhav, Bo Zhai, Steven P. Gygi, und Alfred L. Goldberg. 2012. „Ubiquitylation by Trim32 Causes Coupled Loss of Desmin, Z-Bands, and Thin Filaments in Muscle Atrophy“. *The Journal of Cell Biology* 198 (4): 575–89. doi:10.1083/jcb.201110067.

Davies, Kay E., und Kristen J. Nowak. 2006. „Molecular Mechanisms of Muscular Dystrophies: Old and New Players“. *Nature Reviews. Molecular Cell Biology* 7 (10): 762–73. doi:10.1038/nrm2024.

Eriksson, John E., Thomas Dechat, Boris Grin, Brian Helfand, Melissa Mendez, Hanna-Mari Pallari, und Robert D. Goldman. 2009. „Introducing Intermediate Filaments: From Discovery to Disease“. *The Journal of Clinical Investigation* 119 (7): 1763–71. doi:10.1172/JCI38339.

Favre, Bertrand, Yann Schneider, Prakash Lingasamy, Jamal-Eddine Bouameur, Nadja Begré, Yves Gontier, Marie-France Steiner-Champliaud, Miguel A. Frias, Luca Borradori, und Lionel Fontao. 2011. „Plectin Interacts with the Rod Domain of Type III Intermediate Filament Proteins Desmin and Vimentin“. *European Journal of Cell Biology* 90 (5): 390–400. doi:10.1016/j.ejcb.2010.11.013.

Franke, W. W., E. Schmid, M. Osborn, und K. Weber. 1978. „Different Intermediate-Sized Filaments Distinguished by Immunofluorescence Microscopy“. *Proceedings of the National Academy of Sciences of the United States of America* 75 (10): 5034–38.

Frisén, J., C. B. Johansson, C. Török, M. Risling, und U. Lendahl. 1995. „Rapid, Widespread, and Longlasting Induction of Nestin Contributes to the Generation of Glial Scar Tissue after CNS Injury“. *The Journal of Cell Biology* 131 (2): 453–64.

Fuchs, E, und K Weber. 1994. „Intermediate filaments: structure, dynamics, function, and disease“. *Annual Review of Biochemistry* 63: 345–82. doi:10.1146/annurev.bi.63.070194.002021.

Fuchs, E, und Y Yang. 1999. „Crossroads on cytoskeletal highways“. *Cell* 98 (5): 547–50.

Gardner, E. E., D. Dahl, und A. Bignami. 1984. „Formation of 10-Nanometer Filaments from the 150K-Dalton Neurofilament Protein in Vitro“. *Journal of Neuroscience Research* 11 (2): 145–55. doi:10.1002/jnr.490110204.

Geisler, N., E. Kaufmann, und K. Weber. 1982. „Proteinchemical Characterization of Three Structurally Distinct Domains along the Protofilament Unit of Desmin 10 Nm Filaments“. *Cell* 30 (1): 277–86.

Gillard, B. K., L. T. Thurmon, R. G. Harrell, Y. Capetanaki, M. Saito, R. K. Yu, und D. M. Marcus. 1994. „Biosynthesis of Glycosphingolipids Is Reduced in the Absence of a Vimentin Intermediate Filament Network“. *Journal of Cell Science* 107 (Pt 12) (Dezember): 3545–55.

Goldfarb, L G, P Vicart, H H Goebel, und M C Dalakas. 2004. „Desmin myopathy“. *Brain: A Journal of Neurology* 127 (Pt 4): 723–34. doi:10.1093/brain/awh033.

Granger, B L, und E Lazarides. 1980. „Synemin: a new high molecular weight protein associated with desmin and vimentin filaments in muscle“. *Cell* 22 (3): 727–38.

Green, Kathleen J., Michael Böhringer, Todd Gocken, und Jonathan C. R. Jones. 2005. „Intermediate Filament Associated Proteins“. *Advances in Protein Chemistry* 70: 143–202. doi:10.1016/S0065-3233(05)70006-1.

Herrmann, H, und U Aebi. 2000. „Intermediate filaments and their associates: multi-talented structural elements specifying cytoarchitecture and cytodynamics“. *Current Opinion in Cell Biology* 12 (1): 79–90.

Herrmann, Harald, und Ueli Aebi. 2004. „Intermediate filaments: molecular structure, assembly mechanism, and integration into functionally distinct intracellular Scaffolds“. *Annual Review of Biochemistry* 73: 749–89. doi:10.1146/annurev.biochem.73.011303.073823.

Herrmann, Harald, Harald Bär, Laurent Kreplak, Sergei V Strelkov, und Ueli Aebi. 2007. „Intermediate filaments: from cell architecture to nanomechanics“. *Nature Reviews. Molecular Cell Biology* 8 (7): 562–73. doi:10.1038/nrm2197.

Herrmann, Harald, Sergei V Strelkov, Peter Burkhard, und Ueli Aebi. 2009. „Intermediate filaments: primary determinants of cell architecture and plasticity“. *The Journal of Clinical Investigation* 119 (7): 1772–83. doi:10.1172/JCI38214.

Herrmann, H, M Häner, M Brettel, N O Ku, und U Aebi. 1999. „Characterization of distinct early assembly units of different intermediate filament proteins“. *Journal of Molecular Biology* 286 (5): 1403–20. doi:10.1006/jmbi.1999.2528.

Herrmann, H, M Häner, M Brettel, S A Müller, K N Goldie, B Fedtke, A Lustig, W W Franke, und U Aebi. 1996. „Structure and assembly properties of the intermediate filament protein vimentin: the role of its head, rod and tail domains“. *Journal of Molecular Biology* 264 (5): 933–53. doi:10.1006/jmbi.1996.0688.

Herrmann, H, I Hofmann, und W W Franke. 1992. „Identification of a nonapeptide motif in the vimentin head domain involved in intermediate filament assembly“. *Journal of Molecular Biology* 223 (3): 637–50.

Hesse, M, T M Magin, und K Weber. 2001. „Genes for intermediate filament proteins and the draft sequence of the human genome: novel keratin genes and a surprisingly high number of pseudogenes related to keratin genes 8 and 18“. *Journal of Cell Science* 114 (Pt 14): 2569–75.

Hijikata, T., A. Nakamura, K. Isokawa, M. Imamura, K. Yuasa, R. Ishikawa, K. Kohama, S. Takeda, und H. Yorifuji. 2008. „Plectin 1 links intermediate filaments to costameric sarcolemma through -synemin, -dystrobrevin and actin“. *Journal of Cell Science* 121 (12): 2062–74. doi:10.1242/jcs.021634.

Hirako, Yoshiaki, Hisashi Yamakawa, Yuki Tsujimura, Yuji Nishizawa, Masayo Okumura, Jiro Usukura, Hiroyuki Matsumoto, Kenneth W Jackson, Katsushi Owaribe, und Osamu Ohara. 2003. „Characterization of mammalian synemin, an intermediate filament protein present in all four classes of muscle cells and some neuroglial cells: co-localization and interaction with type III intermediate filament proteins and keratins“. *Cell and Tissue Research* 313 (2): 195–207. doi:10.1007/s00441-003-0732-2.

Hockfield, S., und R. D. McKay. 1985. „Identification of Major Cell Classes in the Developing Mammalian Nervous System“. *The Journal of Neuroscience: The Official Journal of the Society for Neuroscience* 5 (12): 3310–28.

Inagaki, Masaki, Yoichiro Matsuoka, Kunio Tsujimura, Shoji Ando, Toshiya Tokui, Toshitada Takahashi, und Naoyuki Inagaki. 1996. „Dynamic Property of Intermediate Filaments: Regulation by Phosphorylation“. *BioEssays* 18 (6): 481–87. doi:10.1002/bies.950180610.

Ireland, M E, P Wallace, A Sandilands, M Poosch, M Kasper, J Graw, A Liu, u. a. 2000. „Up-regulation of novel intermediate filament proteins in primary fiber cells: an indicator of all vertebrate lens fiber differentiation?“. *The Anatomical Record* 258 (1): 25–33.

Ishikawa, H., R. Bischoff, und H. Holtzer. 1968. „Mitosis and Intermediate-Sized Filaments in Developing Skeletal Muscle“. *The Journal of Cell Biology* 38 (3): 538–55.

Izmiryan, Araksya, Claudio Areias Franco, Denise Paulin, Zhenlin Li, und Zhigang Xue. 2009. „Synemin isoforms during mouse development: multiplicity of partners in vascular and neuronal systems“. *Experimental Cell Research* 315 (5): 769–83. doi:10.1016/j.yexcr.2008.12.009.

Janssen, Mandy E. W., Hongjun Liu, Niels Volkmann, und Dorit Hanein. 2012. „The C-Terminal Tail Domain of Metavinculin, Vinculin's Splice Variant, Severs Actin Filaments“. *The Journal of Cell Biology* 197 (5): 585–93. doi:10.1083/jcb.201111046.

Kasai, M., E. Nakano, und F. Oosawa. 1965. „POLYMERIZATION OF ACTIN FREE FROM NUCLEOTIDES AND DIVALENT CATIONS“. *Biochimica Et Biophysica Acta* 94 (März): 494–503.

Kerssemakers, Jacob W J, E Laura Munteanu, Liedewij Laan, Tim L Noetzel, Marcel E Janson, und Marileen Dogterom. 2006. „Assembly dynamics of microtubules at molecular resolution“. *Nature* 442 (7103): 709–12. doi:10.1038/nature04928.

Khanamiryan, Luiza, Zhenlin Li, Denise Paulin, und Zhigang Xue. 2008. „Self-assembly incompetence of synemin is related to the property of its head and rod domains“. *Biochemistry* 47 (36): 9531–39. doi:10.1021/bi800912w.

Kirmse, Robert, Stephanie Portet, Norbert Mücke, Ueli Aebi, Harald Herrmann, und Jörg Langowski. 2007. „A quantitative kinetic model for the in vitro assembly of intermediate filaments from tetrameric vimentin“. *The Journal of Biological Chemistry* 282 (25): 18563–72. doi:10.1074/jbc.M701063200.

Kobayashi, M., G. Sjöberg, S. Söderhäll, U. Lendahl, B. Sandstedt, und T. Sejersen. 1998. „Pediatric Rhabdomyosarcomas Express the Intermediate Filament Nestin“. *Pediatric Research* 43 (3): 386–92. doi:10.1203/00006450-199803000-00013.

Konieczny, Patryk, Peter Fuchs, Siegfried Reipert, Wolfram S Kunz, Anikó Zeöld, Irmgard Fischer, Denise Paulin, Rolf Schröder, und Gerhard Wiche. 2008. „Myofiber integrity depends on desmin network targeting to Z-disks and costameres via distinct plectin isoforms“. *The Journal of Cell Biology* 181 (4): 667–81. doi:10.1083/jcb.200711058.

Laemmli, U K. 1970. „Cleavage of structural proteins during the assembly of the head of bacteriophage T4“. *Nature* 227 (5259): 680–85.

Lazarides, E. 1980. „Desmin and Intermediate Filaments in Muscle Cells“. *Results and Problems in Cell Differentiation* 11: 124–31.

Lazarides, E. 1982. „Intermediate filaments: a chemically heterogeneous, developmentally regulated class of proteins“. *Annual Review of Biochemistry* 51: 219–50. doi:10.1146/annurev.bi.51.070182.001251.

Lebowitz, Jacob, Marc S. Lewis, und Peter Schuck. 2002. „Modern Analytical Ultracentrifugation in Protein Science: A Tutorial Review“. *Protein Science: A Publication of the Protein Society* 11 (9): 2067–79. doi:10.1110/ps.0207702.

Leung, C. L., und R. K. Liem. 1996. „Characterization of Interactions between the Neurofilament Triplet Proteins by the Yeast Two-Hybrid System“. *The Journal of Biological Chemistry* 271 (24): 14041–44.

Lichtenstern, Tanja, Norbert Mücke, Ueli Aebi, Monika Mauermann, und Harald Herrmann. 2012. „Complex formation and kinetics of filament assembly exhibited by the simple epithelial keratins K8 and K18“. *Journal of Structural Biology* 177 (1): 54–62. doi:10.1016/j.jsb.2011.11.003.

Liem, R. K. 1993. „Molecular Biology of Neuronal Intermediate Filaments“. *Current Opinion in Cell Biology* 5 (1): 12–16.

Liu, Yi-Hsiang, Chiung-Chi Cheng, Yih-Shyong Lai, Wei-Ting Chao, Ren-Jeng Pei, Yung-Hsiang Hsu, und Chin-Chin Ho. 2011. „Synemin down-regulation in human hepatocellular carcinoma does not destabilize cytoskeletons in vivo“. *Biochemical and Biophysical Research Communications* 404 (1): 488–93. doi:10.1016/j.bbrc.2010.12.008.

Li, Z., E. Colucci-Guyon, M. Pinçon-Raymond, M. Mericskay, S. Pournin, D. Paulin, und C. Babinet. 1996. „Cardiovascular Lesions and Skeletal Myopathy in Mice Lacking Desmin“. *Developmental Biology* 175 (2): 362–66. doi:10.1006/dbio.1996.0122.

Li, Z., M. Mericskay, O. Agbulut, G. Butler-Browne, L. Carlsson, L. E. Thornell, C. Babinet, und D. Paulin. 1997. „Desmin Is Essential for the Tensile Strength and Integrity of Myofibrils but Not for Myogenic Commitment, Differentiation, and Fusion of Skeletal Muscle“. *The Journal of Cell Biology* 139 (1): 129–44.

Magin, T. M., M. Hatzfeld, und W. W. Franke. 1987. „Analysis of Cytokeratin Domains by Cloning and Expression of Intact and Deleted Polypeptides in Escherichia Coli“. *The EMBO Journal* 6 (9): 2607–15.

Milner, D. J., G. Weitzer, D. Tran, A. Bradley, und Y. Capetanaki. 1996. „Disruption of Muscle Architecture and Myocardial Degeneration in Mice Lacking Desmin“. *The Journal of Cell Biology* 134 (5): 1255–70.

Mücke, Norbert, Tatjana Wedig, Andrea Bürer, Lyuben N Marekov, Peter M Steinert, Jörg Langowski, Ueli Aebi, und Harald Herrmann. 2004. „Molecular and biophysical characterization of assembly-starter units of human vimentin“. *Journal of Molecular Biology* 340 (1): 97–114. doi:10.1016/j.jmb.2004.04.039.

Mullis, K B, und F A Faloona. 1987. „Specific synthesis of DNA in vitro via a polymerase-catalyzed chain reaction“. *Methods in Enzymology* 155: 335–50.

Nagai, K, und H C Thøgersen. 1987. „Synthesis and sequence-specific proteolysis of hybrid proteins produced in Escherichia coli“. *Methods in Enzymology* 153: 461–81.

Olivé, Montse, Lev Goldfarb, Ayush Dagvadorj, Nyamkhishig Sambuughin, Denise Paulin, Zhenlin Li, Bertrand Goudeau, Patrick Vicart, und Isidro Ferrer. 2003. „Expression of the intermediate filament protein synemin in myofibrillar myopathies and other muscle diseases“. *Acta Neuropathologica* 106 (1): 1–7. doi:10.1007/s00401-003-0695-0.

Omary, M Bishr. 2009. „‚IF-pathies‘: a broad spectrum of intermediate filament-associated diseases“. *The Journal of Clinical Investigation* 119 (7): 1756–62. doi:10.1172/JCI39894.

Pallari, Hanna-Mari, Julia Lindqvist, Elin Torvaldson, Saima E. Ferraris, Tao He, Cecilia Sahlgren, und John E. Eriksson. 2011. „Nestin as a Regulator of Cdk5 in Differentiating Myoblasts“. *Molecular Biology of the Cell* 22 (9): 1539–49. doi:10.1091/mbc.E10-07-0568.

Park, Donghyun, Andy Peng Xiang, Frank Fuxiang Mao, Li Zhang, Chun-Guang Di, Xiao-Mei Liu, Yuan Shao, u. a. 2010. „Nestin Is Required for the Proper Self-Renewal of Neural Stem Cells“. *Stem Cells (Dayton, Ohio)* 28 (12): 2162–71. doi:10.1002/stem.541.

Parry, David A. D. 2005. „Microdissection of the Sequence and Structure of Intermediate Filament Chains“. *Advances in Protein Chemistry* 70: 113–42. doi:10.1016/S0065-3233(05)70005-X.

Paulin, Denise, und Zhenlin Li. 2004. „Desmin: A Major Intermediate Filament Protein Essential for the Structural Integrity and Function of Muscle“. *Experimental Cell Research* 301 (1): 1–7. doi:10.1016/j.yexcr.2004.08.004.

Pekny, M., C. B. Johansson, C. Eliasson, J. Stakeberg, A. Wallén, T. Perlmann, U. Lendahl, C. Betsholtz, C. H. Berthold, und J. Frisén. 1999. „Abnormal Reaction to Central Nervous System Injury in Mice Lacking Glial Fibrillary Acidic Protein and Vimentin“. *The Journal of Cell Biology* 145 (3): 503–14.

Pitre, Aaron, Nathan Davis, Madhumita Paul, A. Wayne Orr, und Omar Skalli. 2012. „Synemin Promotes AKT-Dependent Glioblastoma Cell Proliferation by Antagonizing PP2A“. *Molecular Biology of the Cell* 23 (7): 1243–53. doi:10.1091/mbc.E11-08-0685.

Pollard, Thomas D. 2002. „Cellular motility powered by actin filament assembly and disassembly“. *Harvey Lectures* 98: 1–17.

Reipert, S, F Steinböck, I Fischer, R E Bittner, A Zeöld, und G Wiche. 1999. „Association of mitochondria with plectin and desmin intermediate filaments in striated muscle“. *Experimental Cell Research* 252 (2): 479–91. doi:10.1006/excr.1999.4626.

Rezniczek, G. A., J. M. de Pereda, S. Reipert, und G. Wiche. 1998. „Linking Integrin alpha6beta4-Based Cell Adhesion to the Intermediate Filament Cytoskeleton: Direct Interaction between the beta4 Subunit and Plectin at Multiple Molecular Sites“. *The Journal of Cell Biology* 141 (1): 209–25.

Russell, M, L Lund, R Haber, K Mckeegan, N Cianciola, und M Bond. 2006. „The intermediate filament protein, synemin, is an AKAP in the heart“. *Archives of Biochemistry and Biophysics* 456 (2): 204–15. doi:10.1016/j.abb.2006.06.010.

Sahlgren, Cecilia M., Andrey Mikhailov, Samuli Vaittinen, Hanna-Mari Pallari, Hannu Kalimo, Harish C. Pant, und John E. Eriksson. 2003. „Cdk5 Regulates the Organization of Nestin and Its Association with p35“. *Molecular and Cellular Biology* 23 (14): 5090–5106.

Sanger, F, S Nicklen, und A R Coulson. 1977. „DNA sequencing with chain-terminating inhibitors“. *Proceedings of the National Academy of Sciences of the United States of America* 74 (12): 5463–67.

Sarria, A. J., S. R. Panini, und R. M. Evans. 1992. „A Functional Role for Vimentin Intermediate Filaments in the Metabolism of Lipoprotein-Derived Cholesterol in Human SW-13 Cells“. *The Journal of Biological Chemistry* 267 (27): 19455–63.

Schröder, Rolf, Alexandra Vrabie, und Hans H. Goebel. 2007. „Primary Desminopathies“. *Journal of Cellular and Molecular Medicine* 11 (3): 416–26. doi:10.1111/j.1582-4934.2007.00057.x.

Selcen, Duygu, Kinji Ohno, und Andrew G. Engel. 2004. „Myofibrillar Myopathy: Clinical, Morphological and Genetic Studies in 63 Patients“. *Brain: A Journal of Neurology* 127 (Pt 2): 439–51. doi:10.1093/brain/awh052.

Shelanski, M. L., F. Gaskin, und C. R. Cantor. 1973. „Microtubule Assembly in the Absence of Added Nucleotides“. *Proceedings of the National Academy of Sciences of the United States of America* 70 (3): 765–68.

Sihag, Ram K., Masaki Inagaki, Tomoya Yamaguchi, Thomas B. Shea, und Harish C. Pant. 2007. „Role of Phosphorylation on the Structural Dynamics and Function of Types III and IV Intermediate Filaments“. *Experimental Cell Research* 313 (10): 2098–2109. doi:10.1016/j.yexcr.2007.04.010.

Sjöberg, G., W. Q. Jiang, N. R. Ringertz, U. Lendahl, und T. Sejersen. 1994. „Colocalization of Nestin and Vimentin/desmin in Skeletal Muscle Cells Demonstrated by Three-Dimensional Fluorescence Digital Imaging Microscopy“. *Experimental Cell Research* 214 (2): 447–58. doi:10.1006/excr.1994.1281.

Stafford, W F. 1992. „Boundary analysis in sedimentation transport experiments: a procedure for obtaining sedimentation coefficient distributions using the time derivative of the concentration profile“. *Analytical Biochemistry* 203 (2): 295–301.

Steinert, P. M., Y. H. Chou, V. Prahlad, D. A. Parry, L. N. Marekov, K. C. Wu, S. I. Jang, und R. D. Goldman. 1999. „A High Molecular Weight Intermediate Filament-Associated Protein in BHK-21 Cells Is Nestin, a Type VI Intermediate Filament Protein. Limited Co-Assembly in Vitro to Form Heteropolymers with Type III Vimentin and Type IV Alpha-Internexin“. *The Journal of Biological Chemistry* 274 (14): 9881–90.

Strelkov, Sergei V, Harald Herrmann, und Ueli Aebi. 2003. „Molecular architecture of intermediate filaments“. *BioEssays: News and Reviews in Molecular, Cellular and Developmental Biology* 25 (3): 243–51. doi:10.1002/bies.10246.

Strelkov, Sergei V., Harald Herrmann, Norbert Geisler, Tatjana Wedig, Ralf Zimbelmann, Ueli Aebi, und Peter Burkhard. 2002. „Conserved Segments 1A and 2B of the Intermediate Filament Dimer: Their Atomic Structures and Role in Filament Assembly“. *The EMBO Journal* 21 (6): 1255–66. doi:10.1093/emboj/21.6.1255.

Styers, Melanie L, Gloria Salazar, Rachal Love, Andrew A Peden, Andrew P Kowalczyk, und Victor Faundez. 2004. „The endo-lysosomal sorting machinery interacts with the intermediate filament cytoskeleton“. *Molecular Biology of the Cell* 15 (12): 5369–82. doi:10.1091/mbc.E04-03-0272.

Sun, Ning, David R Critchley, Denise Paulin, Zhenlin Li, und Richard M Robson. 2008. „Identification of a repeated domain within mammalian alpha-synemin that interacts directly with talin“. *Experimental Cell Research* 314 (8): 1839–49. doi:10.1016/j.yexcr.2008.01.034.

Sun, Ning, Ted W. Huiatt, Denise Paulin, Zhenlin Li, und Richard M. Robson. 2010. „Synemin interacts with the LIM domain protein zyxin and is essential for cell adhesion and migration“. *Experimental Cell Research* 316 (3): 491–505. doi:10.1016/j.yexcr.2009.10.015.

Szeverenyi, Ildiko, Andrew J Cassidy, Cheuk Wang Chung, Bernett T K Lee, John E A Common, Stephen C Ogg, Huijia Chen, u. a. 2008. „The Human Intermediate Filament Database: comprehensive information on a gene family involved in many human diseases“. *Human Mutation* 29 (3): 351–60. doi:10.1002/humu.20652.

Tao, Guo-Zhong, Kok Sun Looi, Diana M. Toivola, Pavel Strnad, Qin Zhou, Jian Liao, Yuquan Wei, Aida Habtezion, und M. Bishr Omary. 2009. „Keratins Modulate the Shape and Function of Hepatocyte Mitochondria: A Mechanism for Protection from Apoptosis“. *Journal of Cell Science* 122 (Pt 21): 3851–55. doi:10.1242/jcs.051862.

Toivola, Diana M, Guo-Zhong Tao, Aida Habtezion, Jian Liao, und M Bishr Omary. 2005. „Cellular integrity plus: organelle-related and protein-targeting functions of intermediate filaments“. *Trends in Cell Biology* 15 (11): 608–17. doi:10.1016/j.tcb.2005.09.004.

Towbin, H, T Staehelin, und J Gordon. 1979. „Electrophoretic transfer of proteins from polyacrylamide gels to nitrocellulose sheets: procedure and some applications“. *Proceedings of the National Academy of Sciences of the United States of America* 76 (9): 4350–54.

Turowski, P., T. Myles, B. A. Hemmings, A. Fernandez, und N. J. Lamb. 1999. „Vimentin Dephosphorylation by Protein Phosphatase 2A Is Modulated by the Targeting Subunit B55“. *Molecular Biology of the Cell* 10 (6): 1997–2015.

Vaittinen, S, R Lukka, C Sahlgren, T Hurme, J Rantanen, U Lendahl, J E Eriksson, und H Kalimo. 2001. „The expression of intermediate filament protein nestin as related to vimentin and desmin in regenerating skeletal muscle“. *Journal of Neuropathology and Experimental Neurology* 60 (6): 588–97.

Voter, W A, und H P Erickson. 1984. „The kinetics of microtubule assembly. Evidence for a two-stage nucleation mechanism“. *The Journal of Biological Chemistry* 259 (16): 10430–38.

Wegner, A, und J Engel. 1975. „Kinetics of the cooperative association of actin to actin filaments“. *Biophysical Chemistry* 3 (3): 215–25.

Wickert, Ute, Norbert Mücke, Tatjana Wedig, Shirley A. Müller, Ueli Aebi, und Harald Herrmann. 2005. „Characterization of the in Vitro Co-Assembly Process of the Intermediate Filament Proteins Vimentin and Desmin: Mixed Polymers at All Stages of Assembly“. *European Journal of Cell Biology* 84 (2-3): 379–91. doi:10.1016/j.ejcb.2005.01.004.

Wiese, C., A. Rolletschek, G. Kania, P. Blyszczuk, K. V. Tarasov, Y. Tarasova, R. P. Wersto, K. R. Boheler, und A. M. Wobus. 2004. „Nestin Expression--a Property of Multi-Lineage Progenitor Cells?“. *Cellular and Molecular Life Sciences: CMLS* 61 (19-20): 2510–22. doi:10.1007/s00018-004-4144-6.

Xue, Z G, Y Cheraud, V Brocheriou, A Izmiryan, M Titeux, D Paulin, und Z Li. 2004. „The mouse synemin gene encodes three intermediate filament proteins generated by alternative exon usage and different open reading frames“. *Experimental Cell Research* 298 (2): 431–44. doi:10.1016/j.yexcr.2004.04.023.

8 Table of figures

9 Appendices

9.1 Abbreviations and chemical formulas

aa	amino acid
Ab	antibody
APS	ammoniumperoxodisulfate (4 Amidinphenyl)-methansulfonylfluoride- hydrochloride-monohydrate
AUC	analytical ultracentrifugation
BSA	bovine serum albumin
cDNA	complentary *deoxyribonuclein acid*
C-terminal	carboxyterminal
DAPI	4,6-diamidino 2-phenylindole
DesΔhead	headless desmin
DesΔtail	tailless desmin
Des rod	rod domain of desmin
DesWT	desmin wild-type
DMSO	dimethyl sulfoxide
DNA	*deoxyribonuclein acid*
DNase	deoxyribonucleases
dNTP	deoxynucleotides

DTT	dithiothreitol
E.coli	*escherichia coli*
EDTA	thylendiamintetraacetic acid
EGTA	ethylene glycol tetraacetic acid
h	human
hum	human
HRP	horseradish peroxidase
IF	Intermediate filament
iP	isoelektric point
KCl	potassium chloride
LB	“Luria broth”, full media for bacteria
N-terminal	aminoterminal
NP 40	Nonidet P40 (octyl-phenyl-polyethylenglykol)
OD	optical density
P	pellet
PAGE	polyacryle amide gel electrophoresis
PCR	polymerase chain reaction
Pen/ Strep	penicillin/ Streptomycin
PMSF	phenylmethylsulphonyl fluoride
RNase	ribonucleases
Rpm	revolutions per minute
RT	22°C
s	sedimentation coefficient

S	Svedberg unit (10^{-13} seconds)
SDS	sodium dodecyl sulfate
SN	supernatant
TAE	Tris-Acetat-EDTA
Taq DNA polymerase	thermus aquaticus DNA polymerase
TB	„Terrific broth“
TE	Tris/EDTA buffer
TEMED	N-N-N’-N’-Tetramethylethylendiamine
Tris	N,N,N-Tris[hydroxymethyl]aminomethane
v/v	volume per volume
w/v	weight per volume

Prefixes, units and symbols

A	ampere
bp	basepair
°C	degree Celsius
cm	centimeter
Da	dalton
g	gram
h	hour
kb	kilo basepair
kDa	kilo dalton
L	Liter
M	molar
µg	microgram
µm	micro meter
mA	milli-Ampere
min	minute
nm	nanometer
S	Svedberg
sec	Sekunde
U	„Unit“, Einheit der Enzymaktivität
rpm	round per minute
V	Volt

Amino acids

amino acids	3-Letter	1-Letter	codons
Alanine	Ala	A	GCA GCC GCG GCU
Arginine	Arg	R	AGA AGG CGA CGC CGG CGU
Asparagine	Asn	N	AAC AAU
Aspartic acids	Asp	D	GAC GAU
Cysteine	Cys	C	UGC UGU
Glutamine	Gln	Q	CAA CAG
Glutamic acids	Glu	E	GAA GAG
Glycine	Gly	G	GGA GGC GGG GGU
Histidine	His	H	CAC CAU
Isoleucine	Ile	I	AUA AUC AUU
Leucine	Leu	L	UUA UUG CUA CUC CUG CUU
Lysine	Lys	K	AAA AAG
Methionine	Met	M	AUG
Phenylalanine	Phe	F	UUC UUU
Proline	Pro	P	CCA CCC CCG CCU
Serine	Ser	S	AGC AGU UCA UCC UCG UCU
Threonine	Thr	T	ACA ACC ACG ACU
Tryptophane	Trp	W	UGG
Tyrosine	Tyr	Y	UAC UAU
Valine	Val	V	GUA GUC GUG GUU

10 Supplementary

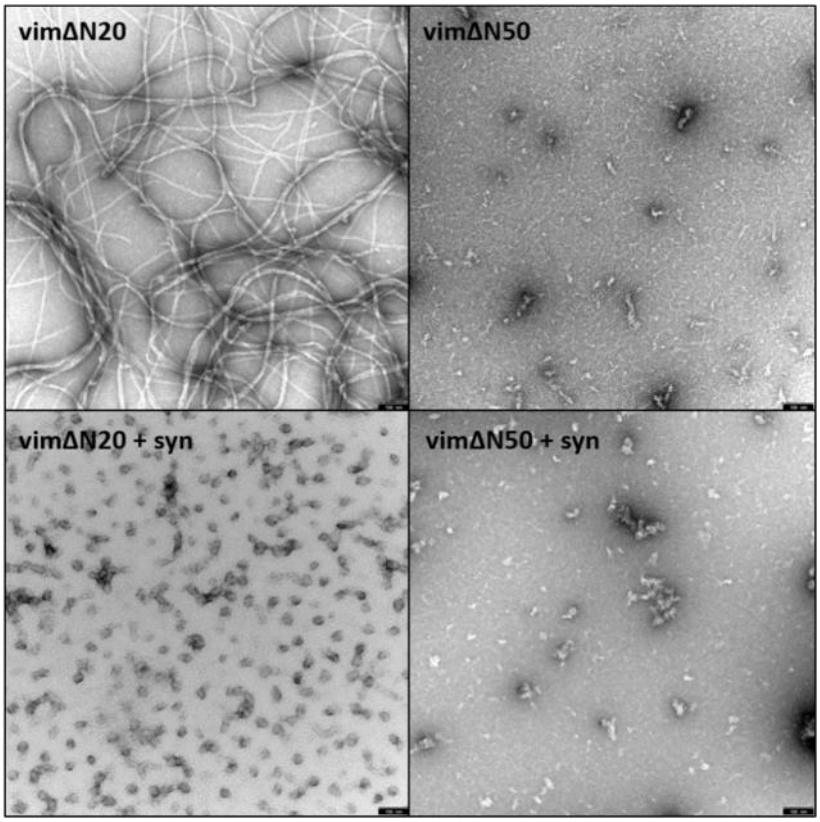

Figure 50: electron micrographs of negatively stained samples of head truncated variants of vimentin assembled in the presence of synemin. Assembly was performed at 37°C by addition of an equal amount of "assembly buffer" and stopped by adding 0.1% glutaraldehyde at 1 hour.

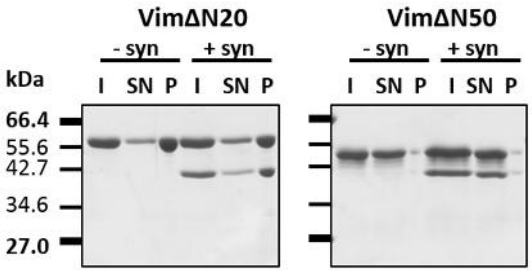

Figure 51: Sedimentation analysis of head-truncated variants of vimentin assembled in the presence of synemin. The protein was dialyzed into 5 mM Tris-HCl, pH 8.4 and assembly was started through adding the assembly buffer containing 40 mM Tris-HCl, 100 mM NaCl, pH 7.0. After assembly, the sample was centrifuged at 30 PSI for 15 minutes. The fraction are shown after separation by gel electrophoresis. (I: input; SN: supernatant; P: pellet).

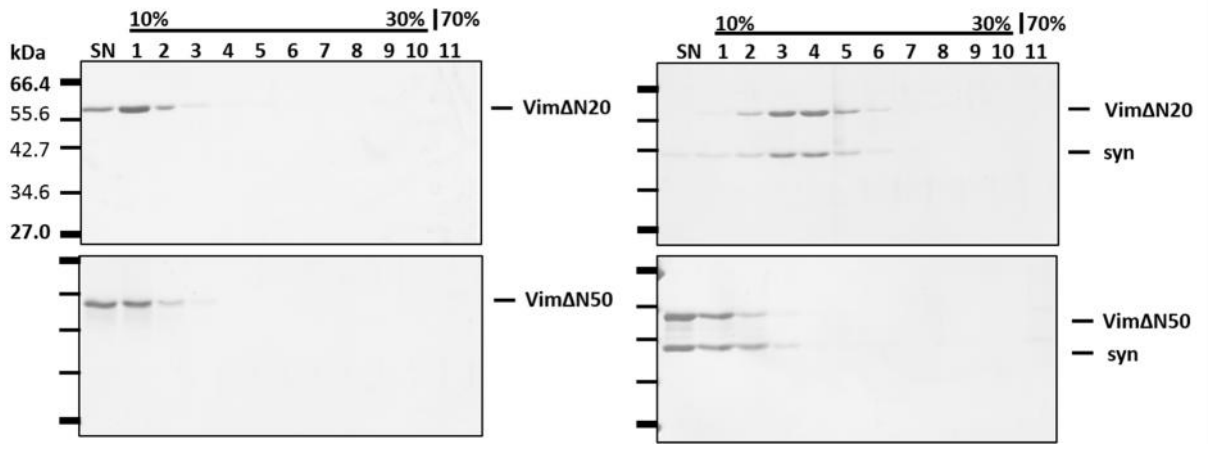

Figure 52: sucrose gradient analysis of assembled variants of head- truncated vimentin. The protein was dialyzed into 5 mM Tris-HCl, pH 8.4 and assembly was started through adding the assembly buffer containing 40 mM Tris-HCl, 100 mM NaCl, pH 7.0. After assembly, the sample was centrifuged at 28.000 rpm, 4°C for 5 hours. The fraction are shown after separation by gel electrophoresis. (SN: supernatant; Fraction 1 – 10: 10 – 30 % gradient; 11: 70 % cushion.)

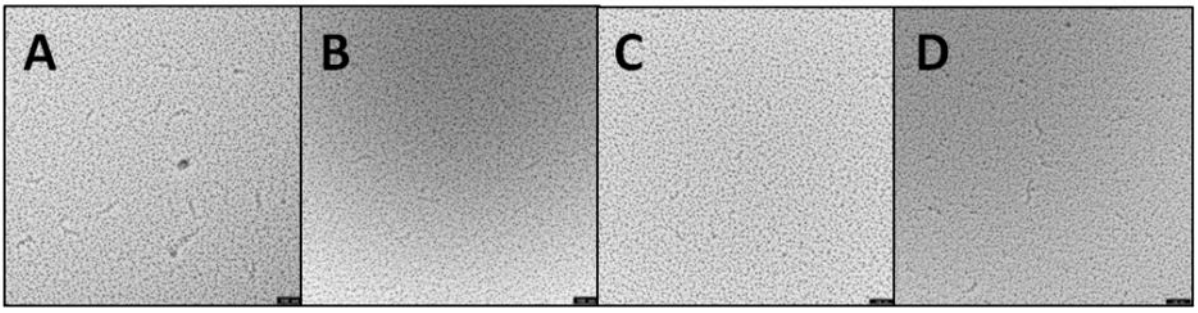

Figure 53 : Rotary shadowing of structures formed by synemin-L and desmin in 10 mM Tris-HCl, pH 7.5. After dialysis from 8 M urea into 5 mM Tris-HCl, pH 8.4, the samples were dialyzed for 1 hour into 10 mM Tris-HCl, pH 7.5. The protein concentration of all protein samples was 0.1 g/L for rotary shadowing. **A:** Synemin-L **B:** Desmin **C:** Synemin-L and desmin mixed before renaturation **D:** Synemin-L and desmin mixed after renaturation; bar 100 nm.

Synemin-L

```
 Continuous From: 1 To: 339   Length: 340
     Summary for whole sequence:
Molecular weight =   38968.19     Residues =    339
Average Residue Weight = 114.950     Charge = -21
Isoelectric point =  4.71

Residue           Number      Mole Percent
A = Ala              48            14.159
B = Asx               0             0.000
C = Cys               5             1.475
D = Asp              16             4.720
E = Glu              57            16.814
F = Phe               1             0.295
G = Gly              18             5.310
H = His               4             1.180
I = Ile               4             1.180
K = Lys               3             0.885
L = Leu              56            16.519
M = Met               5             1.475
N = Asn               4             1.180
P = Pro               7             2.065
Q = Gln              19             5.605
R = Arg              49            14.454
S = Ser              10             2.950
T = Thr              10             2.950
V = Val              11             3.245
W = Trp               5             1.475
Y = Tyr               7             2.065
Z = Glx               0             0.000

Small       (A+G)             66      19.469
Hydroxyl    (S+T)             20       5.900
Acidic      (D+E)             73      21.534
Acid/Amide  (D+E+N+Q)         96      28.319
Basic       (H+K+R)           56      16.519
Charged     (D+E+H+K+R)      129      38.053
Small hphob (I+L+M+V)         76      22.419
Aromatic    (F+W+Y)           13       3.835
```

Nestin

```
Continuous From: 1 To: 313   Length: 313
     Summary for whole sequence:
Molecular weight =   35370.48     Residues =    313
Average Residue Weight = 113.005     Charge =  -6
Isoelectric point =  5.71

Residue            Number      Mole Percent
A = Ala              50            15.974
B = Asx               0             0.000
C = Cys               5             1.597
D = Asp               5             1.597
E = Glu              49            15.655
F = Phe               2             0.639
G = Gly              20             6.390
H = His               5             1.597
I = Ile               1             0.319
K = Lys               6             1.917
L = Leu              43            13.738
M = Met               5             1.597
N = Asn               6             1.917
P = Pro               8             2.556
Q = Gln              24             7.668
R = Arg              42            13.419
S = Ser              11             3.514
T = Thr               7             2.236
V = Val              15             4.792
W = Trp               6             1.917
Y = Tyr               3             0.958
Z = Glx               0             0.000

Small       (A+G)             70      22.364
Hydroxyl    (S+T)             18       5.751
Acidic      (D+E)             54      17.252
Acid/Amide  (D+E+N+Q)         84      26.837
Basic       (H+K+R)           53      16.933
Charged     (D+E+H+K+R)      107      34.185
Small hphob (I+L+M+V)         64      20.447
Aromatic    (F+W+Y)           11       3.514
```